1-1-2014

Trial-by-Trial Coding of Instructive Signals in the Cerebellum: Insights From Eyeblink Conditioning in Mice

Farzaneh Najafi
University of Pennsylvania, farznaj@gmail.com

Trial-by-Trial Coding of Instructive Signals in the Cerebellum: Insights From Eyeblink Conditioning in Mice

Abstract
The cerebellum is an area of the brain that plays a crucial role in the learning of motor skills. This process involves climbing fibers, which provide teaching signals to Purkinje cells in the cerebellar cortex when perturbations occur during a movement. However, controversy has arisen over climbing fibers contribution to cerebellar learning. This is because climbing-fiber signals are described as "all-or-nothing": they fire a single burst of action potentials in response to all supra-threshold stimuli, regardless of their strength. On the contrary, motor learning is not all-or-nothing: the amount of learning is driven by the strength of perturbations. In this dissertation, I describe the experiments that I performed to unravel how climbing fibers may encode the strength of teaching signals. In **Chapter 2**, I present my behavioral studies in mice, which involved a simple cerebellar-dependent motor learning task, eyeblink conditioning. I show that mice take into account the strength of unexpected perturbations to adapt their movements trial-by-trial. In **Chapter 3**, I present a review of the previous literature and provide a hypothesis on how climbing fibers can encode the strength of teaching signals in a single trial. In **Chapter 4**, I present the findings of my in vivo two-photon calcium imaging experiments, which suggest climbing-fiber signals may not be all-or-nothing at the post-synaptic level. Finally, in **Chapter 5** I describe the different mechanisms that we discovered for coding the intensity of teaching signals by Purkinje cells in the cerebellum of awake mice.

Degree Type
Dissertation

Degree Name
Doctor of Philosophy (PhD)

Graduate Group
Biology

First Advisor
Javier F. Medina

Keywords
calcium imaging, cerebellum, climbing fibers, eyeblink conditioning, motor learning, unconditioned stimulus

Subject Categories
Biology | Neuroscience and Neurobiology | Psychology

TRIAL-BY-TRIAL CODING OF INSTRUCTIVE SIGNALS IN THE CEREBELLUM: INSIGHTS FROM EYEBLINK CONDITIONING IN MICE

Farzaneh Najafi

A DISSERTATION
in
Biology
Presented to the Faculties of the University of Pennsylvania
in
Partial Fulfillment of the Requirements for the
Degree of Doctor of Philosophy
2014

Supervisor of Dissertation

_____

Javier F. Medina, Assistant Professor, Psychology

Graduate Group Chairperson

_____

Doris Wagner, Professor, Biology

Dissertation Committee:

Marc Schmidt, Associate Professor, Biology

Joshua I. Gold, Professor, Neuroscience

Peter Petraitis, Professor, Biology

Isabel Muzzio, Assistant Professor, Psychology

TRIAL-BY-TRIAL CODING OF INSTRUCTIVE SIGNALS IN THE CEREBELLUM:

INSIGHTS FROM EYEBLINK CONDITIONING IN MICE

I dedicate this thesis to

My dearest **mom**,

the symbol of selfless love, care and sacrifice in my life,
I owe to her for all I am

My beloved **dad**,

from whom I learned enthusiasm, perseverance and dedication

My darling **husband**, Morteza

whose thoughtful, calm, and considerate behavior taught me so much

My **twin** sister, Farideh

my exact & opposite, my love & rival, with whom I was born & raised, laughed & cried,
agreed & argued, studied & played

My sweetheart siblings:

elder **sister**, Azadeh
younger **brother**, Mohammad Amin

my closest friends forever, whose cheer, kindness and sense of humor lighted up my life

&

My beloved departed **grandma**,

who helped raise me and is my symbol of tolerance, respect and empathy

I love you all dearly

ACKNOWLEDGMENTS

"Your depression is connected to your insolence and refusal to praise."

- Rumi (13th-century Persian Poet)

The completion of my PhD has been a long journey, in which I would not have been able to succeed without the support and guidance of the following people. It is to them that I owe my deepest gratitude.

My principal adviser, Javier Medina, with whom I have had the privilege of working as the first and only student over the past six years. His persistent help and guidance, immense motivation and dedication, and his humorous manners have been instrumental in inspiring and encouraging me during these years. I am indebted to him for all the hours he spent discussing science with me, assisting with my research projects, commenting on my writing, and training me as a scientist.

My collaborator and adviser at Princeton University, Samuel Wang, in whose lab I spent two years of my PhD doing exciting experiments on optical imaging, which formed an essential part of my thesis. The techniques that I learned in Sam's lab were invaluable. I am also particularly grateful to Sam for inviting me to stay in his attic during the first few months of my research at Princeton.

My thesis committee members:

- Marc Schmidt, the first person from Penn that I was introduced to and interviewed by, over the phone, almost 8… (ahh! the time passes so quickly!) years ago. An

affable person who encouraged me to come to Penn, a decision that I eventually made and am truly happy about. I am grateful to Marc for his support at different points during my PhD.

- Joshua Gold, whose scientific comments inspired me and professional way of dealing with problems taught me a lot. I am especially thankful to him for helping me at various times during my PhD.
- Peter Petraitis, who was welcoming and very helpful to me whenever I reached out to him, by email or in person, with my statistical questions.
- Isabel Muzzio, whose extremely cordial conversations with me in our random meetings in the hallways and lavatory of Solomon Building meant a lot to me.
- Bob Rescorla, who I was honored to have in my thesis committee for a couple of years, and whose influential work provided a lot of inspiration for my thesis (ref. the dissertation intro).

My current lab members: Shane Heiney, Shogo+Keiko Ohmae, and Divya Subramanian. I am so fortunate to have such great lab-mates. Not only did I enjoy discussing science with them, but I also gained precious career-related advice from all of them. They have been extremely friendly and helpful to me during the last years of my PhD. I also would like to acknowledge my previous lab members: Sam McDougle, Luis Ruffolo, Selman Chettih, Madi Moser, Tori Nault, and Margot Wohl, whose company I enjoyed during my early years in the lab.

My friends in Sam Wang's lab at Princeton University: Andrea Giovannucci, my affable collaborator who I enjoyed working with, and especially learned from his programming skills. Ilker Ozden, who taught me how to do optical imaging, and generously answered

my technical and scientific questions. Laura Lynch, Richard Sun, Alex Kloth, and Eve Schneider who were friendly and helpful to me whenever I asked for their help.

Colleen Gasiorowski, Doris Wagner and Mike Nusbaum: Colleen, the Biology Graduate Group coordinator, a truly kind person who has been helping me since the moment I entered Penn. Doris and Mike, professors of Biology and Neuroscience, who have been very welcoming whenever I reached out to them, and have given me some precious advice at different points during my PhD.

My friends outside of work, who are too many to list here, but they know who I mean! They provided the valuable friendship that I needed to deal with the nostalgia for my family and home country during the past 7 years. I am thankful to them for their kind support.

My family, … "though miles may lie between us, we are never far apart, for love doesn't count the miles, it is measured by the heart" …. I absolutely cannot find the right words to express my gratitude to my parents, twin sister, elder sister and younger brother. I truly love them and I wouldn't have made it this far without them.

And last, but certainly not least, my best friend, soul mate and husband, Morteza, who I met at Penn in the second year of my PhD. His love, support, discipline and compromise have taught me so much. These years of graduate school have not been an easy ride, but we both learned a lot…not just to fill our schedules, but to fulfill our lives. We could strengthen our commitment and determination to live life to the fullest. You are the best outcome of my PhD, Morteza.

ABSTRACT

TRIAL-BY-TRIAL CODING OF INSTRUCTIVE SIGNALS IN THE CEREBELLUM: INSIGHTS FROM EYEBLINK CONDITIONING IN MICE

Farzaneh Najafi

Javier F. Medina

The cerebellum is an area of the brain that plays a crucial role in the learning of motor skills. This process involves climbing fibers, which provide teaching signals to Purkinje cells in the cerebellar cortex when perturbations occur during a movement. However, controversy has arisen over climbing fibers contribution to cerebellar learning. This is because climbing-fiber signals are described as “all-or-nothing”: they fire a single burst of action potentials in response to all supra-threshold stimuli, regardless of their strength. On the contrary, motor learning is *not* all-or-nothing: the amount of learning is driven by the strength of perturbations. In this dissertation, I describe the experiments that I performed to unravel how climbing fibers may encode the strength of teaching signals. In **Chapter 2**, I present my behavioral studies in mice, which involved a simple cerebellar-dependent motor learning task, eyeblink conditioning. I show that mice take into account the strength of unexpected perturbations to adapt their movements trial-by-trial. In **Chapter 3**, I present a review of the previous literature and provide a hypothesis on how climbing fibers can encode the strength of teaching signals in a single trial. In **Chapter 4**, I present the findings of my in vivo two-photon calcium imaging experiments, which suggest climbing-fiber signals may *not* be all-or-nothing at the post-synaptic level. Finally, in **Chapter 5** I describe the different mechanisms that we discovered for coding the intensity of teaching signals by Purkinje cells in the cerebellum of awake mice.

TABLE OF CONTENTS

LIST OF ILLUSTRATIONS

CHAPTER 1:

General Introduction

"The measure of intelligence is the ability to change."

- Albert Einstein

1.1 Prediction errors: the learning drive

Learning, in its most basic form, can be viewed as a process by which we acquire the ability to anticipate what happens in the future using the past and present information (Schultz and Dickinson, 2000; Niv and Schoenbaum, 2008). Learning can occur as a result of Pavlovian conditioning during which an animal learns to predict an event (unconditioned stimulus, US) through establishing association with a pre-occurring event (conditioned stimulus, CS). For instance, if a dog receives repeated presentations of a tone stimulus followed by a fluid reward, the animal will gradually learn to associate the two stimuli. This will result in eliciting a response to the tone that anticipates the reward (e.g. salivation). Pavlov called this response, which is acquired through experience, a conditioned response (CR) (Pavlov and Anrep, 1927).

Animals learn to improve their predictions through comparing their expectations with the outcomes, and, subsequently, correcting for the discrepancy (prediction error) between the two variables. This is the basis of the powerful conditioning model

suggested by Rescorla and Wagner in 1972 (Rescorla and Wagner, 1972). Rescorla-Wagner learning rule is formulated as:

$$\Delta V = \alpha\,(\lambda - \sum V) = \alpha\,(oucome - prediction) \qquad \text{Eq. 1}$$

, Where ΔV determines how much the current prediction will be updated in the next presentation of stimuli (i.e. the next "trial"); α is the learning rate determining how much the new experience will be weighted in the future prediction; λ is the actual outcome (equal to a "perfect" prediction); and $\sum V$ is the overall current expectation provided by all the available stimuli in a trial. The key term in this equation that drives learning is $(\lambda - \sum V)$, which is the prediction error, i.e. a measure of the discrepancy between the occurred outcome and the expected outcome.

Neurons in several brain areas compute prediction errors related to reward, punishment, external stimuli, motor performance, etc. (Schultz and Dickinson, 2000). The first neurons that met the criteria for coding for prediction errors were the midbrain dopamine neurons (Schultz, 1986; Schultz et al., 1997). The discharge rate of these neurons is modulated depending on the sign of the error term: $(oucome - prediction)$; i.e. any violation of the error term above zero, such as when a reward is unexpectedly given to the animal, or when the reward is bigger than expected (for example when the association between the conditioned stimulus and the reinforcer (reward) is yet not completely established), will result in the excitation of dopamine neurons. However if the error term is negative, e.g. if the animal expects a reward to happen but it does not

receive it, dopamine neurons will be inhibited (Schultz et al., 1997; Bermudez and Schultz, 2010; Steinberg et al., 2013).

Signals related to the sign of the prediction error have been found in a qualitative way in many brain areas besides the midbrain dopamine neurons. However, the literature is very sparse on demonstrating a neural code that explicitly and in a quantitative manner represents the difference between the actual and expected outcomes. My PhD thesis was concerned with studying the neural basis of λ (actual outcome) magnitude, which is a critical parameter in determining the size of the prediction error, hence the magnitude of learning. I have used eyeblink conditioning in mice as the model system. The behavioral properties of this simple form of motor learning have been extensively studied and many of the underlying neural substrates have been identified, thereby making this paradigm ideal for examining the neuronal coding of motor error signals. In the next sections, I briefly describe the role of the cerebellum and its associated circuitry in eyeblink conditioning.

1.2 Cerebellum: the neuronal machine

Detailed anatomical and electrophysiological description of the cerebellum microcircuitry was first provided in the landmark book 'The Cerebellum as a Neuronal Machine' published by Eccles and his colleagues in 1967 (Eccles and et al., 1967). The most outstanding feature of this circuitry is perhaps its precise geometrical arrangement (Ito, 2006). Purkinje cells, which are the sole output neurons of the cerebellar cortex, receive two types of input from parallel fibers and climbing fibers (Fig. 1). Parallel fibers originate from granule cells, which in turn receive excitatory input from mossy fibers.

Mossy fibers convey information from many different sources in the central nervous system including the spinal cord and numerous structures in the brain stem, such as the Pons. Climbing fibers, on the other hand, are formed by the axons of the inferior olive neurons and convey sensory information into the cerebellar cortex. Inhibitory axons of Purkinje cells innervate Deep Cerebellar Nuclei (DCN), which in turn project to targets outside the cerebellum. It was further shown that there are inhibitory projections from the interpositus nucleus, which is one of the cerebellar nuclei, to the inferior olive (Andersson and Hesslow, 1987a; Andersson et al., 1988). Thereby olivo-cerebellar, cortico-nuclear, and nucleo-olivary projections form the olivo-cerebello-olivary loop that is particularly relevant to my PhD thesis (Fig. 1).

The cerebellar cortex is structurally partitioned into microzones that represent the minimal functional units of the cerebellum. All Purkinje cells within a microzone receive climbing fiber input from the same peripheral receptive field, and innervate the same subset of cerebellar nuclei cells. Moreover nuclear cells send inhibitory collaterals only to the olivary neurons that correspond to the same microzone; hence discrete olivo–cortico–nuclear complexes are formed (Oscarsson, 1979; Andersson and Hesslow, 1987b; Apps and Garwicz, 2005). Olivary neurons projecting to the same microzone are electrically coupled through gap junctions and have synchronized activity.

Eccles and colleagues also provided detailed characterization of electrophysiological responses triggered by parallel fibers and climbing fibers in the Purkinje cells. Two types of spikes are produces in Purkinje cells. Simple spikes are conventional action potentials that are generated in response to parallel fiber inputs.

However, climbing fibers evoke multi-component, calcium-based, action potentials called complex spikes, aka climbing fiber responses.

But what is the function of the highly stereotyped cerebellar circuitry? A few years after the classic description of the cerebellar neuronal circuitry was published, theorists Marr and Albus proposed seminal models of cerebellar function based on its neural circuitry (Marr, 1969; Albus, 1971). These models proposed that climbing fiber responses represent prediction error signals and function as a 'teacher' to modify the motor output of the cerebellum. This modification is done through inducing plasticity at the parallel fiber-Purkinje cell synapses which are concurrently active with the climbing fibers. Much of the evidence in support of the classic Marr-Albus theories has come from a simple form of motor learning: eyeblink conditioning.

1.3 Eyeblink conditioning: a simple cerebellar-dependent learning task

The classic conditioning of the eyeblink reflex is a simple and robust model for the evaluation of cerebellar motor learning. Repeated presentations of a neutral stimulus such as a light or an auditory stimulus (conditioned stimulus, CS), and an eyeblink-reflex eliciting stimulus, such as an airpuff to the eye (unconditioned stimulus, US) (Strughold, 1930) will result in a closing movement of the eyelid that anticipates the occurrence of the airpuff (conditioned response, CR) (Gormezano et al., 1962).

Previous work from many laboratories has demonstrated a straightforward mapping between the CS, US, CR, and the cerebellar neural circuitry (Medina et al., 2000; Thompson and Steinmetz, 2009; Boele et al., 2010). In brief it is shown that the CS is conveyed via mossy fibers, and the US is transferred through climbing fibers. The

cerebellar cortex is involved in forming the CR, possibly through the induction of plasticity in the form of LTD (long-term depression), which results from the coactivation of parallel fibers and climbing fibers (Ito and Kano, 1982; Ito, 2006; Dean et al., 2010). This plasticity will in turn result in the disinhibition of interpositus nucleus which relays conditioned responses to the eyeblink-related motor neurons (Fig. 1).

Of particular relevance to the research in this dissertation is the role that climbing fibers play in adaptation of conditioned eyelid responses. Various studies (Hesslow and Ivarsson, 1996; Kim et al., 1998; Medina et al., 2002) indicate that climbing fibers are activated in response to the US at the beginning of conditioning, when the animals still have not learned to blink in response to the CS, and are therefore committing errors. However, the US-related climbing fiber response is lost when the animals close their eyelid at the time of the US, hence making prediction errors nil. Therefore, the activity of climbing fibers is generally consistent with coding for prediction errors.

It has been hypothesized that olivary neurons that give rise to climbing fibers act as *neural comparators*, i.e. they compare the excitatory input which comes from the US and represents the 'occurred outcome', with the inhibitory input which originates from the interpositus nucleus and represents the 'predicted outcome'. Thereby the net activity of olivary neurons (and their climbing fiber axons) in response to the US is an indicative of the prediction error (Simpson et al., 1996; De Zeeuw et al., 1998). This hypothesis provides a neural implementation of the Rescorla-Wagner model (Eq.1) during cerebellar learning.

Learning theories suggest that the magnitude of the prediction error is the quantity that drives trial-by-trial adaptation (Rescorla and Wagner, 1972; Sutton and

Barto, 1998). However, this parameter has received sparse attention in the eyeblink-conditioning field. The motivation behind the studies in my dissertation was to address this gap, and discover the trial-by-trial representation of the magnitude of prediction errors during cerebellar learning. We took an initial step to address this problem by studying the encoding of the intensity of the unconditioned stimulus, which represents the actual outcome in the Rescorla-Wagner model (Eq.1, λ), during eyeblink conditioning. In the first chapter of my thesis, I will examine the relationship between US intensity and the amount of trial-by-trial adaptation during eyeblink conditioning in mice. In the remaining chapters we will take advantage of two-photon imaging tools to explore climbing fiber representation of US intensity in awake naïve mice.

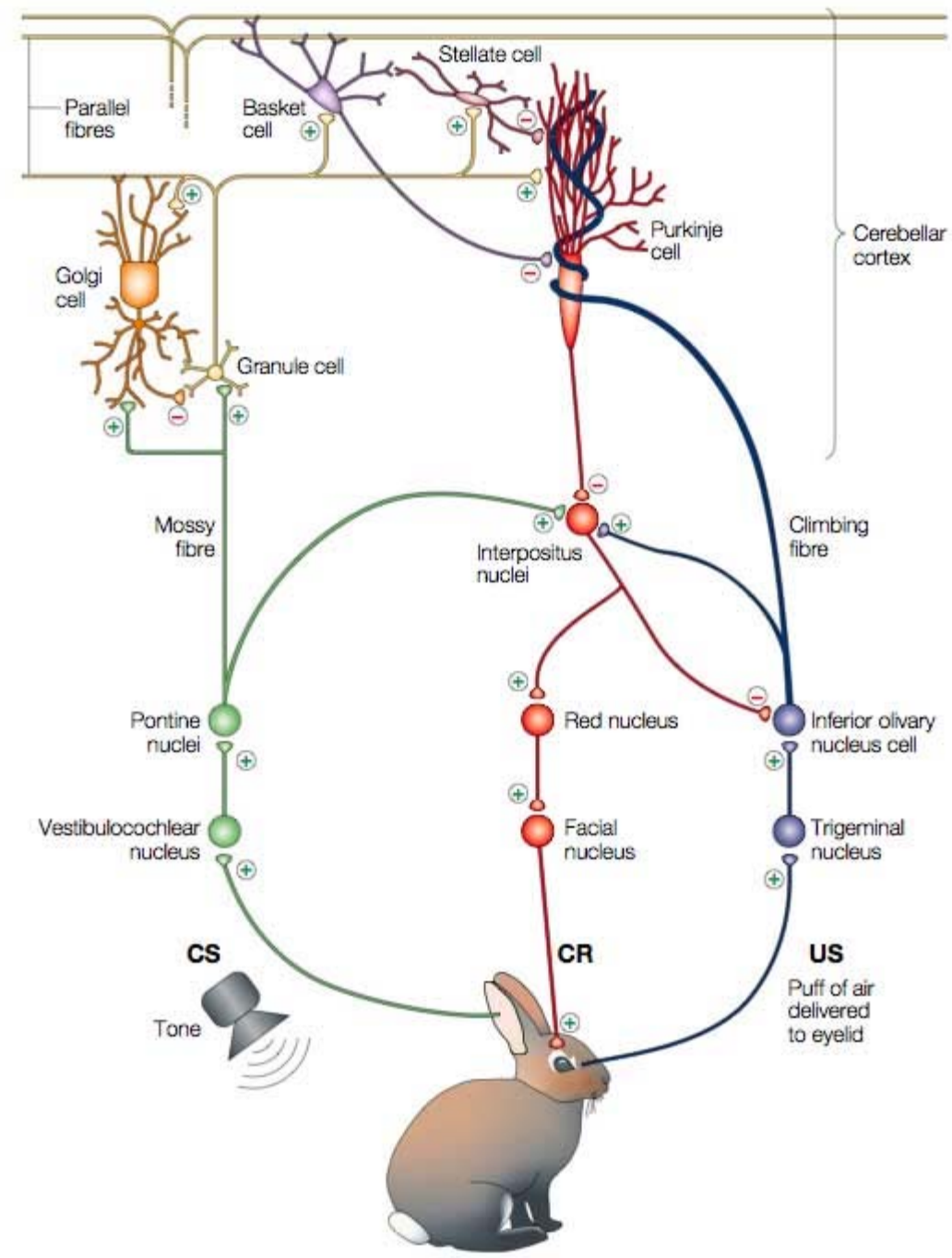

Figure 1-1 Cerebellar circuitry and the eyelid conditioning

CS, US, and CR pathways are mapped onto the cerebellar neural circuitry. CS: Conditioned Stimulus; US: Unconditioned Stimulus. CR: Conditioned Response. Figure from (Medina et al., 2002).

CHAPTER 2:

Contribution of short-term memory to single-trial motor adaptation in mice

Farzaneh Najafi [1] and Javier F. Medina [2]

[1] Department of Biology, University of Pennsylvania, Philadelphia, PA, USA
[2] Department of Psychology, University of Pennsylvania, Philadelphia, PA, USA

2.1 Novel method for doing eyeblink conditioning in mice

The classic animal models for doing eyeblink conditioning are rabbits (Gormezano et al., 1962). These animals acquire conditioned responses (CRs) gradually, after several training sessions that include hundreds of paired presentations of the conditioned and unconditioned stimuli (CS and US, respectively). Such gradual learning is expected given that eyeblink conditioning is a form of motor learning, and the learning of motor skills occurs gradually. This is in contrast to other forms of learning, particularly fear conditioning, which occur immediately only after the exposure to the fearful stimulus (Maren, 2001). Additionally, rabbits demonstrate proper timing of conditioned responses, such that their maximum eyelid closure occurs near the time of US delivery (Smith, 1968). Proper adaptive timing is another distinguishing characteristic of motor learning.

Eyeblink conditioning in mice is by far more challenging compared to rabbits (Takatsuki et al., 2001; Woodruff-Pak, 2006). Conventionally, it is performed in freely

moving mice using very strong unconditioned stimuli. In such conditions, mice generally demonstrate very rapid learning, within only a few trials. Additionally their conditioned responses possess poor temporal characteristics that do not match the timing of the US. Such learning properties are inconsistent with the features of motor learning, implying that the current methods of eyeblink conditioning in mice may chiefly induce fear conditioning (Boele et al., 2010). This is a major drawback since fear conditioning and classical eyeblink conditioning involve different neuronal circuitries (McCormick and Thompson, 1984; Maren, 2001).

We initially used the freely moving approach in order to set up eyeblink conditioning in our lab (Fig. 1A; see methods for details). A brief tone was used as the CS, and the US was a puff of air delivered to the animal's eye. In order to record the eyelid closure I used the Magnetic Distance Measurement Technique (Koekkoek et al., 2002) (Fig. 1B). In this method a very small magnet is glued on the lower eyelid and an electro-magnetometer is used to measure the magnetic field produced by the magnet. The strength of the magnetometer signal is a function of its distance with the magnet (Fig. 1C). Figure 1D demonstrates the performance of example mice trained by this method. Approximately 30% of the mice could achieve proper learning (Fig. 1D, left). The rest of the mice, however, showed poor learning and failed to acquire reliable conditioned responses (Fig. 1D, right).

Since eyeblink conditioning in freely moving mice was not efficient, we used a novel method to condition mice (Fig. 2A). We mounted head-fixed mice on top of a treadmill, which allowed them to move despite being head-restrained. This method proved to be remarkably efficient. Mice achieved learning criteria comparable to those of

rabbits that were quite unprecedented in the literature of mouse eyeblink conditioning. Figures 2B-C show the average eyelid position and the CR% for one of the earliest mice that I trained using the head-fixed locomotive method.

The behavioral data that I present in the next sections come from head-fixed mice on a cylindrical treadmill. I used a light-emitting diode (LED) as the CS, and periocular airpuff stimulation as the US. Additionally, a high-speed camera, instead of the magnetic system, was used to record eyelid movements (Chettih et al., 2011). This helped with eliminating the non-linearity inherent in the magnetic system (see Fig. 1C).

2.2 Learning the strength of the unconditioned stimulus

A key prediction of learning theories such as the Rescorla-Wagner model is that the amount of adaptation scales proportionally with the magnitude of the prediction error. Evidence from motor learning tasks, which involved visual (Franklin and Wolpert, 2008) or mechanical perturbations of the movement (Shadmehr and Mussa-Ivaldi, 1994; Scheidt et al., 2001), is generally consistent with the hypothesis on proportionality of learning with error magnitude (cf. chapter 6.1).

Pertinent to the proportionality hypothesis is the influence of the intensity of the unconditioned stimulus on the magnitude of learning. As mentioned in the introduction of my dissertation, the strength of the US represents the magnitude of the actual outcome. Therefore, an unexpected change in US strength will produce a prediction error, whose magnitude will be related to how much the US intensity was modified.

The influence of US intensity has been briefly examined in some classic studies of conditioning. For example, it was first shown by Pavlov that a weak CS, which normally is not suitable for eliciting CRs, could be changed to an effective CS by increasing the strength of the US (Passey, 1948). Further studies in humans and rabbits also showed a positive effect of the US intensity upon the rate of acquisition of conditioned eyelid responses (Passey, 1948; Spence and Taylor, 1951; Spence, 1953; Spence et al., 1958; Hoehler and Leonard, 1981; Kehoe and White, 2002). However, a thorough experimental analysis of the influence of US intensity on conditioning is still lacking. In particular, no evidence is available for the effects of US intensity on eyeblink conditioning in mice.

In my first behavioral experiment, I tested the hypothesis that the magnitude of conditioned eyelid responses scales proportionally with the intensity of the US. After mice were fully trained and asymptotic learning was achieved, I introduced daily sessions that included several blocks of trials (11 blocks, 50 trials per block). The strength of the US was kept constant for each block, but it was randomly varied from one block to the next. To study the influence of US intensity on learning, I computed the average position (Fig. 3A) and velocity (Fig. 3B) of eyelid traces across the last 30 trials of each block. Figure 3 illustrates the summary of all sessions (n=13; slid lines: average; shades: s.e.m.), demonstrating that mice adjust their conditioned responses according to the strength of the unconditioned stimulus. Next I quantified the CR magnitude by taking the average of eyelid signal in the last 30ms prior to airpuff delivery. Mean CR position (Fig. 3C) and CR velocity (Fig. 3D) are shown for different blocks of US intensity for

each session (black dots: individual sessions; red: average). Our results demonstrate a positive correlation between the magnitude of CR and the US intensity.

2.3 Time course of gain-up and gain-down adaptation to the US intensity

The time course of motor adaptation has been suggested to depend on the direction of learning (Li et al., 1995; Boyden and Raymond, 2003; Kojima et al., 2004; Smith et al., 2006). For instance, it has been shown that vestibulo-ocular reflex (VOR) adaptation, which is a cerebellar-learning task, occurs at different time courses during gain-up (increasing the gain of normal VOR) and gain-down (decreasing the gain of normal VOR) trainings (Boyden and Raymond, 2003). Similarly, a study of saccadic adaptation, which also depends on cerebellar circuitry, has shown that decreasing and increasing the gain of saccades are not simply mirror images of each other, suggesting that distinct mechanisms may underlie these two directions of motor learning (Kojima et al., 2004).

In the previous section, we showed that mice could adapt the magnitude of their conditioned eyelid responses based on the US intensity. Here, we examined the time course of CR adaptation, within single sessions, to US intensity. In particular we compared the temporal properties of adaptation between the following two conditions. 1) ”Gain-up”, in which the airpuff strength is changed from weak to strong. 2) “Gain-down”, in which a strong-to-weak change in airpuff intensity occurs.

Fully trained mice were given daily sessions in which the airpuff strength was changed after ~50 trials, and then it was kept constant for hundreds of trials, until the end of the session. Figure 4A represents the CR magnitude, trial-by-trial, for 4

consecutive sessions in an example mouse. Sessions in which the strength of the airpuff was increased are shown in black, and sessions in which the strength of the airpuff was decreased are shown in blue. In agreement with our previous experiment (ref. section 2.2), we found that a weak-to-strong change of the US (gain-up) induced an increase in the amplitude of the CRs (Fig. 4A, black), and a strong-to-weak US change (gain-down) resulted in smaller CRs (Fig. 4A, blue). We will refer to these two directions of adaptation as gain-up and gain-down, respectively.

The time course of adaptation to the gain-up and gain-down conditions appeared quite different: CR adaptation occurred rapidly when the US intensity was increased (Fig. 4A, black). However CRs were much more gradually adapted to decreases in US intensity (Fig. 4A, blue). We quantified this effect by fitting exponentials to the magnitude of all CRs after the change point. The gain-down adaptation could be fit by a single exponential with a slow time constant (Fig.6A, black exponentials on panels “Gain-down1” and “Gain-down2”; time constant: 194 and 117 trials, respectively). The gain-up adaptation, however, was better fit by two exponentials, one very fast (Fig. 4A, red exponentials on panels “Gain-up1” and “Gain-up2”; time constant: 23 and 27 trials, respectively), and one much slower (Fig. 4A, green exponentials on panels “Gain-up1” and “Gain-up2”; time constant: 159 and 116 trials, respectively).

The population summary of all gain-up and gain-down sessions (n=6; Fig. 4B-E) confirm the results of the representative data shown in Figure 4A. The time constant of the gain-up adaptation was 25±2 trials for the fast exponential (Fig. 4B,C red; mean±s.e.m.) and 138±22 trials for the slow exponential (Fig. 4B,C, green; mean±s.e.m.). On the other hand, the time constant of the gain-down adaptation was

171±18 trials (Fig. 4B,C, black exponential; mean±s.e.m.). The mean eyelid traces before the puff change (Fig. 4D, blue) and in consecutive blocks of trials after the puff change (Fig. 4D, cyan, green, orange, red, respectively) are shown for the gain-up (Fig. 4D, top) and gain-down (Fig. 4D, bottom) conditions. The corresponding CR positions (Fig. 4E) demonstrate the gradual learning induced by the reduction of US intensity (Fig. 4D,E, bottom), and the rapid learning induced by the enhancement of US intensity (Fig. 4D,E, top).

2.4 CR adaptation to single perturbations of US intensity

Insights about the mechanisms underlying motor adaptation have come from studies that examined how humans adjust their movements trial-by-trial during the learning process (Thoroughman et al., 2007). However, there are limited reports of trial-by-trial motor adaptation in other animal models despite the obvious advantages they offer for understanding the neural underpinnings. Here we studied, for the first time, trial-by-trial adaptation during eyeblink conditioning in mice.

Mice were initially trained with a medium-strength airpuff. To assess single-trial adaptation, we introduced sessions in which the medium-strength trials (‘normal’ trials) were interspersed with ~10% “perturbation” trials, i.e. occasional trials in which the LED (conditioned stimulus) was presented with either no airpuff (Fig. 5A, cyan box) or with a strong airpuff stimulus (Fig. 5D, red box) (inter-trial interval, ITI, for all trials: ~7sec). The mean difference traces (n=8 mice; ~20 sessions per mouse; ~50 perturbation trials per session), which demonstrate the change in the eyelid-position trace from one trial to the next, are shown for the normal (no perturbation) condition (Fig. 5B,E, black), as well as

the two perturbation conditions (Fig. 5B blue: no-puff, Fig. 5E, red: strong-puff). We found that the magnitude of the learned blinks (CRs) was slightly decreased on the trial immediately following the no-puff perturbation (Fig. 5B blue), and it was slightly increased on the trial after the strong-puff perturbation (Fig. 5E red). This is in contrast to normal trials, after which no change in the eyelid position occurred (Fig. 5B,E black). The change in CR magnitude is quantified for individual mice (Fig. 5C,F), demonstrating that the majority of mice adapted their CRs on the trial that immediately follows a perturbation trial (Fig. 5C blue; Fig. 5F red). Additionally CR adaptation occurred in the direction of perturbation, i.e. CR got smaller after the no-puff perturbation (Fig. 5C blue), and they got bigger after the strong-puff perturbation (Fig. 5F red); however CRs were not changed after a normal trial (Fig. 5C,F, black).

Next, we studied if the single-trial adaptation described above relied on an associative process. In other words, we studied if the reduction in CR amplitude after the no-puff trial is a form of non-associative learning merely induced by the absence of airpuff; or, if this CR adaptation occurs because the light stimulus is presented but the US is unexpectedly omitted. Similarly, the single-trial adaptation after a strong puff could be due to a sensitization process merely induced by the presence of a strong airpuff; or, it could be due to the unexpected association of the light stimulus with a strong airpuff, in lieu of a normally medium airpuff.

In other to address the potential non-associative mechanisms mentioned above, we omitted the light stimulus in some of the perturbation trials (Fig. 5A,D, green box). Therefore, a “gap” trial, i.e. a trial without CS or US (Fig. 5A, green box), was used to control for the no-puff-driven adaptation. On the other hand, a puff-alone trial, i.e. a trial

with a strong US and no CS (Fig. 5D, green box), was used to control for the adaptation after the strong airpuff. We found that the eyelid trace after the gap condition was not significantly changed (Fig. 5B green); however it was significantly enhanced after the strong-puff-alone condition (Fig. 5E green). The quantification of CR change in individual mice (Fig. 5C,F, green) confirms these results. Therefore, we conclude that the adaptation after a no-puff perturbation relies on an associative process that requires presentation of the light stimulus in the absence of the periocular airpuff. In contrast, other non-associative factors such as sensitization seem to largely explain the single-trial effect after a strong-airpuff perturbation.

2.5 Temporal properties of single-trial adaptation to US intensity

Previous studies have suggested that single-trial motor memory may be short-lived (Huang and Shadmehr, 2007; Yang and Lisberger, 2010). To study how long single-trial memory lasts in eyeblink conditioning, we randomly varied the time interval following the perturbation trial (Fig. 6A, middle, bottom). In particular, mice were trained in sessions that included occasional (~10%) no-puff or strong-puff perturbation trials in addition to the normal medium-airpuff trials. The trial following the perturbation trial was delivered at a random interval within [1 60] sec (ITI for the rest of the trials: ~7sec). In order to control for the effects of passage of time on learning in the absence of perturbation, we did additional experiments in which all trials were normal and the ITI was randomly varied in occasional trials, similar to how it was varied in perturbation experiments (Fig. 6A, top).

Figure 6B illustrates the mean difference traces (i.e. the change in eyelid position from the trial under study to the next trial; n=16 mice; ~25 session per mouse) for the perturbation conditions (Fig. 6B, no-puff: blue traces in the middle; strong-puff: red traces in the bottom), and the normal condition (Fig. 6B, black traces on top; also superimposed on the no-puff and strong-puff conditions for comparison). Our results indicate that learning following normal trials as well as the perturbation trials is ITI-dependent (Fig. 6B).

We found that in the absence of any perturbations, the size of conditioned responses starts to decrease after ~10 seconds (Fig. 6B top). On the other hand, the comparison of single-trial adaptation between the normal and no-puff trials (Fig. 6B, middle, black, blue, respectively) reveals that CR magnitude decreases after a no-puff trial. However, this adaptation lasts only for 60 seconds. In other words, if the trial following the no-puff perturbation arrives later than 60 seconds, CR magnitude will not be any longer modified by the perturbation (Fig. 6B, middle; 60-80sec; Note that the blue and black traces are superimposed). Similarly, a strong-puff perturbation induced an increase in CR magnitude (Fig. 6B, bottom), an effect that lasted only up to 60 seconds (Fig. 6B, bottom, 60-80sec).

A quantification of change in CR magnitude following the perturbation trials relative to the normal trials is shown (Fig. 6C). In brief, our findings suggest that single-trial adaptation to US intensity is transient; i.e. the amplitude of the CR is adaptively modified only within a narrow window of time, lasting ~60 seconds after the perturbation trial. Additionally, in the absence of any perturbations, a decrement in CR magnitude

occurs after ~10 seconds. A forgetting or an extinction-like mechanism could drive this effect.

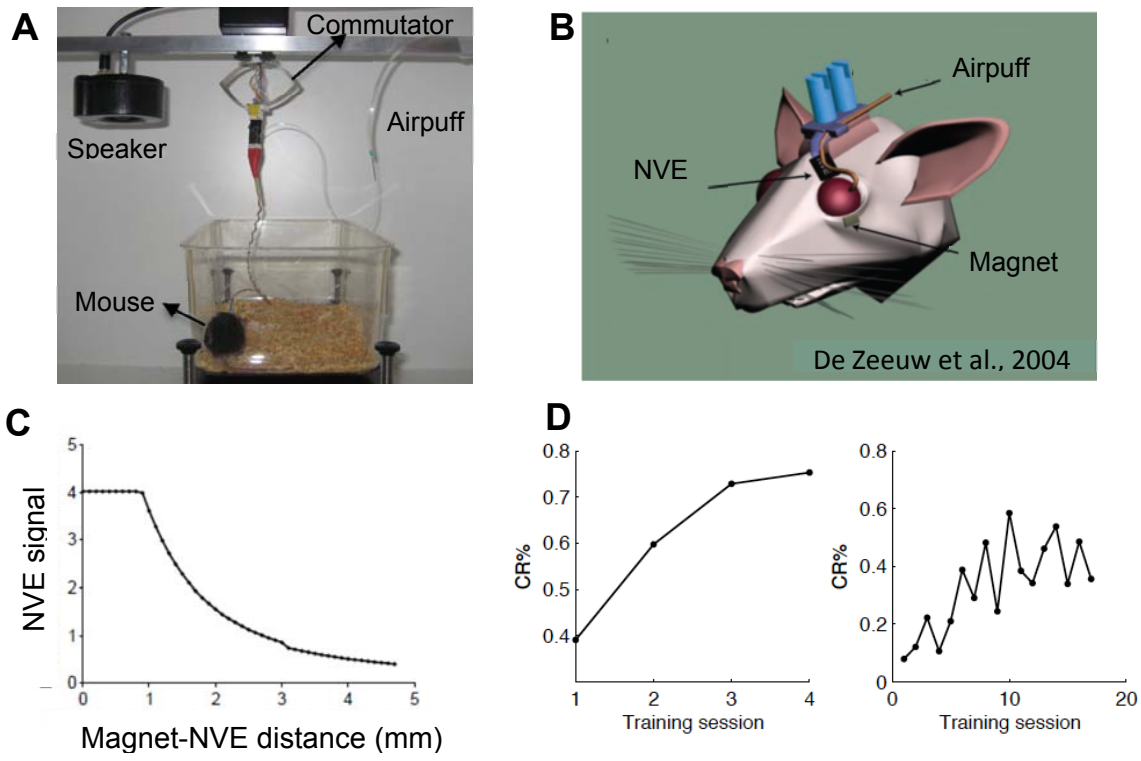

Figure 2-1 Eyeblink conditioning in freely moving mice

(A) The freely moving setup. Commutator allows the mouse to freely move in the cage. The speaker delivers the tone stimulus (CS). **(B)** Adopted from (De Zeeuw et al., 2004), it demonstrates the magnet-based technique used for measuring the eyelid closure. **(C)** Relation between the magnetometer (NVE chip) signal and the distance between the magnet and the chip. **(D)** Performance of two example mice conditioned with the freely moving setup. Proper learning was observed in almost 30% of the mice (left). The rest of the mice demonstrated poor learning (right).

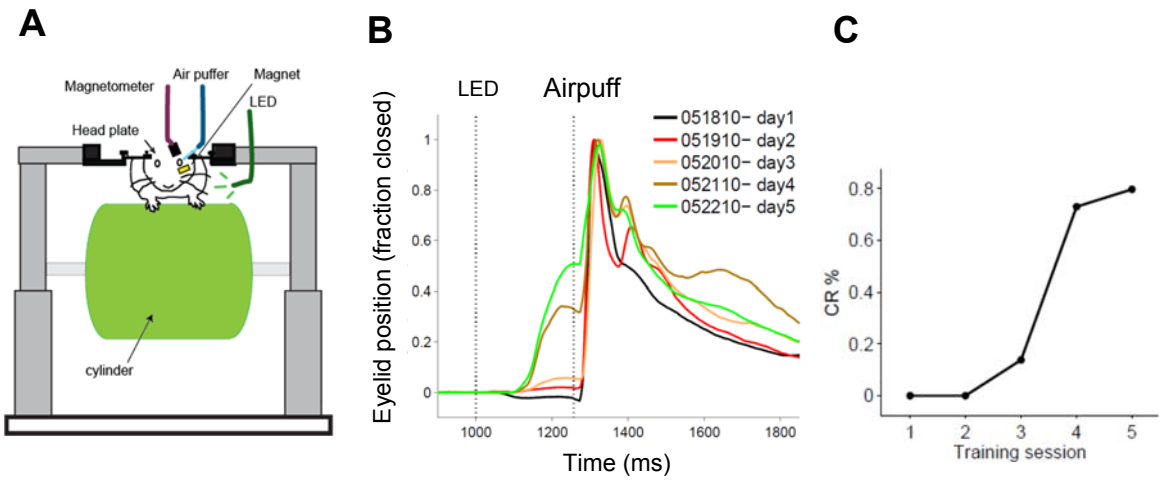

Figure 2-2 Eyeblink conditioning in head-fixed locomotive mice

(A) Mice are mounted on top of a treadmill. LED and airpuff provide the CS and US, respectively. Eyelid movement is recorded with a magnetometer. **(B)** Average eyelid position is shown for the first 5 training days of one of the earliest mice that I trained using this method. **(C)** CR percentage for the same mouse is shown. The performance is comparable to rabbit eyeblink conditioning.

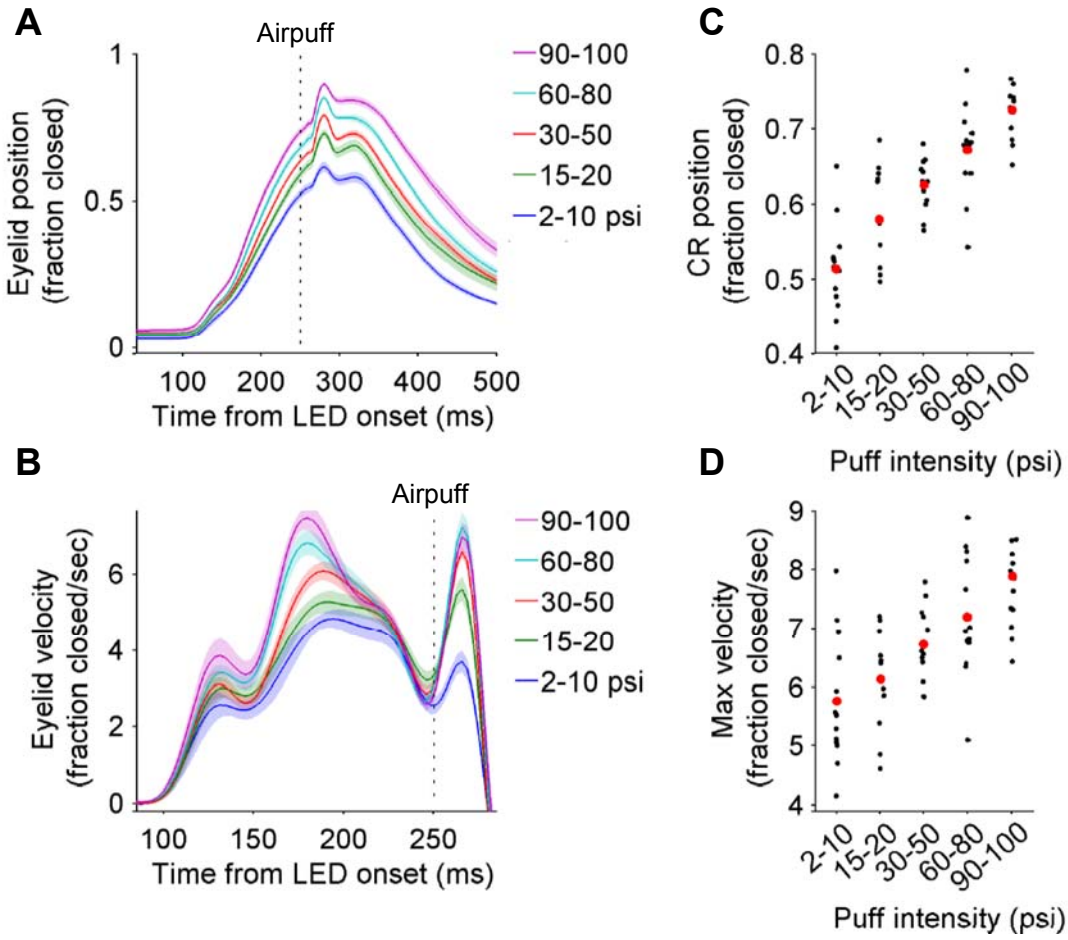

Figure 2-3 CR adaptation to the US intensity

Mean eyelid position **(A)** and eyelid velocity **(B)** across sessions in which different intensities of the airpuff were used as the US. Legend indicates US intensity. Mean CR position **(C)** and CR velocity **(D)** across sessions in which different intensities of the airpuff were used as the US.

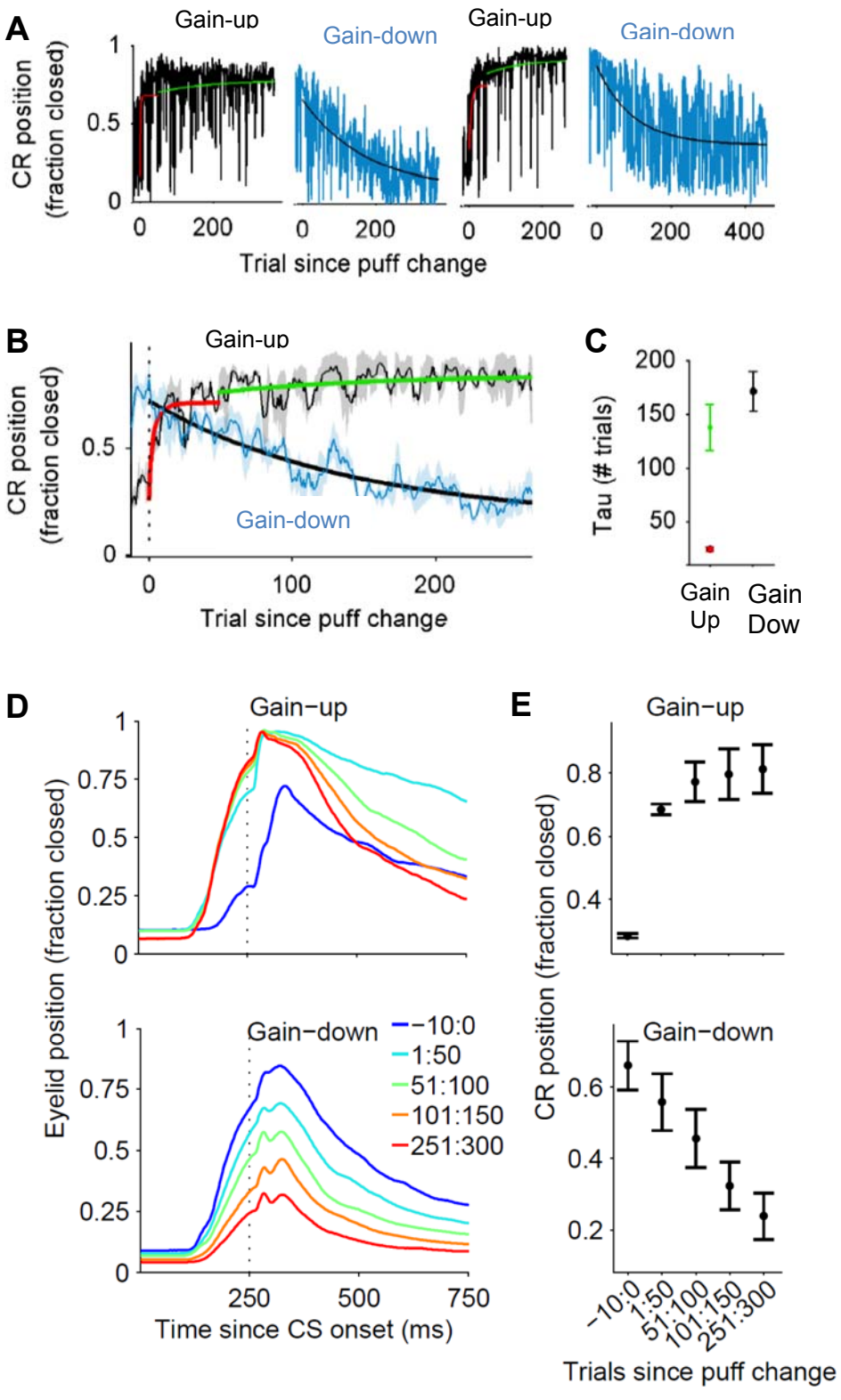
A
Gain-up
Gain-down
Gain-up
Gain-down
CR position (fraction closed)
1
0.5
0
0
200
0
200
0
200
0
200
400
Trial since puff change
B
Gain-up
Gain-down
CR position (fraction closed)
0.5
0
0
100
200
Trial since puff change
C
Tau (# trials)
200
150
100
50
Gain Up
Gain Dow
D
Gain−up
Gain−down
−10:0
1:50
51:100
101:150
251:300
Eyelid position (fraction closed)
1
0.75
0.5
0.25
0
250
500
750
Time since CS onset (ms)
E
Gain−up
Gain−down
CR position (fraction closed)
0.8
0.6
0.4
0.2
−10:0
1:50
51:100
101:150
251:300
Trials since puff change

Figure 2-4 Time course of gain-up and gain-down adaptation to US intensity

(A). CR position is shown, trial-by-trial, in 4 consecutive sessions that included a single change of US intensity (trial 0). In “Gain-up” sessions (black), US was made stronger after the change point. In “Gain-down” sessions (blue), US was made weaker. Exponential fits to the CRs after the change point are shown (red and green for the gain-up; black for the gain-down). **(B-E)** Population summary of all gain-up and all gain-down sessions (n=6). **(B)** Trial-by-trial CR position averaged across all gain-up (black) and gain-down (blue) sessions. (Shade: s.e.m.). Superimposed are the exponential fits (red and green for the gain-up; black for the gain-down). **(C)** Time constants of exponential fits to CR adaptation (mean±s.e.m); red and green correspond to the fast and slow exponentials of the gain-up condition. Black corresponds to the single exponential fit to the gain-down condition**. (D)** Average of eyelid traces before the puff change (blue, trials -10:0) and in blocks of 50 trials after the puff change (cyan, green, orange, and red, respectively) shown for gain-up (top) and gain-down (bottom) conditions. **(E)** Average CR magnitude for each block of trials surrounding the change point (±s.e.m). Gain-up condition (top) induces a rapid learning which will be followed by a much more gradual learning. In contrast, the gain-down condition induces a gradual, slow adaptation (bottom).

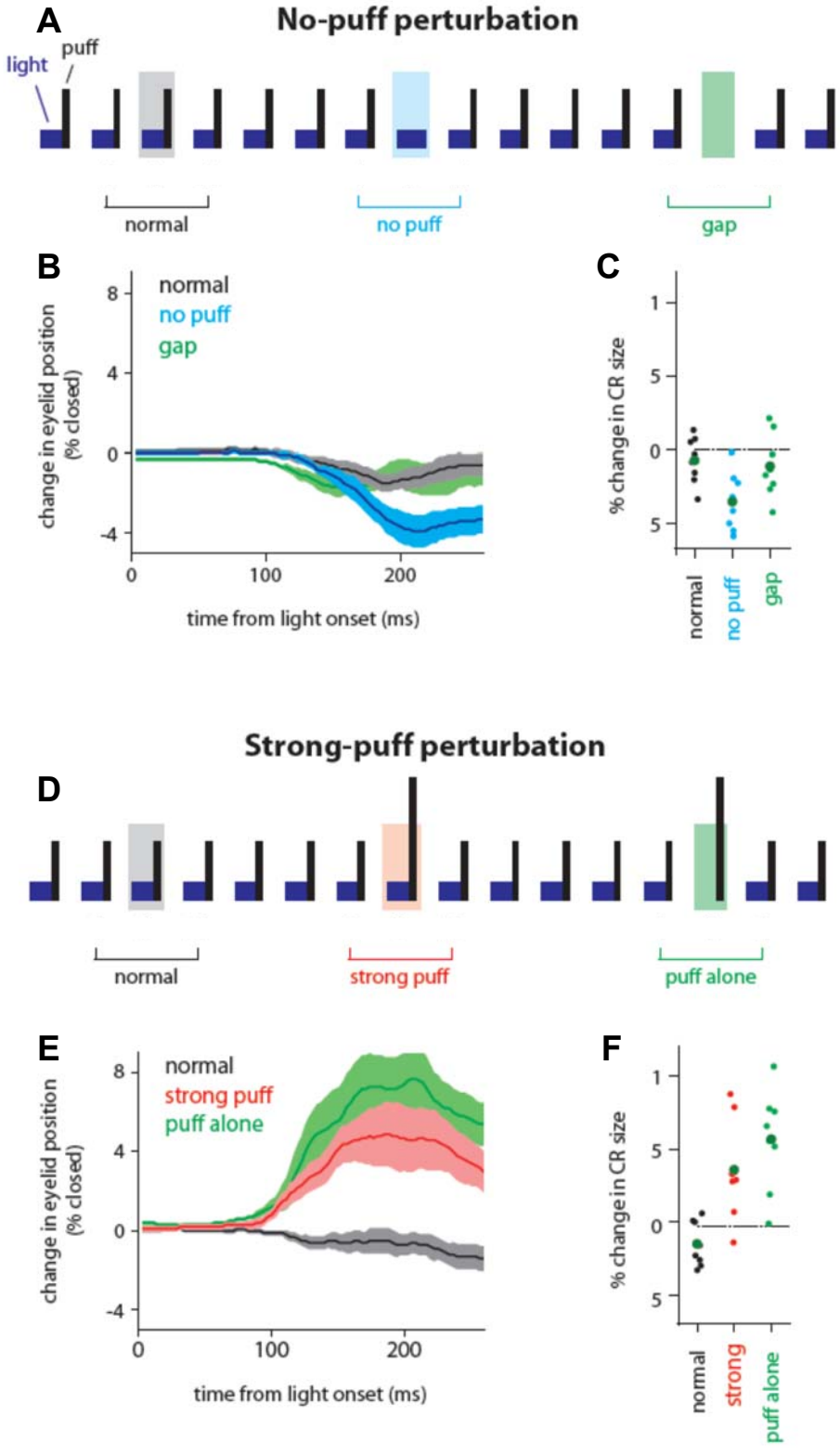
A
No-puff perturbation
light
puff
normal
no puff
gap
B
normal
no puff
gap
change in eyelid position (% closed)
8
4
0
-4
0
100
200
time from light onset (ms)
C
% change in CR size
1
5
0
5
normal
no puff
gap
Strong-puff perturbation
D
normal
strong puff
puff alone
E
normal
strong puff
puff alone
change in eyelid position (% closed)
8
4
0
-4
0
100
200
time from light onset (ms)
F
% change in CR size
1
5
0
5
normal
strong
puff alone

Figure 2-5 Single-trial adaptation to US intensity

No-puff perturbation: (A) Schematic illustrates the no-puff perturbation experiments. The airpuff was medium on most of the trials, but it was removed on some occasional trials (”no puff”, cyan box). In order to control for any non-associative effect, the light stimulus was also removed from some of the no-puff trials (”gap”, green box). **(B)** The “difference” traces demonstrating the change in eyelid position following a normal, no-puff, and gap trial (n = 8 mice, solid lines: average; shaded areas: s.e.m). **(C)** Each data point corresponds to an individual mouse and represents the change in CR size following a particular condition (normal, no-puff, and no-light). The large green dots represent the average across mice (n=8). **Strong-puff perturbation:** Similar to the no-puff perturbation experiments, except that the airpuff was made stronger on some occasional trials. **(D-F)** Same as (A-C), but for strong-puff experiments.

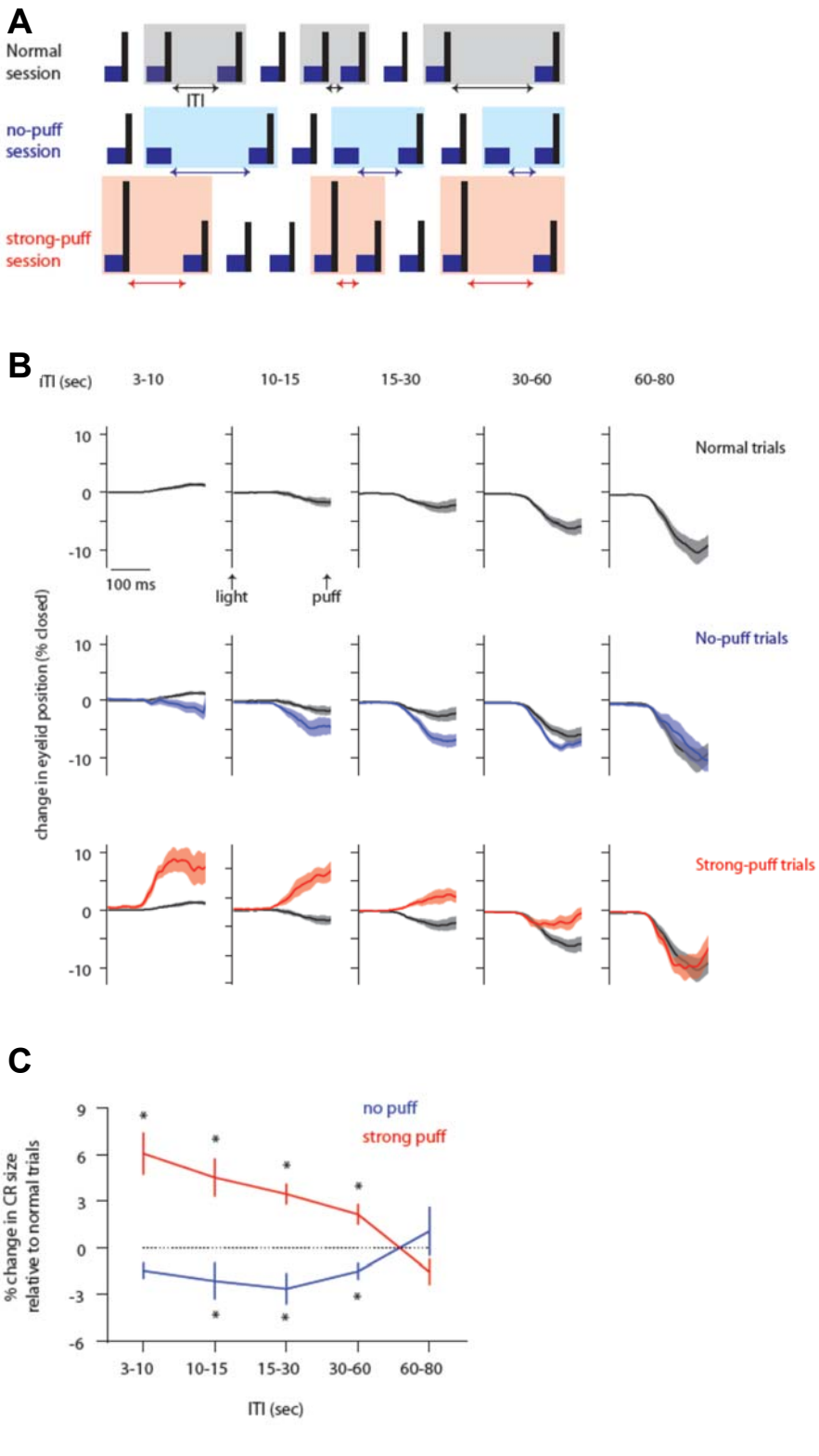
A
Normal session
ITI
no-puff session
strong-puff session
B
iTI (sec)
3-10
10-15
15-30
30-60
60-80
Normal trials
No-puff trials
Strong-puff trials
change in eyelid position (% closed)
10
0
-10
100 ms
light
puff
C
no puff
strong puff
% change in CR size relative to normal trials
9
6
3
0
-3
-6
3-10
10-15
15-30
30-60
60-80
ITI (sec)

Figure 2-6 Single-trial adaptation to US intensity is transient

(A) Schematic illustrates the experiments that examined the timescale of single-trial adaptation. Normal sessions only included medium-strength airpuff trials; the inter-trial intervals were selected randomly from the range [1 60] sec. No-puff and strong-puff sessions included occasional no-puff or strong-puff perturbation trials in addition to the medium-strength airpuff trials. The trial following the perturbation trial was delivered at a random interval within [1 60] sec. Shaded boxes indicate the trials that were used for computing the "difference" traces in B. **(B)** "Difference" traces, which demonstrate the change in eyelid position following the normal, no-puff, and strong-puff trials, are shown for different ITIs (n = 16 mice; mean±s.e.m). The traces for the normal condition are superimposed on the no-puff and strong-puff conditions for comparison. **(C)** Average change in CR size after the no-puff (blue) and strong-puff (red) trials relative to the change following the normal trials is shown for different ITIs (n=16 mice; bars: s.e.m; asterisks indicate significance relative to the normal condition, $p < 0.05$).

CHAPTER 3:

Beyond "all-or nothing" climbing fibers: graded representation of teaching signals in Purkinje cells

Farzaneh Najafi [1] and Javier F. Medina [2]

[1] Department of Biology, University of Pennsylvania, Philadelphia, PA, USA
[2] Department of Psychology, University of Pennsylvania, Philadelphia, PA, USA

Frontiers in Neural Circuits. 2013 Jul 2;7:115

3.1 Abstract

Arguments about the function of the climbing fiber (CF) input to the cerebellar cortex have fueled a rabid debate that started over 40 years ago, and continues to polarize the field to this day. The origin of the controversy can be traced back to 1969, the year David Marr published part of his dissertation work in a paper entitled "A theory of cerebellar cortex." In Marr's theory, CFs play a key role during the process of motor learning, providing an instructive signal that serves as a "teacher" for the post-synaptic Purkinje cells. Although this influential idea has found its way into the mainstream, a number of objections have been raised. For example, several investigators have pointed out that the seemingly "all-or-nothing" activation of the CF input provides little information and is too ambiguous to serve as an effective instructive signal. Here, we take a fresh look at these arguments in light of new evidence about the peculiar physiology of CFs. Based on recent findings we propose that at the level of an individual Purkinje cell, a

graded instructive signal can be effectively encoded via pre- or post-synaptic modulation of its one and only CF input.

Marr's idea that cerebellar climbing fibers (CFs) play the role of "teachers" during motor learning was a stroke of genius. Like the rest of the hypotheses first introduced in his revolutionary "A theory of cerebellar cortex" (Marr, 1969), the idea that CFs provide instructive signals was built from the ground up, based on first principles and a deep understanding of the computational problems that need to be solved in motor control. In addition, Marr relied extensively on detailed knowledge about the wiring circuit and the physiology of the cerebellar cortex, which had been compiled just a few years before in a remarkable book by (Eccles and et al., 1967). We may never know with certainty what led to the aha moment that sparked the idea that CFs could act as "teachers"; but one can only imagine that in developing his pioneering theory, Marr must have been particularly intrigued by the unique properties of the CF input and the peculiar response it generates in the post-synaptic Purkinje cell.

3.2 "All-or-Nothing" Instructive Signals

Climbing fibers are the axons sent by neurons in the inferior olive to the contralateral cerebellum (Figure 1A; red; (Eccles et al., 1966a; Desclin, 1974; Schmolesky et al., 2002; Ohtsuki and Hirano, 2008). One of the most striking features of this olivo-cerebellar projection is that in the adult cerebellar cortex, each Purkinje cell is innervated by a single CF (Eccles et al., 1966a; Schmolesky et al., 2002; Ohtsuki and Hirano, 2008). This is one of the most powerful excitatory synapses in the brain (Eccles et al., 1966b), comprising more than 1000 contacts distributed all along the proximal

portion of the Purkinje cell dendritic tree (Palay and Chan-Palay, 1974; Strata and Rossi, 1998). As a result, activation of a single olivary neuron results in a large electrical event in the soma of the post-synaptic Purkinje cell, termed the “complex spike” (CS; (Thach, 1967) because it consists of a fast initial spike followed by several slower spikelets of smaller amplitude separated from each other by 2–3 ms (Figure 1B5; asterisk; (Eccles et al., 1966b). The CS can be easily distinguished from the so called “simple spikes” (Thach, 1967), normal action potentials fired constantly by the Purkinje cells at high rates (Figure 1B5; thin lines). The cause of the spikelets in the CS was disputed for years (Armstrong and Rawson, 1979; Campbell et al., 1983), but recent work has demonstrated that they are a result of the interaction between local resurgent sodium currents in the Purkinje cell soma (Raman and Bean, 1997, 1999a, b; Schmolesky et al., 2002), and the characteristic activation of the pre-synaptic CFs, which tend to fire in brief high-frequency bursts of 1–6 spikes (Figure 1B1; (Crill, 1970; Armstrong, 1974; Mathy et al., 2009).

From the very beginning, the somatic CS was described as being “all-or-nothing” (Eccles et al., 1966b), a label that has stuck to this day. This characterization of the CS is based on the finding that direct microstimulation of the inferior olive causes a seemingly binary response in the post-synaptic Purkinje cell (Eccles et al., 1966b): “nothing” if the strength of stimulation is below a certain threshold, or a unitary (“all”) CS for all strengths above threshold (Figure 1B5; same CS for weak or strong inferior olive stimulation). In other words, the CS evoked in an individual Purkinje cell is unaffected if additional CFs are activated by increasing the strength of stimulation in the inferior olive. These groundbreaking experiments hold an important place in history, partly because in

showing that the post-synaptic CF response does not depend on the number of stimulated cells in the inferior olive, they helped demonstrate that each Purkinje cell must receive input from one-and-only-one CF. Importantly, the “all-or-nothing” quality of the post-synaptic CS also implies that the response of the sole pre-synaptic CF input is not graded with the strength of olivary stimulation, and must itself be “all-or-nothing” as well (Figure 1B1; same 3-spike burst for weak or strong IO stimulation). Later studies confirmed this prediction by recording directly from individual neurons in the inferior olive, and showing that their spiking response varies little with the strength of stimulation (Crill, 1970). This finding has far-reaching implications and is at the center of a heated debate about the functional role of the CF input.

3.3 Spontaneous Climbing Fibers and the Signal-to-Noise Problem

To Marr, the idiosyncratic properties of the olivo-cerebellar system could only mean one thing: each individual “all-or-nothing” CF input represents an “elemental” instruction that provides information about what the correct movement should be in a given context (Marr, 1969). It is important to remember that in the original theory, these instructive signals could be encoded in either motor or sensory coordinates (Marr, 1969). For example, if an obstacle is placed in front of the right foot causing the subject to trip while walking on a treadmill, the appropriate elemental instruction could be represented using motor commands coming from cerebral cortex (e.g., “lift right foot”), or sensory-related inputs coming from peripheral activation of cutaneous receptors (e.g., “the right foot hit an obstacle”). In either case, the idea was that the CF input would be providing an instructive signal to the Purkinje cell, triggering mechanisms of plasticity that would

be used to correct subsequent movements (i.e., lift the right foot higher on the next step cycle and avoid the obstacle).

Almost 45 years after Marr's original proposal, his hypothesis remains controversial and the cerebellar field is still divided with regards to how CF signals are used to exert control over our movements (De Schutter and Maex, 1996; Simpson et al., 1996; Llinas, 2011). It appears that at least in some motor learning tasks, CFs are activated in a manner that is compatible with their presumed role as "teachers" (Gilbert and Thach, 1977; Raymond et al., 1996; Simpson et al., 1996; Kitazawa et al., 1998; Raymond and Lisberger, 1998; Ito, 2006; Medina and Lisberger, 2008; Rasmussen et al., 2008; Soetedjo et al., 2008b). Further support comes from *in vitro* studies showing that CF inputs can trigger a variety of synaptic plasticity mechanisms in Purkinje cells (for reviews, see (Hansel et al., 2001; Gao et al., 2012). However, a number of questions have been raised about the potential instructive role of CFs during motor learning, particularly with regards to the problems inherent in representing information with "all-or-nothing" signals from spontaneously active neurons (Llinas and Welsh, 1993; Llinas et al., 1997).

One argument against the idea that CFs act as "teachers" is that the "all-or-nothing" CF input is ambiguous from the point of view of an individual Purkinje cell, and suffers from the so-called "signal-to-noise" problem (Llinas et al., 1997). The trouble is that CFs are spontaneously active about once per second (Armstrong, 1974; Simpson et al., 1996), and at least in the prevailing view (Figure 1B), the post-synaptic Purkinje cell would have no way of distinguishing between these frequent spontaneous activations ("noise"), and the few which occur during motor learning and presumably encode

elemental instructions (“signal”). Even if Purkinje cells were somehow able to discriminate between instructive and spontaneous CF inputs, the “all-or-nothing” character of the CF signal would put a hard limit on how much information can be encoded. At best, a CF could fire (“all”) to signal “lift right foot” or remain silent (“nothing”) to signal “do not lift right foot,” but it would not be able to provide useful parametric information about how far to lift it. These theoretical considerations call into question the ability of individual CFs to provide efficient instructive signals for motor learning. But are CFs really such “bad teachers?”

3.4 Pooling Together CF Signals: there is Strength in Numbers

Previous theoretical studies have suggested that even though a single “all-or-nothing” CF signal is ambiguous, an individual Purkinje cell could still solve the “signal-to-noise” problem by collecting information from its CF input across many trials (Sejnowski, 1977; Kawato and Gomi, 1992; Gilbert, 1993; Mauk and Donegan, 1997; Mauk et al., 1997; Kenyon et al., 1998; Spoelstra et al., 2000; Dean et al., 2010). In these computational models, CF activity works as an equilibrium point signal: the CF fires (“all”) to trigger plasticity when an error is made and the movement needs to be adjusted, but is silent (“nothing”) if the movement is performed correctly. Because a single spontaneous CF input cannot be distinguished from a single error-related CF input, it is assumed that both types of CF signals are equally capable of inducing plasticity. However, only those CF signals that are repeatedly triggered with high probability in a specific learning context would lead to an enduring change in the Purkinje cell. This solves one problem, but leaves unanswered one important question: how can “all-or-nothing” CFs provide parametric information about the size of the error?

After all, an effective instructive signal should indicate whether the movement (Wise et al., 2010) requires just a small adjustment or a major overhaul.

An “all-or-nothing” CF signal cannot carry much information by itself, but instructive signals with details about error size could be encoded, at least in theory, by pooling together the activity of many olivary neurons. For example, the instructive signal “lift right foot” could be represented by activating any one of ten CFs, while at the same time graded information about how far to lift it could be encoded by modulating how many of the ten are simultaneously activated. The olivo-cerebellar system seems perfectly suited for this type of synchronous population coding: neighboring neurons in the inferior olive are electrically coupled by dendrodendritic gap junctions (Llinas et al., 1974; Sotelo et al., 1974; De Zeeuw et al., 1996; De Zeeuw et al., 1997; Marshall et al., 2007), and as a result, small groups of CFs converging on the same narrow parasagittal strip of cerebellar cortex have a tendency to fire synchronously (Bell and Kawasaki, 1972; Llinas and Sasaki, 1989; Sugihara et al., 1993; Simpson et al., 1996; Lang et al., 1999; Kitazawa and Wolpert, 2005). Furthermore, the level of co-activation in the CF population appears to encode sensorimotor-related information (Lou and Bloedel, 1992; Welsh et al., 1995; Wylie et al., 1995; Lang, 2002; Ozden et al., 2009; Schultz et al., 2009; Wise et al., 2010).

As pointed out by others (Ozden et al., 2009; Schultz et al., 2009; Bengtsson et al., 2011; Otis et al., 2012), the level of CF co-activation could potentially be read out and used as an instructive signal in downstream neurons of the deep cerebellar nuclei which receive convergent input from many Purkinje cells (Palkovits et al., 1977; Person and Raman, 2012). However, our concern here is with the representation of instructive

signals at the level of an individual Purkinje cell, which receives input from a single CF (Eccles et al., 1966b; Schmolesky et al., 2002; Ohtsuki et al., 2009), and therefore does not have easy access to information encoded in the population. Note that in theory, a Purkinje cell could receive information about activation of neighboring CFs through spillover mechanisms (Szapiro and Barbour, 2007; Mathews et al., 2012), but this possibility will not be considered further in this paper. Instead, we will discuss alternative ways to enhance the information capacity of individual olivary neurons, using mechanisms that challenge the conventional view that all CF signals are created equal.

3.5 Modulation of the Pre-Synaptic Climbing Fiber Burst

New discoveries about the spike-generating mechanisms of olivary neurons are challenging conventional wisdom about the way CFs encode information. As noted earlier, CFs fire in brief high-frequency bursts, comprising 1–6 spikes separated from each other by 2–3 ms (Crill, 1970; Armstrong, 1974; Mathy et al., 2009). The burst is generated in the olivary axon itself, as a result of an intrinsic positive feedback loop (Mathy et al., 2009): the first spike is initiated in the axon, but it also backpropagates into the dendrites where it opens high-voltage-activated calcium channels that cause a prolonged depolarization lasting up to 10 ms. When this depolarization reaches the axon, it triggers the rest of the spikes in the burst.

At first glance, this seemingly automatic and self-driven burst mechanism appears to fit well with the “all-or-nothing” character of the CF response to brief olivary stimulation (Crill, 1970), which was mentioned earlier and is characterized by a single burst of spikes that varies little whether the initial depolarization is just above threshold

or much stronger (Figure 1B1). However, it is known that the processes underlying spike generation and dendritic depolarization are both influenced by a variety of factors, including the resting potential of the inferior olivary neuron (Llinas and Yarom, 1981; Ruigrok and Voogd, 1995). This opens up the possibility that information may be transmitted by modulating the number of spikes in the CF burst.

Indeed, the era of the “all-or-nothing” CF may be coming to an end. Recent studies have shown that the burst size, i.e., the number of spikes in the CF burst, is tightly regulated and provides extra information not available in the conventional binary signal (Maruta et al., 2007; Mathy et al., 2009; Bazzigaluppi et al., 2012; De Gruijl et al., 2012). For example, burst size is correlated with a number of critical parameters which together define the state of olivary neurons. These cells have a characteristic subthreshold membrane potential oscillation which is synchronized across neighboring olivary neurons via gap junctions (Lampl and Yarom, 1993, 1997; Devor and Yarom, 2002; Leznik and Llinas, 2005). It has been shown that the number of spikes in the CF burst varies systematically according to the phase of the oscillation *in vitro* (Mathy et al., 2009), the amplitude of the oscillation *in vivo* (Bazzigaluppi et al., 2012), and the extent of electrotonic coupling and synchrony in a computer model of the olivary network (De Gruijl et al., 2012). In addition, burst size can be used to distinguish between spontaneous and sensory-related CF signals evoked by sinusoidal whole-field visual stimulation (Maruta et al., 2007). This last study also found that the number of spikes in the CF burst varied systematically depending on the direction of the visual stimulus.

The findings of the studies mentioned in the preceding paragraph must be interpreted with some caution. As was also the case in previous experiments (Eccles et

al., 1966; Armstrong and Rawson, 1979), the number of spikes per CF burst was quite variable from one burst to the next and always fell within the same limited range (1–6 spikes), regardless of condition or behavioral state. Therefore, the changes in burst size for any given situation were small (<1 spike per burst) and could only be detected in the average as a slight probability bias toward generating more bursts with many (>4) or few (1) spikes. It remains to be seen whether such a fickle modulation of the CF-burst signal could play a functional role during motor learning, perhaps by regulating the induction of plasticity in the post-synaptic Purkinje cell (Mathy et al., 2009). Nonetheless, these groundbreaking experiments have demonstrated that the number of spikes in the CF burst is not entirely random and can thus provide parametric information not available in a binary code.

Figure 1C illustrates a straightforward way to encode a graded instructive signal by systematically modulating the number of spikes in the CF burst, e.g., 2 spikes for “no instruction” due to spontaneous activation, 3 for “lift right foot a little,” and 4 for “lift right foot a lot.” Clearly, this example is an oversimplification. In reality, codes based on burst size would be inherently noisy because as mentioned above, the number of spikes in the CF burst is subject to stochastic variations within a limited range. However, the information capacity of an individual CF would still be enhanced under conditions in which burst size is probabilistic and only slightly biased one way or another depending on the parametric details of the instruction. A similar proposal for encoding parametric information in the CF system was formulated on theoretical grounds almost 40 years ago (Gilbert, 1974).

One advantage of the code in Figure 1C1 is that it can be unambiguously read-out because a difference of just one spike in the CF burst has a substantial impact on the response evoked in the post-synaptic Purkinje cell. In the dendrites, burst size regulates the duration of the depolarizing plateau potential (Campbell et al., 1983a), the number of calcium spikes (Mathy et al., 2009), and the ability of the CF input to induce plasticity (Mathy et al., 2009; Figure 1C4). With regards to Purkinje cell output, burst size has a strong influence on both the number of CS-related spikes that are sent down the axon (Mathy et al., 2009), and the duration of the characteristic pause in simple spike activity that follows the CS (Mathy et al., 2009; Figure 1C5).

3.6 Modulation of the Post-Synaptic Climbing Fiber Response

It is often overlooked that the same groundbreaking paper that coined the term "all-or-nothing" to describe the Purkinje cell CS also made it very clear that the excitatory post-synaptic potential (EPSP) evoked after activation of the CF input could itself be graded (Eccles et al., 1966a): the size of the EPSP was shown to depend critically on the membrane potential. This observation has important implications for the coding of instructive signals in Purkinje cells, particularly as it pertains to the regulation of CF-evoked calcium influx in the dendrites.

Activation of the CF input causes a massive depolarization of the proximal dendrites of the Purkinje cell (Eccles et al., 1966a), triggering regenerative calcium spikes that propagate and cause calcium influx throughout the dendritic tree (Ross and Werman, 1987), including the terminal spiny branchlets (Konnerth et al., 1992; Miyakawa et al., 1992), where the excitatory parallel fiber (PF) synapses are located

(Figure 1A; cyan). Dendritic calcium is the trigger for a wide variety of short-term (Batchelor and Garthwaite, 1997; Glitsch et al., 2000; Brenowitz and Regehr, 2003; Maejima et al., 2005; Rancz and Hausser, 2006) and long-term (Sakurai, 1990; Konnerth et al., 1992; Kano et al., 1996; Hansel and Linden, 2000; Miyata et al., 2000; Wang et al., 2000; Coesmans et al., 2004; Tanaka et al., 2007) mechanisms of plasticity in Purkinje cell synapses, and for this reason it is considered the neural implementation of behaviorally driven instructive signals at the most fundamental molecular level (for reviews, see (Hansel et al., 2001; Gao et al., 2012).

What is important about the CF-triggered dendritic calcium signal from a neural coding perspective is that just like the evoked EPSP, its amplitude can be modulated *in vitro* (Miyakawa et al., 1992; Midtgaard et al., 1993; Callaway et al., 1995; Wang et al., 2000) and *in vivo* (Kitamura and Hausser, 2011) by a variety of factors that influence the membrane potential of the Purkinje cell. For example, activation of inhibitory synapses from molecular layer interneurons (Figure 1A; green) causes a conductance shunt that reduces the amplitude of the CF-triggered calcium signal (Callaway et al., 1995). Conversely, dendritic calcium influx is significantly enhanced if the CF input is preceded by stimulation of the excitatory PF pathway (Wang et al., 2000), which by itself causes a small graded calcium response via activation of voltage-gated calcium channels as well as metabotropic receptor-dependent release from intracellular stores (Eilers et al., 1995; Takechi et al., 1998).

Figure 1D illustrates a straightforward way to encode a graded instructive signal by systematically modulating the amplitude of the CF-triggered calcium response in the Purkinje cell dendrites. The three signals corresponding to “no instruction” due to

spontaneous activation of the CF input, “lift right foot a little” and “lift right foot a lot” are associated with progressively increasing levels of PF excitation (Figure 1D3), and as a result, they are encoded in the dendrite as progressively larger calcium responses (Figure 1D4). Note that in this example there is a parallel systematic modulation of the characteristic post-CF pause in Purkinje cell activity (Figure 1D5), which is consistent with the recently described effect of extra dendritic calcium spikes on somatic spiking (Davie et al., 2008). On the other hand, the CS itself provides no parametric information about the instruction because it is the same regardless of the context in which the CF was activated (Figure 1D5). This is consistent with previous work demonstrating that the burst pattern of the CS is largely unaffected by dendritic events because the CF input causes a functional division between dendritic and axosomatic compartments (Davie et al., 2008).

We have made one key assumption in Figure 1D: the instructive signal that activates the CF input also activates some of the PF synapses on the same Purkinje cell. In other words, our proposal requires a high degree of spatial convergence in the cerebellar cortex: PF’s and CFs inputs representing the same type of information must come together at the level of individual Purkinje cells.

The field is currently divided with regards to this “convergence” hypothesis (Apps and Garwicz, 2005). Previous studies have provided irrefutable evidence that the CF receptive field of an individual Purkinje cell matches that of the mossy fibers located in the granular layer directly underneath (Garwicz et al., 1998; Brown and Bower, 2001; Voogd et al., 2003; Odeh et al., 2005; Pijpers et al., 2006; Apps and Hawkes, 2009). What is less clear is whether this vertically aligned spatial organization would result in

the Purkinje cell receiving the CF signal together with excitatory input from mossy fiber-driven PF's (Cohen and Yarom, 1998; Brown and Bower, 2001); Figure 1D), or with inhibitory input from mossy fiber-driven molecular layer interneurons ((Ekerot and Jorntell, 2001; Ekerot and Jorntell, 2003) Figure 1E). Based on classic work (Eccles and et al., 1967; Eccles et al., 1972; Eccles, 1973), as well as more recent studies using *in vivo* imaging of peripherally evoked inhibitory responses in the cerebellar cortex (Gao et al., 2006) or patchy photostimulation of granule cells *in vitro* (Dizon and Khodakhah, 2011), we think both scenarios are possible. We suspect that the levels of local excitatory and inhibitory input may differ between groups of Purkinje cells, depending on their precise location relative to the activated PF's. This raises the intriguing possibility that the mossy fiber pathway may be used to set the membrane potential of the Purkinje cell, and in this way adjust the efficacy of CF-related instructive signals.

3.7 Epilog: CF-Driven Plasticity in Purkinje Cells

Our paper highlights how graded modulation of individual CF inputs may be used for encoding parametric information about instructive signals. But to really understand the role of CFs in motor learning, we must first answer one fundamental question: if CFs are the "teachers," who might the students be and what do they learn? In "A theory of cerebellar cortex," Marr predicted that CFs would teach by modifying the strength of excitatory PF synapses (Figure 1A; cyan). Immediately after the publication of his revolutionary theory, Marr himself worked with Eccles on this topic, but "failed to discover any significant modification even after some hundreds of parallel fiber-climbing fiber inputs" (Eccles, 1973). This initial failure did not stop others from trying to induce plasticity by stimulating CFs with more physiological patterns. More than a decade later,

Masao Ito would become the first person to demonstrate CF-dependent long-term depression (LTD) of PF synapses (Ito and Kano, 1982). Since then, research about cerebellar plasticity has exploded (Gao et al., 2012). We now know that CFs can trigger a variety of long-term modifications in PF synapses (Figure 1A; cyan; (Ito and Kano, 1982), in molecular layer interneuron synapses (Figure 1A; green; (Kano et al., 1992; Duguid and Smart, 2004; Mittmann and Hausser, 2007), and even in the CF synapse itself (Figure 1A; red; (Hansel and Linden, 2000; Bosman et al., 2008; Ohtsuki and Hirano, 2008). The functional significance of these plasticity mechanisms remains largely unknown. We can only imagine that in contrast to the conventional "all-or-nothing" instructive CF input, the type of graded CF signals we have described here could provide an extra degree of flexibility for choosing carefully who the students are and what to teach them.

Acknowledgments

We are grateful to K. Ohmae and J. Chin for help with the figure and to S. Wang for helpful discussion. Work supported by grant R01MH093727 from the National Institutes of Mental Health to Javier F. Medina.

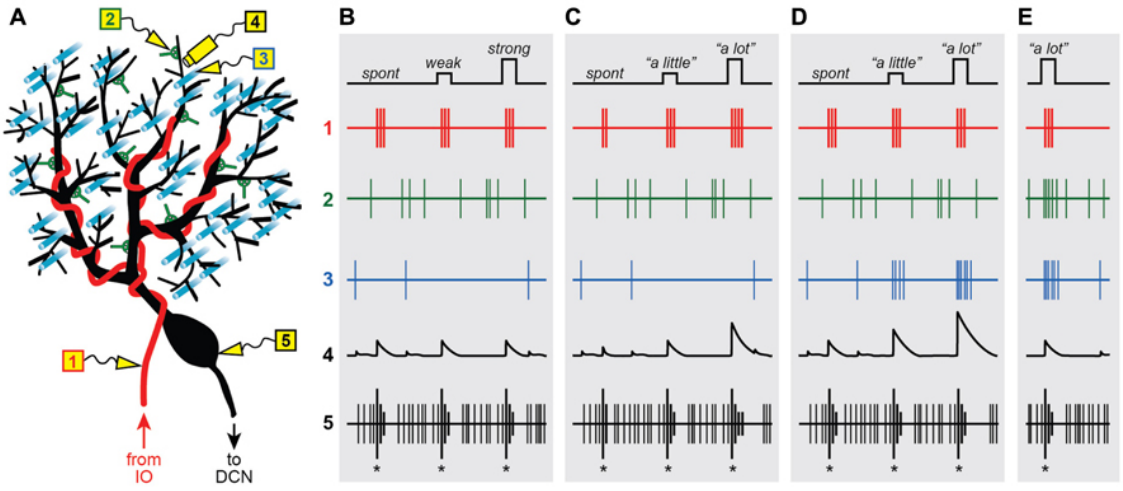

Figure 3-1 Graded instructive signals in a Purkinje cell

(A) A schematic diagram of a Purkinje cell and its different synaptic inputs. Electrodes are placed in different locations to measure the extracellular spiking activity of the climbing fiber (1; red), a molecular layer interneuron (2; green), a parallel fiber (3; cyan) and the Purkinje cell axon (5; black). In addition, intracellular calcium signals are imaged in one of the Purkinje cell's distal dendrites (4; black), near electrodes 2 and 3. **(B–E)** Spikes and calcium signals measured in the five locations shown in (A), under four different scenarios: when all climbing fiber signals are "all-or-nothing" whether firing is spontaneous (spont) or when the strength of stimulation in the inferior olive is weak or strong (B), when instructive signals to lift the foot "a little" or "a lot" influence the number of spikes in the climbing fiber burst (C), or when the instructive signals activate the climbing fiber simultaneously with parallel fiber inputs (D) and input from the molecular layer interneurons (E).

CHAPTER 4:

Sensory-driven enhancement of calcium signals in individual Purkinje cell dendrites of awake mice

Farzaneh Najafi[1], Andrea Giovannucci[2], Samuel S.-H. Wang[2], Javier F. Medina[3]

[1]Department of Biology, University of Pennsylvania, Philadelphia, PA 19104, USA

[2]Department of Molecular Biology and Princeton Neuroscience Institute, Princeton University, Princeton, NJ 08544, USA

[3]Department of Psychology, University of Pennsylvania, Philadelphia, PA 19104, USA

Cell Reports. 2014 Mar 13;6(5):792-8

4.1 Abstract

Climbing fibers are thought to contribute to cerebellar plasticity and learning by triggering a large influx of dendritic calcium in the postsynaptic Purkinje cell to signal the occurrence of an unexpected sensory event. However, climbing fibers fire about once per second whether or not an event occurs, raising the question of how sensory-driven signals might be distinguished from a background of ongoing spontaneous activity. Here we report that in Purkinje cell dendrites of awake mice, climbing fiber-triggered calcium signals are enhanced when the trigger is a sensory event. In addition, we show that a large fraction of the total enhancement in each Purkinje cell dendrite is driven by an additional boost of calcium provided by sensory activation of a non-climbing fiber input.

We suggest that sensory stimulation may enhance dendritic voltage and calcium in Purkinje cells to increase the strength of plasticity signals during cerebellar learning.

4.2 Introduction

Calcium is the trigger for cellular mechanisms of plasticity in many neurons throughout the brain and as such, it is thought to play a central role during learning and memory formation (Zucker, 1999; Sjostrom and Nelson, 2002). For Purkinje cells (PCs) of the cerebellar cortex, the job of generating the calcium signals necessary for plasticity and learning is often attributed to the powerful climbing fiber (CF) input (Thach et al., 1992; Raymond et al., 1996; Simpson et al., 1996; De Zeeuw et al., 1998; Ito, 2013). This is because in many learning tasks, CFs seem to play the role of “teachers” by firing a burst of action potentials to signal that an unexpected sensory event has occurred (Gilbert and Thach, 1977; Kitazawa et al., 1998; Raymond and Lisberger, 1998; Medina and Lisberger, 2008; Rasmussen et al., 2008; Soetedjo et al., 2008b). In turn, the CF burst produces a strong depolarization of the post-synaptic PC and causes a calcium-based dendritic spike that serves as the trigger for a variety of plasticity mechanisms (Schmolesky et al., 2002; Kitamura and Kano, 2013). In this paper, we use calcium imaging of PC dendrites in awake mice to resolve a long-standing question about the way CF inputs encode information and generate plasticity signals in the cerebellum.

It was pointed out 40 years ago that from the perspective of an individual PC, CF signals are potentially ambiguous (Gilbert, 1975). In the adult cerebellum each PC receives input from a single CF (Ito, 1984), and every CF fires bursts of action potentials spontaneously at a rate of about once per second *in vivo* (Ito, 1984). Furthermore, early

investigators demonstrated that because CF bursts are “all-or-nothing” (Crill, 1970), they evoke the same electrical response in the soma of the postsynaptic PC (i.e. a complex spike), regardless of whether the CF input fired spontaneously or in response to a sensory event (Eccles et al., 1966b). These classic electrophysiology studies have led to the current view of cerebellar learning, in which individual CF bursts are equivocal and for this reason, information about sensory-driven instructive signals must be accumulated by collecting the responses to CF inputs over many learning trials or many PCs (Houk et al., 1996; Mauk and Donegan, 1997; Gibson et al., 2004; Ozden et al., 2009; Schultz et al., 2009).

Our experiments challenge the classical view that spontaneous and sensory-driven CF inputs are equivalent. This view does not take into account that the somatic and dendritic compartments of the PC are functionally separate and process CF signals independently during synaptic activation (Llinas and Sugimori, 1980; Davie et al., 2008). Therefore, we designed our experiments to test whether spontaneous and sensory-driven CF inputs are different from each other, not by recording the electrical complex spike response near the PC soma as in previous work (Eccles et al., 1966b), but by measuring CF-triggered calcium spikes and visualizing dendritic plasticity signals directly.

4.3 Material and Methods

Animal preparation. Experimental procedures were approved by the Princeton University Institutional Animal Care and Use Committee and performed in accordance with the animal welfare guidelines of the National Institutes of Health. C57BL/6J mice 8-

14 weeks old were anesthetized with isoflurane and a small craniotomy was made over the cerebellum. A coverslip with a pre-molded Kwik-Sil plug was placed on the exposed brain and held in place by a two-piece headplate. On the following day, animals were anesthetized with isoflurane and a calcium indicator or viral construct was injected in the cerebellar cortex (2-3 injections, ~300 nl, 150-200 microns below the dura surface). The injections contained either the calcium indicator Oregon Green BAPTA-1/AM (OGB-1/AM) or a combination of AAV2/1.CMV.PI.Cre.rBG and AAV2/1.CAG.Flex.GCaMP6f.WPRE.SV40 (U. Penn. Vector Core). Hyperosmotic D-mannitol (15% in PBS) was given IP ~15 min before virus injection to reduce toxicity associated with AAV injections and GCaMP6f overexpression.

Two-photon imaging. Imaging was performed immediately after animals recovered from anesthesia for OGB-1/AM injections, or after 7-10 days for AAV injections. Mice were head-fixed on top of a cylindrical treadmill while airpuff stimuli (30 ms, 20-50 psi) were delivered through a blunted hypodermic needle pointed at the ipsilateral eye (~4 s inter-trial interval, ~35 trials/experiment). Fluorescence signals were acquired with a custom-built two-photon microscope that collected data as movies of 32x128 pixels (64 ms/frame). Dendritic calcium spikes were detected with a three-step process as described before (Ozden et al., 2012): (1) Pixels corresponding to individual dendrites were determined with an algorithm that uses the independent spatial components estimated by PCA/ICA, (2) the fluorescence trace ($\Delta F/F$) of a PC dendrite was computed as $(F-F_b)/F_b$, where F is the mean fluorescence intensity of the pixels contributing to a dendrite in each frame, and F_b is the baseline defined as the lowest 8th percentile of all fluorescence values within a 1-sec window surrounding each frame, (3) calcium spikes

were detected by examining the fluorescence trace for each dendrite frame by frame using a template-matching algorithm and setting a threshold. Essentially, this algorithm identifies transient increases in fluorescence with the characteristic temporal profile of CF-triggered calcium spikes and a peak amplitude larger than a threshold value.

GCaMP6f cell specificity. In order to quantify the cellular origin of the signal recorded in the molecular layer, we estimated the expression density of Purkinje cells (PCs), molecular layer interneurons (MLIs) and granule cells (GCs). In vivo, within GCaMP6f expressing zones, visible structures were counted up to the maximum optical penetration depth of 260 μm and compared with published total density values (Sturrock, 1989). We found 13.6±0.8 stained PCs per 10^4 μm^2 (76% of all estimated PCs; mean±s.e.m, n=3), 6.0±1.3 dimly stained MLIs per 10^6 μm^3 (7% of all estimated MLIs; mean±s.e.m, n=5), and no GCs with brightness >2.5% of the average PC brightness (n=5). MLI and GC visibility in vivo is dependent on the animal's behavioral state (Ozden et al., 2012); therefore, we repeated our measurements in fixed brain slices (n=3), which are optically more uniform and in which calcium concentrations are expected to be uniformly high, we found that 75% of PCs were visible, 7% of MLIs were visible at 40% the brightness of PCs, and 1.1% of GCs were visible at 6% the brightness of PCs. In summary, the relative fraction of PC: MLI: GC expression was 1:0.09:0.01 with a relative brightness of 1:0.4:0.01, indicating that more than 95% of the signal in the molecular layer arises from PC dendrites. In the selected ROIs, which include PC dendrites only, we expect a much higher value.

Analysis of calcium signals. All $\Delta F/F$ traces, except for those shown in Figures 1C and 1D, were normalized for each dendrite separately such that the peak value of the

average spontaneous calcium spike was '1'. To limit the analysis to single CF inputs, we removed segments of the fluorescence trace containing more than one calcium spike separated from each other by less than 100 ms (doublets or multiples). Trials with a single calcium spike in a 50-150 ms interval after the periocular airpuff were used for the analysis of evoked calcium spikes. Trials without any calcium spikes in this interval were used for the analysis of the non-CF signal. The size of each individual calcium spike was computed by taking the integral of the normalized $\Delta F/F$ signal in a 100 ms window starting at the peak ("$\Delta F/F$-integral"). The size of the non-CF signal was measured similarly, by taking the integral of the normalized $\Delta F/F$ signal in a 100 ms window starting at a point selected randomly within 50-150 ms of the periocular airpuff. See also Figure S1.

ROC analysis. True-positive rate (TPR) and false-positive rate (FPR) were computed under the assumption that the amplitude of evoked calcium spikes is larger than the amplitude of spontaneous spikes. TPR was calculated as the fraction of evoked spikes that would have been correctly identified because their amplitude was bigger than the criterion, and FPR was calculated as the fraction of spontaneous spikes that would have been incorrectly identified because their amplitude was bigger than the criterion.

4.4 Results

We used two-photon microscopy to image spontaneous and sensory-driven calcium spikes triggered by activation of the CF input to individual PC dendrites. Awake mice were head-fixed on top of a cylindrical treadmill while we delivered periocular airpuffs via a needle pointed toward the eye (Figure 1A). We imaged 13 locations in 5

mice and found CF-triggered calcium spikes in response to the periocular airpuff in a total of 76 PCs distributed broadly within three separate zones of cerebellar cortex (Figure 1B): vermis of lobule VI and paravermis of lobule IV/V and VI.

As in earlier imaging studies (Sullivan et al., 2005; Ozden et al., 2008), PC dendrites appeared as elongated structures separated from each other by 5-10 μm (Figures 1C and 1D, top). We used two different fluorescent calcium indicators with complementary advantages: OGB-1/AM (Figure 1C), a fast-responding synthetic indicator that can be bulk-loaded and is taken up by a variety of cell types in the cerebellar cortex (Sullivan et al., 2005), and GCaMP6f (Figure 1D), a genetically-encoded calcium indicator with slower kinetics that allows a much higher level of cell-type-specific expression (Figures 1E and 1F; see Experimental Procedures). With GCaMP6f, we observed labeled PCs at an average density of 13.6 ± 1.4 cells per 10^4 μm^2 cortical surface area, an estimated 76% of all PCs (percentages calculated in comparison with cell densities reported in (Sturrock, 1989). In comparison, other cell types were sparser and dimmer: 7% of molecular layer interneurons (MLIs) were visible at an average of 0.4 times the brightness of PC dendrites, and 1% of granule cells (GCs) were visible at 0.06 times the brightness of PC dendrites. Thus, under our expression conditions nearly all the GCaMP6f signal in molecular layer neuropil arises from PC dendrites, even before identification of regions of interest (ROIs).

Calcium spikes in individual PC dendrites were apparent as a rapidly-rising transient increase in the fluorescence signal (Figures 1C and 1D, bottom). We have shown previously that these dendritic calcium spikes are generated when the CF input fires and generates a complex spike (CS) in the PC (Ozden et al., 2008). Our imaging

tools and template-and-threshold algorithm can detect approximately 95% of all CSs with less than an 8% false-positive rate (Ozden et al., 2008). In PC dendrites, calcium spikes occurred at the expected spontaneous rate of once per second (Figures 1C and 1D, blue dots; rate=0.90±0.25 Hz, mean±s.d.), and also in response to periocular airpuff stimulation (Figures 1C and 1D, red dots; response probability=0.58±0.24, mean±s.d.). We termed these events spontaneous and evoked calcium spikes, respectively.

Sensory-driven enhancement of calcium spikes in a representative dendrite

Figure 2 shows data for an example PC dendrite in a GCaMP6f experiment. The average evoked calcium spike (Figure 2A, red; 27 spikes) was larger in amplitude than the average spontaneous calcium spike (Figure 2A, blue; 65 spikes; difference between evoked and spontaneous shown in black). Note that all fluorescence traces have been normalized so that the peak of the average signal for spontaneous calcium spikes in the PC is '1' (see Experimental Procedures). As an index of the size of the calcium spike we computed the integral of each normalized fluorescence signal in the 100 ms window following its peak (Figure 2A; "integral"). We will refer to this quantity as ΔF/F-integral. In the example shown, the ΔF/F-integral of the calcium spike was on average 50% larger for evoked vs. spontaneous events (Figure 2B; red vs. blue, Kolmogorov-Smirnov test, $P<0.001$).

Next, we used receiver-operating-characteristic (ROC) analysis to quantify the degree to which the ΔF/F-integral of the calcium spike was sufficient to distinguish sensory-evoked from spontaneous signals (see Experimental Procedures). The ROC curve (Figure 2C) was constructed by sliding the value of a discriminability criterion

along the horizontal axis in Figure 2B. For each value of the criterion, we plotted a point in the ROC curve with coordinates (FPR, TPR), where FPR is the false-positive rate (i.e. fraction of calcium spikes in the spontaneous distribution whose ΔF/F-integral is bigger than criterion), and TPR is the true-positive rate (i.e. fraction of calcium spikes in the evoked distribution whose ΔF/F-integral is bigger than criterion). The area under the ROC curve provides a standard measure of % correct in a two-alternative discrimination task (Green and Swets, 1966). In the example dendrite, the area under the ROC curve was 76% (Figure 2C; gray shaded area), indicating that for each pair of calcium spikes randomly drawn, one from the evoked and one from the spontaneous distributions (Figure 2B), the spike with the larger ΔF/F-integral would be sensory-evoked in 76% of cases. In comparison, identical spontaneous and evoked distributions would give an ROC area of 50% (dotted diagonal, Figure 2C).

Population analysis

Evoked calcium spikes were bigger than spontaneous calcium spikes in nearly all PC dendrites we examined, both in experiments using OGB-1/AM (Figures 3A-3C; n=33/35 dendrites) and in experiments using GCaMP6f (Figures 3D-3F; n=40/41 dendrites). This enhancement was apparent in the population difference trace (Figures 3A and 3D), which was obtained by averaging the difference between evoked and spontaneous traces across all dendrites. Note that the fluorescence signal of each individual dendrite was first normalized separately as before and as a result, the difference traces shown in Figures 3A and 3D are relative to the average size of spontaneous calcium spikes. The ΔF/F-integral for evoked spikes was on average 32±20% larger than for spontaneous spikes in OGB-1/AM experiments (Figure 3B, red

circle; mean±s.d.), and 41±24% larger in GCaMP6f experiments (Figure 3E, red circle; mean±s.d.). This sensory-driven enhancement was statistically significant (two-sample Kolmogorov-Smirnov test, $p<0.05$) for 69% of OGB-1/AM-labeled dendrites and 73% of GCaMP6f-expressing dendrites (Figures 3B and 3E; black circles). ROC analysis (Figures 3C and 3F) showed that sensory-evoked and spontaneous calcium spikes could be discriminated above chance level in most dendrites (median %correct is 81% in Figure 3C and 73% in Figure 3F). The small mismatch between the two calcium indicators is consistent with the known nonlinearity of GCaMP6f (Chen et al., 2013), which would tend to differentially amplify calcium spikes depending on the baseline level and cause greater variability in $\Delta F/F$ values.

Sensory-driven calcium signals in trials without CF-triggered calcium spikes

In addition to the CF input, PC dendrites receive input from granule cells and molecular layer interneurons (Ito, 1984), both of which are capable of modulating the amplitude of the CF-triggered calcium spike (Callaway et al., 1995; Wang et al., 2000; Kitamura and Hausser, 2011). To assess the role of non-CF inputs, we examined the same population of dendrites as in Figure 3 but this time we analyzed the fluorescence signal in trials without a detectable sensory-driven calcium spike. The average fluorescence signal in these trials revealed a small but clear rise of dendritic calcium in response to the periocular airpuff stimulus, both for OGB-1/AM (Figure 4A, left; green trace) and GCaMP6f experiments (Figure 4A, right; green trace). For direct comparison with traces in previous figures, we have normalized the fluorescence signals in Figure 4A exactly as before (i.e. ‘1’ represents the average peak of the spontaneously evoked calcium spikes, computed for each dendrite separately). These signals were not

detected as calcium spikes by our template-matching-and-threshold algorithm because they were much smaller (Figure 4A, Figure S1) and much slower (rise time is 154±48 vs. 10±3ms for calcium spikes; mean±s.d., two-sample Kolmogorov-Smirnov test, $p<0.0001$).

We refer to the fluorescence signal in Figure 4A as the non-CF calcium signal because it was measured in trials without a detectable calcium spike. We have previously shown that our algorithm for identifying calcium spikes detects nearly all complex spikes correctly (Experimental Procedures; (Ozden et al., 2008), which means that the lack of a detectable calcium spike in any given trial can be taken as a reliable indicator that the periocular airpuff failed to activate the CF input. In our experiments, approximately 40% of all trials did not show a sensory-driven calcium spike, consistent with the low CF response probability to peripheral stimulation reported in past studies (Eccles et al., 1972; Gilbert and Thach, 1977; Kitazawa et al., 1998; Medina and Lisberger, 2008; Soetedjo et al., 2008a; Ozden et al., 2012). Nonetheless, spike detection is not perfect and some CF events were probably missed. To reduce the number of missed CF events we lowered the threshold for detecting calcium spikes by as much as 50% (Figure S2). Under this condition, we still observed a sensory-driven non-CF signal (Figure S2C), which indicates that the non-CF signal is unlikely to arise from small CF-triggered calcium spikes that our algorithm might have failed to detect.

A potential source of the non-CF calcium signal in a PC dendrite is neighboring CF inputs to nearby PCs, which could contribute either by providing a source of diffuse fluorescence signal, or by spillover-mediated effects (Mathews et al., 2012; Coddington et al., 2013). To test for these potential contributions, we examined the non-CF signals

of individual PC dendrites in trials in which the periocular airpuff failed to evoke calcium spikes in the two nearest dendrites. Relative to the size of spontaneous calcium spikes, the average ΔF/F-integral of the non-CF signal was 28±17% in trials with calcium spikes in adjacent dendrites, and 27±22% in trials without (mean±s.d; two-sample Kolmogorov-Smirnov test, p=0.7). Thus, our results demonstrate that sensory events are capable of triggering a measurable rise of calcium in the PC dendrite in the absence of any CF activation in the immediately adjacent neuropil, suggesting that spillover effects do not make a major contribution. However, a contribution from more distant CFs cannot be entirely ruled out (Coddington et al., 2013).

The average non-CF signal (Figure 4A; green) was similar in its magnitude and time course to the difference signal previously shown in Figures 3A and 3D (re-plotted for comparison in Figure 4A; dashed line). This suggests that the non-CF signal and the sensory-driven enhancement of the calcium spike might share a common origin. We evaluated this possibility further in a subset of dendrites with significant enhancement and enough trials with and without sensory-driven calcium spikes (13 dendrites for OGB-1/AM and 11 for GCaMP6f experiments). In many of these dendrites, the average ΔF/F-integral of the non-CF signal (Figure 4B, green; error bars, s.e.m.) was comparable to the average ΔF/F-integral of the difference signal (Figure 4B, black). Indeed, the two signals were significantly different from each other in only 1 of the 24 dendrites (Figure 4B, asterisk). On average, we found that the non-CF signal could account for 76% of the total sensory-driven enhancement of the calcium spike (Figure 4B), consistent with the hypothesis that the majority of enhancement in CF trials arose from non-CF sources.

4.5 Discussion

We have demonstrated that calcium spikes in individual Purkinje cell (PC) dendrites are significantly larger when the climbing fiber (CF) input fires in response to an instructive stimulus than when it fires spontaneously. As revealed by our ROC analysis, this sensory-driven enhancement of the calcium spike could potentially be used to tag the occurrence of unexpected sensory events, thus allowing an individual PC to distinguish instructive signals from ongoing background activity.

The mechanisms underlying the sensory-driven enhancement of the dendritic calcium spike are currently unknown. One possibility is that sensory stimuli like periocular airpuffs drive the enhancement by directly amplifying signals along the CF pathway itself. For example, recent work has shown that certain types of vestibular/visual stimulation can increase the number of action potentials within a single (~10 ms) CF burst (Maruta et al., 2007), which is known to enhance the PC dendritic depolarization and result in more calcium entry (Mathy et al., 2009). Similarly, delivery of an unexpected periocular airpuff may recruit arousal centers like the locus coeruleus which could potentiate CF signals by releasing noradrenaline in the cerebellar cortex (Moises et al., 1981). However, in cerebellar slices the direct application of noradrenaline decreases the probability of release at the CF synapse and reduces the amplitude of CF-triggered calcium spikes (Carey and Regehr, 2009).

Our findings suggest an additional mechanism for enhancing dendritic calcium signals that is based on sensory-driven activation of a non-CF input, possibly via the mossy fiber (MF) pathway to the cerebellar cortex. This hypothesis is consistent with

previous work showing that the amplitude of the CF-triggered calcium spike depends on the membrane potential of the PC dendrite (Kitamura and Hausser, 2011), and can be regulated by two types of MF-driven inputs to the PC: inhibitory inputs from molecular layer interneurons (MLIs) (Callaway et al., 1995), and by excitatory inputs from the parallel fibers (PFs) of granule cells (Wang et al., 2000). Additional evidence supporting a contribution of the MF pathway comes from extracellular recording studies which have demonstrated that cutaneous stimulation of the limb can activate PF, MLI and CF inputs converging on the same PC (Eccles et al., 1972; Ekerot and Jorntell, 2003; Apps and Garwicz, 2005).

It is of note that in previous electrophysiological studies, MF and CF convergence usually results in sensory-driven suppression of somatic PC spiking at the time of the CF input (Eccles et al., 1972; Ekerot and Jorntell, 2003), whereas we only found reliable enhancement of CF-triggered dendritic calcium spikes. This unexpected finding may reflect inherent differences in how synaptic inputs are processed to independently generate electrical signals in the PC soma and calcium signals in the dendrites (Llinas and Sugimori, 1980; Denk et al., 1995; Wang et al., 2000; Davie et al., 2008), and could be explained if spiking were influenced by factors such as somatic inhibition that come downstream of dendritic integration. Another difference is that we used periocular airpuff stimuli which are rare and unexpected sensory events, whereas previous studies used cutaneous stimulation of hindlimb or toes which are frequently experienced events during self-generated movements and have presumably resulted in depressed PF synapses and potentiated MLI inputs (Ekerot and Jorntell, 2003). Indeed, CFs appear to be particularly sensitive to this type of contextual modulation because they respond

much more reliably to peripheral stimulation when it is unexpected than when it can be anticipated (Apps, 1999; Ozden et al., 2012).

Our findings have important implications for theories of cerebellar learning. In the prevailing view, instructive signals are encoded at the level of an individual PC as all-or-nothing calcium spikes that are triggered once for every CF firing event, whether spontaneous or in response to an unexpected sensory event (Houk et al., 1996; Kitamura and Hausser, 2011; Najafi and Medina, 2013). Our results challenge this view in two ways. First, we have shown that the amplitudes of sensory-driven and spontaneous calcium spikes are significantly different from each other. Second, we found that sensory stimulation causes a small rise of dendritic calcium in the PC dendrite even when its CF input does not fire, consistent with the idea that instructive signals may be relayed to the cerebellar cortex via multiple pathways, including both the MF and CF pathways (Raymond et al., 1996).

In the cerebellum, short- and long-term synaptic modification of PC inputs is tightly regulated by the precise amplitude and duration of the dendritic calcium signal (Gao et al., 2012). For example, PF-PC plasticity is steeply dependent on calcium concentration (Tanaka et al., 2007), and small variations in dendritic calcium are sufficient to differentially drive either long-term potentiation or long-term depression (Coesmans et al., 2004). Our observations reflect both differences in PC dendritic depolarization and in the ensuing amount of calcium entry in response to single sensory events in contrast to spontaneous conditions. Thus, the type of sensory-driven enhancement of the calcium spike reported here may help modulate the efficacy of the CF input to serve as an instructive signal and drive plasticity and learning.

Acknowledgements

FN and AG developed analysis tools, established the behavioral and imaging setup and performed the experiments in the laboratory of SW. FN, AG and JM analyzed the data, and prepared the figures. FN and JM wrote the first draft of the manuscript. FN, AG, SW, and JM designed experiments and edited the manuscript. We thank A. Kloth for help with eyelid acquisition software, and I. Ozden and D. Dombeck for help with imaging in awake mice. This work was supported by grants to JM (Searle Scholars Program, NIH R01 MH093727), AG (New Jersey Commission on Brain Injury Research CBIR12FE1031), and SW (NIH R01 NS045193, W.M. Keck Distinguished Young Investigator, NIH RC1 NS068414). The authors declare no competing financial interests.

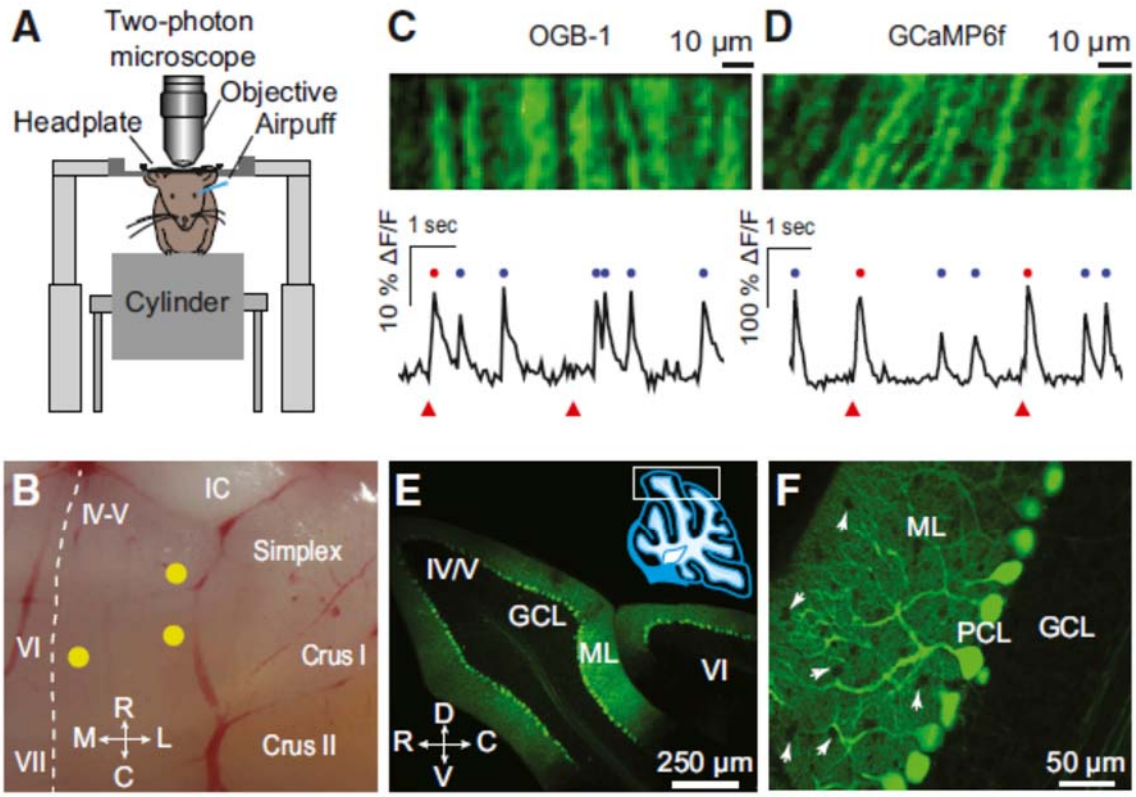

Figure 4-1 Imaging calcium spikes in PC dendrites of awake mice

(A) Two-photon microscopy of cerebellar cortex in awake mice, head-fixed on a cylindrical treadmill. Airpuff stimuli were delivered to the ipsilateral eye. **(B)** Imaged locations in cerebellar cortex (yellow circles). Dashed line indicates the midline. **(C)** Top: field of view showing PC dendrites in an example OGB-1/AM experiment. Bottom: an example fluorescence trace representing spontaneous (blue dots) and sensory-evoked (red dots) calcium spikes in response to periocular airpuff stimuli (triangles). **(D)** Same as (C), for an example GCaMP6f experiment. **(E, F)** Expression of GCaMP6f (green) in PCs (PCL; Purkinje cell layer) located in the area marked by a rectangle in the inset of (E). Notice the absence of staining in the granule cell layer (GCL) and molecular layer (ML) interneurons (white arrows in F). R: rostral; C: caudal; M: medial; L: lateral. D: dorsal; V: ventral; IC: inferior colliculus. IV-V, VI, VII, simplex, and crusI/II are different lobules.

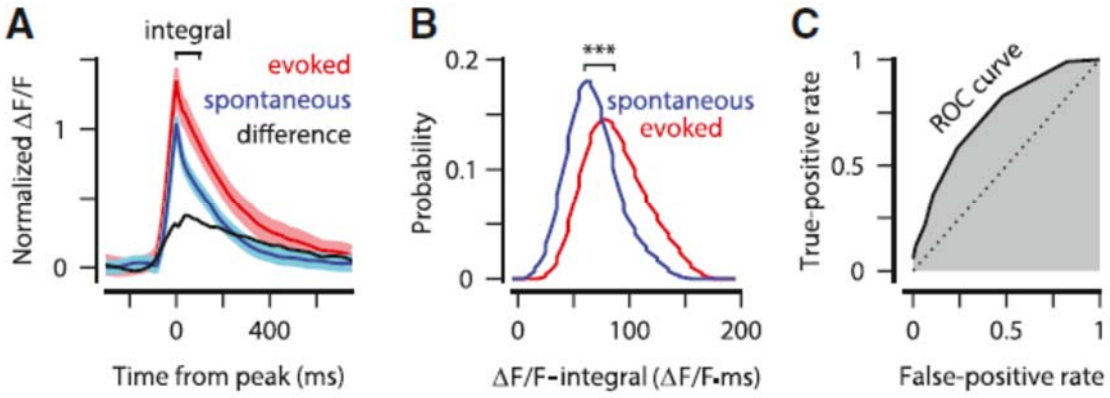

Figure 4-2 Sensory-driven enhancement of calcium spikes in a representative dendrite

(A) Average of spontaneous (blue) and sensory-evoked (red) calcium spikes (± s.e.m.). Difference trace (black) is the difference between evoked and spontaneous traces. All traces are normalized to the peak of the spontaneous trace. **(B)** Histograms of the size of spontaneous (blue) and evoked (red) calcium spikes computed by taking the ΔF/F integral in the window shown in (A; "integral"). Bin width=20 ΔF/F.ms. **(C)** ROC curve (black solid line) and the corresponding area under the curve (shaded gray) computed from the histograms shown in (B). Dotted diagonal is the ROC curve if the two histograms were completely overlapping.

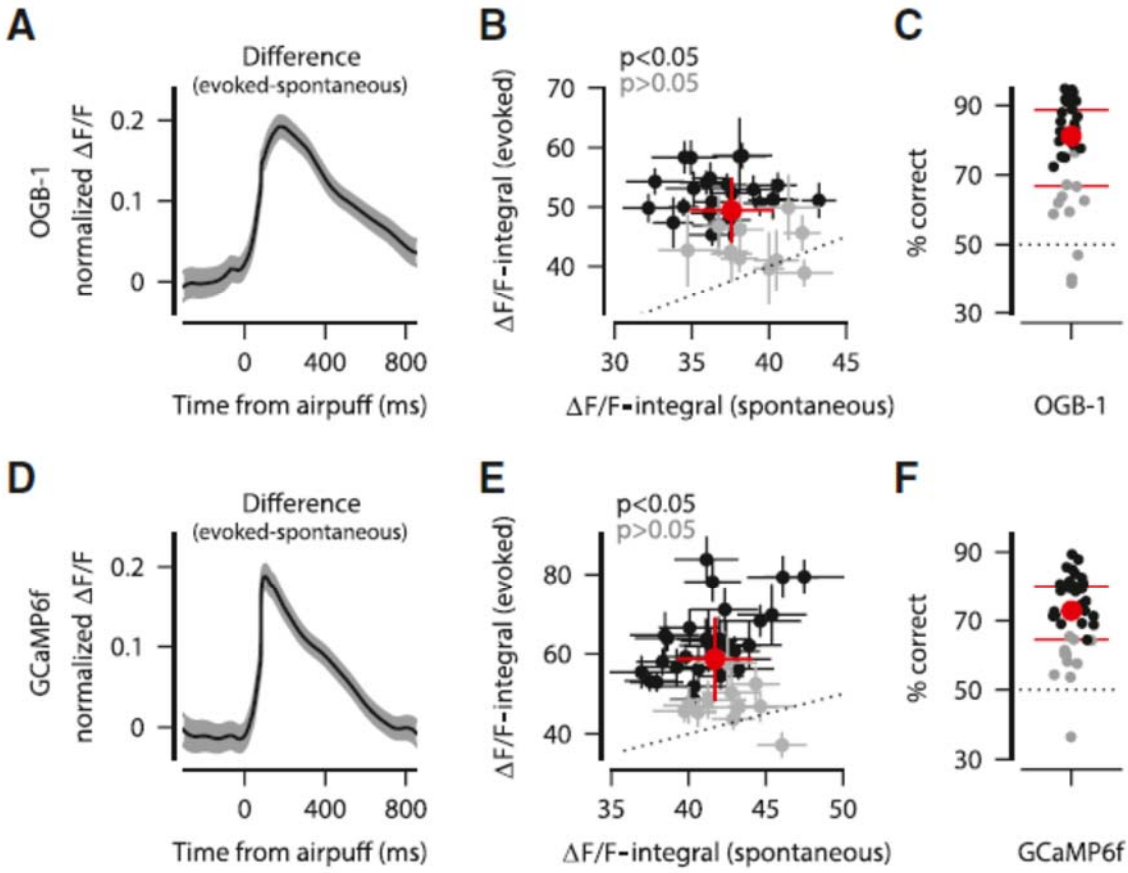

Figure 4-3 Sensory-driven enhancement of calcium spikes

(A-C) OGB-1/AM. **(D-F)** GCaMP6f experiments. **(A, D)** Difference between evoked and spontaneous CF-triggered fluorescence signals averaged across all dendrites (± s.e.m.). All traces are normalized to the peak of the spontaneous trace of each dendrite separately. **(B, E)** Average size of evoked and spontaneous calcium spikes in dendrites with a significant sensory-driven enhancement (black: mean±s.e.m.), and without (gray: mean±s.e.m.). Average ± s.d. of all dendrites is shown in red. **(C, F)** ROC analysis showing % correct discrimination of sensory-evoked and spontaneous calcium spikes, for individual dendrites (black and gray as in (B,E)), and averaged across population (red: circle is median and lines are inter-quartile range). Dotted line indicates the chance discrimination level.

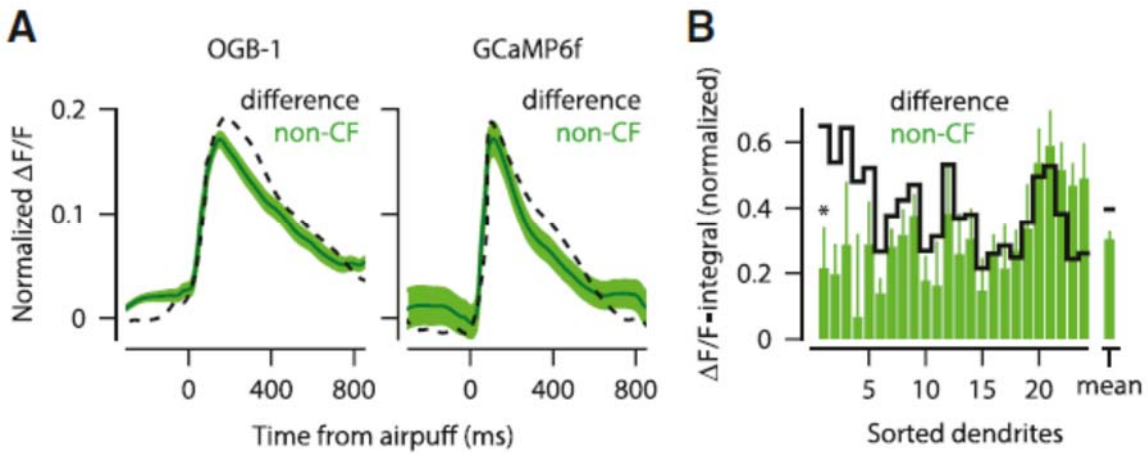

Figure 4-4 Sensory stimulation triggers non-CF calcium signals in PC dendrites

(A) Average fluorescence signal (± s.e.m.) in response to sensory stimulation when there was no CF-triggered calcium spike (green, non-CF). Difference traces in Figures 3A and 3D are superimposed (dashed). Left: OGB-1/AM, right: GCaMP6f experiments. All traces are normalized to the peak of the spontaneous trace of each dendrite separately. **(B)** Average size of non-CF (green, error bars: s.e.m.) and difference (black) calcium signals shown for each dendrite separately after normalizing to the average size of its spontaneous spike. Dendrites are sorted by the difference of the two signals. “Mean” indicates the average across all dendrites. Asterisk indicates significantly different non-CF and difference signals. See also Figure S2.

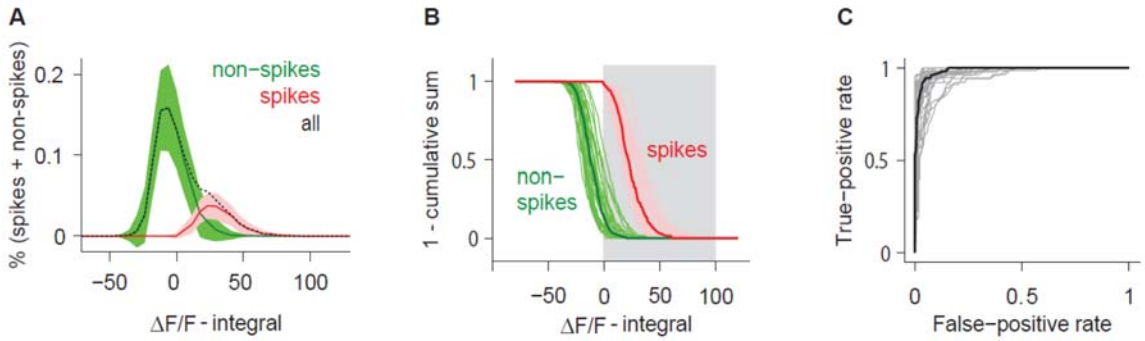

Figure 4-5 (Supp. Fig.) Calcium spikes are largely separable from non-spikes based on their ΔF/F-integral value

Calcium spikes were identified by our spike-detection algorithm, which involved template matching and threshold setting (see Experimental Procedures). In this figure we compare the ΔF/F-integral value of calcium spikes with non-spikes. Panel **A** shows the distribution of ΔF/F-integral values for calcium spikes (red), non-spikes (green), and the pooled data (dashed). Calcium spikes and non-spikes have largely distinct ΔF/F integrals (Figure S1**A**; mean±s.d.; bin width=6 ΔF/F.ms); however, there is a slight overlap between the two distributions. This overlap results from fluorescence signals that, despite having a rather large ΔF/F integral, were not identified as calcium spikes, because their temporal profile was different from the template used in our spike-identification algorithm. Figure S1**B** shows one minus the cumulative distributions of calcium spikes (red) and non-spikes (green) for all the dendrites (thick lines: median). These curves represent the rate of true positives (red) and false positives (green) in discriminating the spike, non-spike distributions based on the ΔF/F-integral values. In order to quantify the separation of the two distributions, we performed ROC analysis by plotting true-positive rates against false-positive rates for each dendrite (Figure S1**C**; black: median). The highly bowed ROC curves indicate that the distribution of ΔF/F integrals is largely separable for calcium spikes compared to non-spikes. Area under ROC curve, which represents the performance in discriminating spikes from non-spikes, equals 0.98±0.02, (mean±s.d.), demonstrating a very high discrimination rate.

CHAPTER 5:

Climbing-fibers code for the intensity of unconditioned stimuli: an awake study

Farzaneh Najafi[1], Andrea Giovannucci[2], Samuel S.-H. Wang[2], Javier F. Medina[3]

[1]Department of Biology, University of Pennsylvania, Philadelphia, PA 19104, USA

[2]Department of Molecular Biology and Princeton Neuroscience Institute, Princeton University, Princeton, NJ 08544, USA

[3]Department of Psychology, University of Pennsylvania, Philadelphia, PA 19104, USA

5.1 Introduction

Climbing fibers are thought to provide teaching signals to their postsynaptic Purkinje cells, where these signals are used to induce mechanisms of neural plasticity which will ultimately result in motor learning (Ito, 1989; Raymond et al., 1996; Simpson et al., 1996; De Zeeuw et al., 1998). Some of the evidence for this hypothesis comes from eyeblink conditioning, a simple example of cerebellar-dependent motor learning, in which subjects gradually learn to close their eyelid in response to an initially neutral stimulus that is repeatedly paired with an unconditioned stimulus, such as a periorbital airpuff (Kim and Thompson, 1997; Medina et al., 2000). Previous work has shown that climbing fibers originating in the dorsal accessory olive carry teaching signals related to the periocular airpuff (Sears and Steinmetz, 1991; Nicholson and Freeman, 2003), and that these signals are both sufficient and necessary for driving learning of the

conditioned eyelid response (Mauk et al., 1986; Medina et al., 2002). However, much less is known about the way climbing fibers represent the strength of the instructive periocular airpuff, a key parameter that has a major influence on the rate and magnitude of learning (Pavlov and Anrep, 1927; Passey, 1948; Spence, 1953; Smith, 1968).

Climbing fibers have peculiar spiking properties; they have a low firing rate which, in contrast to most other brain areas, is barely modulated by stimulation (Simpson et al., 1996). Moreover, each Purkinje cell receives input from one climbing fiber, and responds with a single all-or-nothing burst of spikes once the climbing fiber input is active (Eccles et al., 1966a). Therefore, climbing fiber teaching signals are thought to be represented as binary events in Purkinje cells (Gilbert and Thach, 1977; Gellman et al., 1985; Andersson and Armstrong, 1987; Simpson et al., 1996; Kenyon et al., 1998). This view suggests that individual Purkinje cells will equivalently register different intensities of a teaching signal if only a single trial is presented. Hence, in order to encode graded instructive stimuli, individual Purkinje cells will need to collect many trials. Alternatively, information about the intensity of instructive signals can be collected across a population of Purkinje cells. It is also known that the climbing fiber input evokes, besides the somatic spike, a large calcium transient in Purkinje cell dendrites (Llinas and Sugimori, 1980; Tank et al., 1988; Sullivan et al., 2005; Kitamura and Hausser, 2011). This provides another potential mechanism, which involves graded modulation of the dendritic calcium signal, for representing the strength of teaching stimuli (Najafi and Medina, 2013).

We studied different mechanisms through which Purkinje cells might encode the intensity of periocular teaching signals by doing two-photon calcium imaging in awake

mice. This technique allowed us to simultaneously monitor climbing fiber inputs across a population of Purkinje cells. Additionally, we were able to examine if climbing fiber-triggered calcium transients can provide an analogue signal for the stimulus intensity. Our results suggest several coding mechanisms at the level of individual dendrites as well as dendrite ensembles.

5.2 Material and Methods

Surgery and two-photon imaging. Experimental procedures were approved by the Princeton University Institutional Animal Care and Use Committee and performed in accordance with the animal welfare guidelines of the National Institutes of Health. The details of the animal preparation are described previously (Dombeck et al., 2007). Briefly, C57BL/6J mice (female, 8-14 weeks) were deeply anesthetized by inhalation of isoflurane (0.5-1%). A small area of the cerebellum was exposed (diameter: 3mm). A Kwik-Sil plug, pre-molded on a coverslip, was secured over dura using a two-piece, stainless steel headplate. Throughout the surgery, sterile saline was used to keep dura wet. Animals' body temperature was monitored and maintained near 37 ^{o}C. Analgesics, Meloxicam, were injected. At the end of the surgery, anesthesia was removed and mice were returned to their cage for recovery.

Two-photon calcium imaging was performed the day after surgery. Mice were anesthetized (Isoflurane). Kwik-Sil plug was removed and calcium indicator (Oregon Green 488 BAPTA-1/AM, Invitrogen) was injected 150-200 μm below dura, by applying brief positive pressure through a glass pipette. A new Kwik-Sil plug was used, anesthesia was removed, and the animal was transferred and mounted on a cylindrical treadmill integrated with the imaging apparatus. In vivo calcium imaging was performed

on awake animals using a custom-built two-photon laser scanning microscopy (Sullivan et al., 2005). Image acquisition was controlled by ScanImage software (Pologruto et al., 2003). 32x128-pixel movies were recorded (64 ms/frame). Animals were monitored throughout the experiment with a camera.

Periocular stimulation. Two different sets of experiments were performed. In one set, duration experiments, the airpuff pressure was kept the same (30 psi) and 4 different durations of airpuff were tested (8,15,30,45 ms). In another set, psi experiments, the airpuff duration was constant (30ms), and 2 different airpuff pressures (10, 50 psi) were applied. A pressure injector system (Toohey Spritzer) was used to deliver airpuff stimuli through a needle to the animal's ipsilateral eye (inter-trial interval: 4s; 35 trials per airpuff condition per experiment).

Identification of dendrites and calcium events. Purkinje cell dendrites were identified from the imaging movies using independent component analysis (Hyvarinen, 1999; Ozden et al., 2012). The fluorescence trace (ΔF/F) of each dendrite was computed, frame-by-frame, as (F-Fb)/Fb, where F is the mean fluorescence intensity of the pixels contributing to a dendrite. Fb is the baseline defined as the lowest 8^{th} percentile of the fluorescence values within a 1-sec window. Climbing fiber-evoked calcium events were identified with a template-matching algorithm (Ozden et al., 2008). In brief, a template was generated by taking the average of the largest fluorescence transients. The template was next de-convolved with the ΔF/F. Transients whose peak amplitude was larger than a predefined threshold were classified as calcium events.

Data analysis. The ΔF/F traces presented in all figures were normalized. Normalization was done for each dendrite separately, by dividing the ΔF/F trace of the dendrite to the

peak value of its mean spontaneous calcium event. Calcium events that occurred within 50-200 ms of the periocular stimulus were considered airpuff-evoked. The latency of calcium events (Fig. 4) was computed manually by inspecting each airpuff-evoked calcium event.

The size of individual calcium events ("ΔF/F-integral", Fig. 5), was computed as in our previous paper (Najafi et al., 2014), by taking the integral of the normalized ΔF/F signal over the interval [t t+100ms], where t is the time point at which the peak of the event occurs. The non-CF signal (Fig. 5B,C) was analyzed from trials without any calcium events within 50-200ms of the airpuff stimulus. The size of the non-CF signal was measured in a similar way as the calcium events, by taking the integral of the normalized ΔF/F signal over the interval [t t+100ms], where t is a time point selected randomly within 50-200ms of the stimulus.

Coactivation (Fig. 6) was defined, for each trial, as the fraction of "responsive" dendrites. This was computed by dividing the number of dendrites with an airpuff-evoked calcium event, by the total number of dendrites present in an imaging movie. To compute joint probability (Fig. 6C), all combinations of dendrite pairs in a movie were first generated. Then, for each pair, the "actual" joint probability was defined as the fraction of trials in which both dendrites represented airpuff-evoked calcium events. "Independent" joint probability was computed by multiplying the calcium-event probability of the two dendrites ($P_{i \cap j} = P_i \times P_j$).

5.3 Results

We used a two-photon microscope to image sensory-related calcium signals in Purkinje cell (PC) dendrites of awake mice. Mice were head fixed on top of a custom-built cylindrical treadmill and allowed to locomote in place while we delivered airpuff stimuli of varying pressures and durations to the periocular area. In some experiments we used airpuffs of 4 different durations (12 experiments, 4 mice, 97 dendrites; durations: 8,15,30,45 ms; pressure: 30psi); in other experiments we used airpuffs of 2 different pressures (6 experiments, 3 mice, 39 dendrites; pressures 10,50 psi; duration: 30ms). We will refer to these two datasets as duration and pressure data, respectively.

Climbing fiber-triggered calcium transients in Purkinje cell dendrites

As in previous reports (Sullivan et al., 2005; Ozden et al., 2008), PC dendrites in our experiments appeared as parasagittally aligned, tube-like structures (Fig. 1A), in which large calcium transients (Fig. 1B, circles) occurred spontaneously and in response to periocular airpuff stimuli (Fig. 1B, triangles). We have previously shown that these calcium transients are triggered in each individual PC dendrite by activation of its one-and-only climbing fiber (CF) input, which also evokes a complex spike in the PC somata (Ozden et al., 2008).

A number of features confirmed the CF origin of these calcium transients in our experiments. First, they occurred spontaneously at about 1Hz (0.4-1.4Hz; median 0.7 Hz; Fig. 1C), which is similar to the characteristic spontaneous firing rate of CFs reported previously in awake animals (Thach, 1968). Second, they had a fast rise (~10ms) and a slow decay ($t_{1/2}$: 74±13ms; mean±s.d.; Fig. 1D), as observed for CF-triggered signals in

other calcium imaging studies (Miyakawa et al., 1992; Eilers et al., 1995; Ozden et al., 2008). Third, calcium transients often occurred at the same time in adjacent PC dendrites, and this pairwise correlation decreased rapidly as the mediolateral distance between dendrites increased (Fig. 1E, black). This finding is consistent with previous studies that have demonstrated synchronous CF input to neighboring PCs in the same parasagittal microzone (Bell and Kawasaki, 1972; Sasaki et al., 1989; Ozden et al., 2009; Schultz et al., 2009). Hereafter, we will use the term “calcium events” to refer to CF-triggered calcium transients.

Periocular zones on the surface of the cerebellar cortex

We imaged 101 spots on the surface of cerebellar cortex in 22 mice, including paravermal locations in lobules V, VI, and more lateral locations in simplex (Fig. 2A,B). We were unable to image the most medial parts of simplex due to the high density of blood vessels in that area. Consistent with the location of trigeminal CFs reported in previous studies (Miles and Wiesendanger, 1975a; Miles and Wiesendanger, 1975b; Manni and Petrosini, 2004), we found that many dendrites in the paravermal regions of lobules V and VI responded to periocular airpuff stimulation with a CF-triggered calcium event (Fig. 2C,D). In contrast, dendrites in lobule simplex were mostly unresponsive, which is compatible with the deep location of periocularly-related CF zones in this lobule (Hesslow, 1994; Mostofi et al., 2010; Heiney et al., 2014).

As in previous electrophysiology work (Hesslow, 1994; Mostofi et al., 2010), we found two types of PC dendrites that could be classified according to the spatial specificity of their CF receptive fields: the majority of dendrites in lobule V responded with a CF-triggered calcium event only after ipsilateral periocular airpuffs (Fig. 2B,C),

while in lobule VI most dendrites had bilateral CF receptive fields, responding with a calcium event after ipsi- and contra-lateral periocular airpuff stimuli (Fig. 2B,D). In the analyses below, we examined the properties of calcium events measured in response to ipsilateral airpuffs. Because our results were the same for both types of PC dendrites, we pooled their data together.

Probability of calcium events

We first examined if CF-triggered calcium events in individual PC dendrites encode the intensity of the periocular airpuff probabilistically across repeated presentations of the stimulus. The raster plots of our entire duration dataset demonstrate that calcium events occurred more reliably as the duration of the airpuff was increased (Fig. 3A bottom; top: average). On average across all our dendrites, we found that the probability of a CF-triggered calcium event increased gradually for periocular airpuffs of longer durations (Fig. 3B, left; two-way ANOVA: $F_{4,96}=238.5$, $p<0.0001$; Tukey's HSD, $P<0.01$), and higher pressures (Fig. 3B, right; two-way ANOVA: $F_{2,38}=58.93$, $p<0.0001$; Tukey's HSD, $P<0.001$).

The monotonically increasing relationship between airpuff intensity and calcium event probability, which is shown for the average of all dendrites in Figure 3B, was also evident in 58% of the individual dendrites in the duration dataset (Fig. 3C, top row). In the rest of the dendrites the calcium event probability was not graded with the intensity of the periocular stimulation; instead, these dendrites were relatively unresponsive to all airpuffs below a certain intensity threshold (Fig. 3C, arrowheads), and responded with equal probability for all intensities higher than the threshold. Among this group, we found dendrites with a wide range of thresholds including highly-sensitive dendrites in which

calcium events were triggered by the weakest airpuffs (Fig. 3C, row 2), and others which were unresponsive except for the strongest airpuffs (Fig. 3C, row 5). Thus, our results indicate that, in theory, PCs could gather information about stimulus intensity by taking into account how reliably their single CF input is activated.

Latency of calcium events

The latency of CF responses varies systematically according to the magnitude of passive forepaw movements (Rushmer et al., 1976). We investigated if information about the intensity of a periocular airpuff stimulus might be encoded similarly, in the timing of CF-triggered calcium events.

In agreement with previous electrophysiological reports of sensory-driven CFs (Ekerot et al., 1987; Kobayashi et al., 1998), we found that calcium events were evoked in PC dendrites at a wide range of latencies relative to the onset of the airpuff stimulus (peak latency: ~50-200ms; Fig. 4A,C). Increasing the duration of the periocular airpuff resulted in progressively more long-latency calcium events (Fig. 4A). The analysis shown in Figure 4B confirmed that in most individual dendrites, long-duration airpuffs evoked significantly more calcium events than short-duration airpuffs in the interval 100-200ms after the periocular stimulation (Fig. 4B; Kolmogorov-Smirnov test, $P<0.0001$) but not in the interval 0-100ms (Fig. 4B; Kolmogorov-Smirnov test, $P>0.05$). In contrast, increasing airpuff pressure did not significantly bias the latency of calcium events (Fig. 4C); in most individual dendrites the number of calcium events was unselectively increased for both the 0-100ms interval (Fig. 4D; Kolmogorov-Smirnov test, $P<0.01$), and in the 100-200ms interval (Fig. 4D; Kolmogorov-Smirnov test, $P<0.001$). Thus, our findings indicate that variations in the latency at which individual CFs become activated

by a periocular airpuff stimulus may provide some information about the duration of the airpuff, but not its pressure.

Amplitude of calcium events

We have recently shown that the amplitude of CF-triggered calcium events is enhanced during sensory stimulation (Najafi et al., 2014). Here, we examined if the magnitude of this sensory-driven enhancement is graded according to the intensity of the periocular stimulation. Average fluorescence traces corresponding to spontaneous (Fig. 5A, “sp”) and sensory-evoked calcium events showed a gradual enhancement as the duration or the pressure of the airpuff was increased (Fig. 5A top; only duration data is displayed). To quantify this effect, we measured the size of each individual calcium event by computing the integral of its fluorescence trace over a 100ms time window after the peak (“ΔF/F-integral”), and normalizing this value to the average ΔF/F-integral of all the spontaneous calcium events for each PC dendrite separately. Note that we only examined the fluorescence traces of individual calcium events and excluded trials in which the periocular stimulation resulted in two or more calcium events separated from each other by less than 100ms. This analysis confirmed that periocular airpuffs of longer duration (Fig. 5A bottom, left) and higher pressure (Fig. 5A bottom, right) evoked progressively larger calcium events in PC dendrites (two-way ANOVA; duration data: $F_{4,96}=80.74$, $p<0.0001$; Tukey’s HSD, $P<0.05$; pressure data: $F_{2,38}=62.88$, $p<0.0001$; Tukey’s HSD, $P<0.01$). Thus, the size of the CF-triggered calcium event provides the PC dendrite with information about the intensity of peripheral stimulation.

What neural mechanisms may contribute to the gradual enhancement of the fluorescence traces in Figure 5A? In addition to triggering calcium events in the PC

dendrite, sensory stimulation also elicits a smaller calcium response that has a non-CF origin ("non-CF" signal; (Najafi et al., 2014). We found that this non-CF signal was graded according to the duration of the periocular stimulation (Fig. 5B, top), progressively increasing in size as the stimulus duration or pressure was increased (Fig. 5B bottom; two-way ANOVA; duration data: $F_{4,96}=122.61$, $p<0.0001$; Tukey's HSD, $P<0.0001$, except for d3-d4 comparison; pressure data: $F_{2,38}=71.85$, $p<0.0001$; Tukey's HSD, $P<0.0001$). For short-duration airpuffs (Fig. 5C, durations 1 and 2), the average non-CF signal closely matched the average "enhancement" trace obtained by taking the difference between the average fluorescence traces for spontaneous and evoked calcium events. However, for long-duration airpuffs (Fig. 5C, durations 3 and 4), the non-CF signal was significantly smaller than the "enhancement" trace. These results are consistent with a model in which each sensory-driven calcium event is composed of two separate signals (Fig. 5D): a non-CF signal that is graded depending on the intensity of stimulation and a fixed signal that is triggered every time the CF input is activated, whether spontaneously or in response to a stimulus. In this model, the two calcium signals add linearly for weak stimuli (Fig. 5D, d1, d2, p1, p2) and supralinearly as the intensity of stimulation increases beyond a certain threshold (Fig. 5D, d3 and d4).

Synchronization of calcium events

Previous work has demonstrated that groups of climbing fibers converging on the same parasagittal strip of cerebellar cortex become synchronized in response to sensory stimulation (Lou and Bloedel, 1992; Welsh et al., 1995; Wylie et al., 1995; Lang, 2002; Ozden et al., 2009; Wise et al., 2010). For each of our experiments, we examined if the degree to which CF-triggered calcium events were synchronized provided information

about the intensity of the periocular airpuff stimulus. We found that the number of synchronized calcium events in a 150ms window after stimulus onset gradually increased in response to airpuffs of longer durations (Fig. 6A and 6B, top: two-way ANOVA, $F_{4,394}=199.75$, $p<0.0001$; Tukey's HSD, $P<0.05$), and higher pressures (Fig. 6B, bottom: two-way ANOVA, $F_{2,209}=106.56$, $p<0.0001$; Tukey's HSD, $P<0.0001$).

Since stronger airpuffs increase the probability of calcium events in individual PC dendrites (see Fig. 3), it is possible that the gradual increase in the number of synchronized calcium events (Fig. 6A, B) could be explained entirely by this increase in probability. To assess this possibility, we measured the joint probability for every pair of dendrites in each one of our experiments, i.e. the probability of observing a CF-triggered calcium event in both dendrites within the same 150 ms time window, and compared it to the joint probability expected for independent dendrites ($P_{ij} = P_i \times P_j$, where P_i and P_j represent the calcium-event probability of dendrites i and j in that same time window). We found that joint probability deviated significantly from independence for all airpuff intensities (Fig. 6C; two sample t-test, $P<0.001$). We call this deviation "extra synchrony" because it represents the synchrony beyond that expected solely from the calcium-event probability of individual dendrites. Figure 6D shows that there was a gradual boost in the amount of extra synchrony as the airpuff duration or pressure was increased (two-way ANOVA; duration data: $F_{4,361}=113.49$, $p<0.0001$; Tukey's HSD, $P<0.0001$, except for d3-d4 comparison; pressure data: $F_{2,136}=10.27$, $p<0.0001$; Tukey's HSD, $P<0.05$, except for p1-p2 comparison). Our data indicate that information about the intensity of sensory stimuli can be conveyed across a population of PCs in a single trial by modulating the degree of CF input synchrony.

5.4 Discussion

Our results, which provide the first systematic study of the representation of stimulus intensity in climbing fibers (CFs), support previous studies (Eccles et al., 1972a; Ozden et al., 2009; Kitamura and Hausser, 2011) and extend them by suggesting several mechanisms through which Purkinje cell (PC) dendrites can encode the intensity of periocular sensory stimuli. These mechanisms are discussed below and their implications for cerebellar motor learning are provided.

Coding stimulus intensity in individual Purkinje cells

Climbing fibers have a limited range of firing rate, 1-10 Hz, and respond with an all-or-none burst of spikes to supra-threshold stimuli; therefore, they are thought to serve as binary event detectors unless their response is averaged across several trials (Eccles et al., 1972b, c; Ekerot et al., 1987). In a classical study performed in anesthetized cats, Eccles et al demonstrated that higher intensities of mechanical footpad stimuli are more effective in evoking complex spikes (Eccles et al., 1972b, c). In agreement with their observation, we found that in awake mice, the probability of CF-triggered calcium signals gradually increases as a function of the duration and pressure of periocular stimuli.

What are the learning implications of a probability code? Since CF inputs are binary, they are thought to gradually teach PCs in steps of constant size, i.e. a constant amount of learning will be induced on each trial (Kenyon et al., 1998). We found that the response probability of CFs varies with stimulus intensity, therefore CFs can, after many trials, induce graded plasticity in PCs which will depend on the stimulus intensity.

However, based on computational models of learning, PCs need access to stimulus strength in individual trials (Pouget and Snyder, 2000).

Our results provide an alternative mechanism that would allow individual PCs to grade the amount of plasticity in a single trial. We have shown, for the first time in awake animals, that CF-triggered calcium signals in PC dendrites are not binary as previously thought; instead, their amplitude is graded and represents information about the intensity of sensory stimuli.

Previous experiments performed in cerebellar slices and anesthetized animals suggest two general mechanisms that can underlie modulation of the amplitude of calcium signals in our dendrites. First, the number of spikes in the pre-synaptic CF burst can influence PC dendritic depolarizations and regulate calcium influx into the dendrites (Mathy et al., 2009). In this hypothesis, different intensities of periocular stimuli would modify CFs burst size, for instance, through the graded modulation of the membrane potential of olivary neurons (Llinas and Yarom, 1981). Alternatively, the amplitude of calcium signals could be modulated through mechanisms that influence the membrane potential of the post-synaptic PC (Miyakawa et al., 1992; Kitamura and Hausser, 2011). For instance, congruent PF activity has been shown to enhance CF-triggered calcium signals in PC dendrites (Fierro et al., 1998; Wang et al., 2000). In this view, different intensities of a stimulus will induce, in addition to CF activation, graded PF activity (Campbell et al., 1983; Chan et al., 1989), which will subsequently result in graded calcium signals in PC dendrites. This hypothesis assumes convergence of PFs and CFs with coinciding receptive fields at the level of individual PCs (Eccles et al., 1972c; Brown and Bower, 2001; Apps and Hawkes, 2009).

Modulation of calcium signals has important implications in cerebellar learning. Calcium is the trigger and regulator of a wide variety of short-term and long-term plasticity mechanisms in PC dendrites (Kitamura and Kano, 2013). For instance, plasticity at the PF-PC synapse has been shown to be tightly controlled by the dynamics of calcium signals in PC dendrites (Coesmans et al., 2004; Tanaka et al., 2007). Therefore, graded calcium signals observed in our data can potentially induce graded plasticity and provide a neural correlate at the level of individual PCs for single-trial motor adaptation that would match the intensity of sensory inputs (Thoroughman and Shadmehr, 2000; Scheidt et al., 2001; Thoroughman et al., 2007). Additionally, enhanced dendritic calcium spikes have been shown to modulate the characteristic post-complex spike pause in simple spike activity of PCs (Davie et al 2008); therefore graded calcium spikes can potentially shape the output of PCs and be employed for the online control of movements.

Coding stimulus intensity by ensembles of Purkinje cells

Several studies have shown that spontaneous complex spikes fire simultaneously in ensembles of Purkinje neurons (Llinas et al., 1974). Additionally an increase in synchrony has been observed during skilled tongue movements (Welsh et al., 1995) as well as following peripheral sensory stimulation (Llinas and Sasaki, 1989; Ozden et al., 2009; Schultz et al., 2009) and motor cortex stimulation (Lang, 2002). Our findings in this paper extend these studies by showing that information about the intensity of sensory stimuli is represented in the coactivation of nearby PC dendrites, which reflects the number of simultaneously active CFs.

We also showed that the calcium spike synchrony in response to sensory stimulation is more than what would be expected from independently active dendrites. This deviation, which we termed “extra synchrony”, indicates that the occurrence of calcium spikes in nearby dendrites is somehow dependent on each other. Previous experiments have demonstrated that olivary neurons are coupled through gap junctions, which allow the transfer of depolarizing currents and spike initiation in nearby neurons (Llinas et al., 1974; Llinas and Sasaki, 1989; Van Der Giessen et al., 2008). Therefore, electrotonic coupling can render the activity of olivary neurons dependent on each other, and could be a likely mechanism underlying “extra synchrony” in our dendrites.

How can calcium spike synchrony influence motor output? Each neuron of the deep cerebellar nuclei (DCN) receives converging input from tens of PCs (Person and Raman, 2012). It has been shown that synchronous complex spikes influence the spiking activity of DCN neurons (Hoebeek et al., 2010), which might subsequently contribute to the induction of plasticity in the cerebellar nuclei (Ohyama et al., 2006; Pugh and Raman, 2006). Additionally, the spiking pattern of DCN neurons could be transmitted to downstream cerebellar targets such as premotor areas, and influence the rate and timing of their responses. Therefore, the graded synchrony of calcium spikes in response to unexpected stimuli provides information that could be useful in online motor control as well as single-trial adaptation.

Functional implications

Our results suggest that an analogue signal about the intensity of sensory stimuli is carried in climbing fibers response probability, synchrony, and the amount of calcium triggered in their post-synaptic Purkinje cells. These mechanisms can potentially

contribute to grade motor adaptation in response to different magnitudes of perturbation, as reported in some human behavioral studies (Thoroughman and Shadmehr, 2000; Scheidt et al., 2001; Thoroughman et al., 2007). Additionally, our findings could have direct implications in cerebellar conditioning, such as eyeblink conditioning. Although the periocular areas that we imaged are different from eyeblink hotspots in the cerebellar cortex (Hesslow, 1994; Mostofi et al., 2010), the signals we have found could still contribute to some aspects of learning, such as the precise adjustment of conditioned response amplitude. Alternatively, the signals we observed could contribute to other forms of blink-system motor learning, such as reflex-blink adaptation (Evinger et al., 1989), which occurs during lid restraint and has been shown to modify PC responses (Pellegrini and Evinger, 1997). Our findings open additional lines of research; in particular, imaging PC dendritic calcium signals during eyeblink conditioning would allow to examine the functional implications of our results in adaptation of conditioned responses to varying intensities of periocular airpuffs.

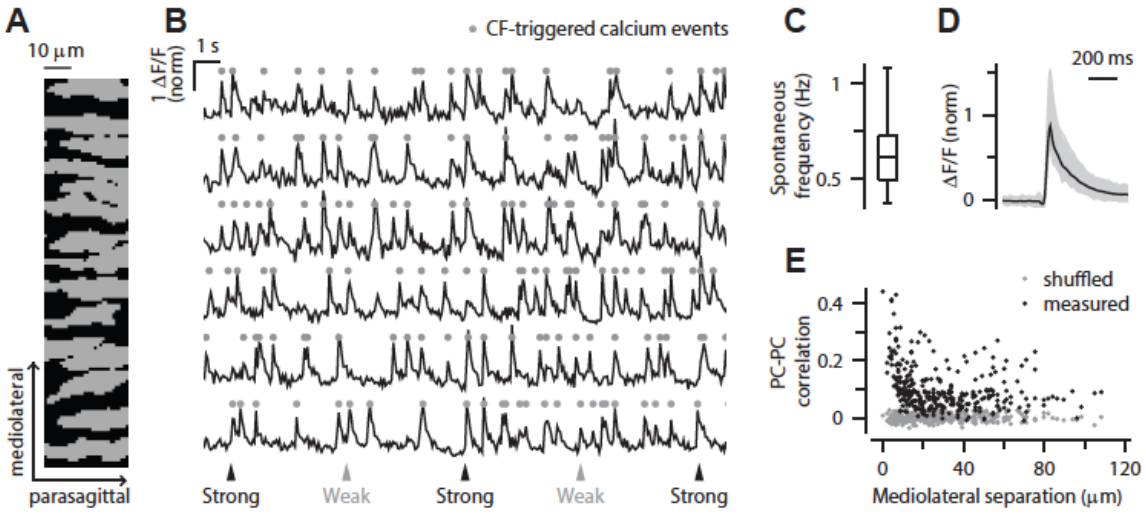

Figure 5-1 Imaging climbing fiber-triggered calcium transients in Purkinje cell dendrites

(A) An example filed of view showing 15 dendrites imaged simultaneously in an experiment. **(B)** Example fluorescence traces of some of the dendrites in (A). Triangles indicate periocular airpuff stimuli of different strengths. Circles mark calcium events. **(C)** Frequency of spontaneous calcium events (central line: median across all dendrites; box edges: 25th and 75th percentiles). **(D)** Mean ΔF/F trace of spontaneous calcium events for each dendrite (gray lines) and their average (black). **(E)** Pearson correlation coefficient of calcium events in pairs of dendrites for the actual (back) and shuffled-frame (gray) data as a function of the mediolateral separation.

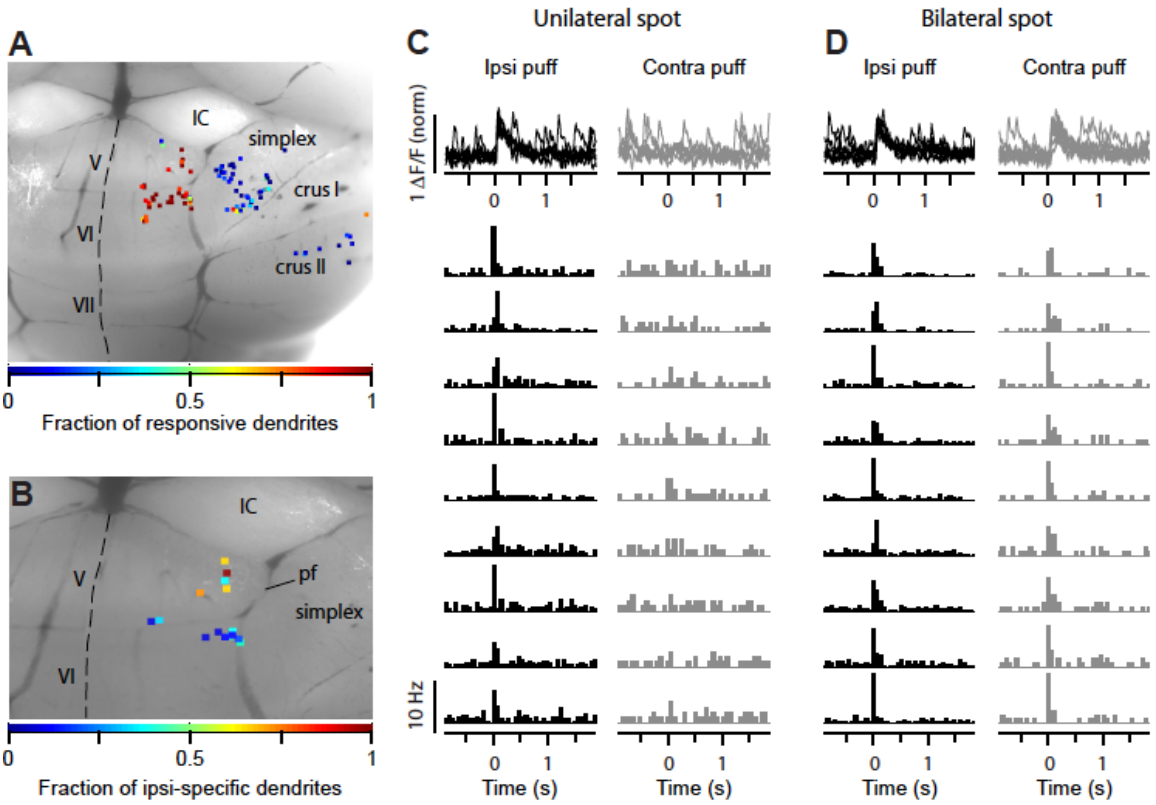

Figure 5-2 Periocular zones on the surface of the cerebellar cortex

(A) Top view of an exposed cerebellum showing all imaged spots (colored dots). Color intensities indicate the fraction of periocular-responsive dendrites in each spot. **(B)** Spots examined for response laterality are shown. Color intensities indicate the fraction of ipsi-specific dendrites in each spot. IC: Inferior Colliculus. IV-V, VI, VII, Simplex, and CrusI/II: cerebellar lobules. pf: primary fissure. Dashed line: midline. **(C) Top:** example ΔF/F traces from an ipsi-specific spot in response to ipsilateral (black, left) and contralateral (gray, right) airpuff stimuli. **Bottom:** each row shows PSTH of a dendrite in the example ipsi-specific spot. **(D)** Same as (C), however a representative bilateral spot is shown.

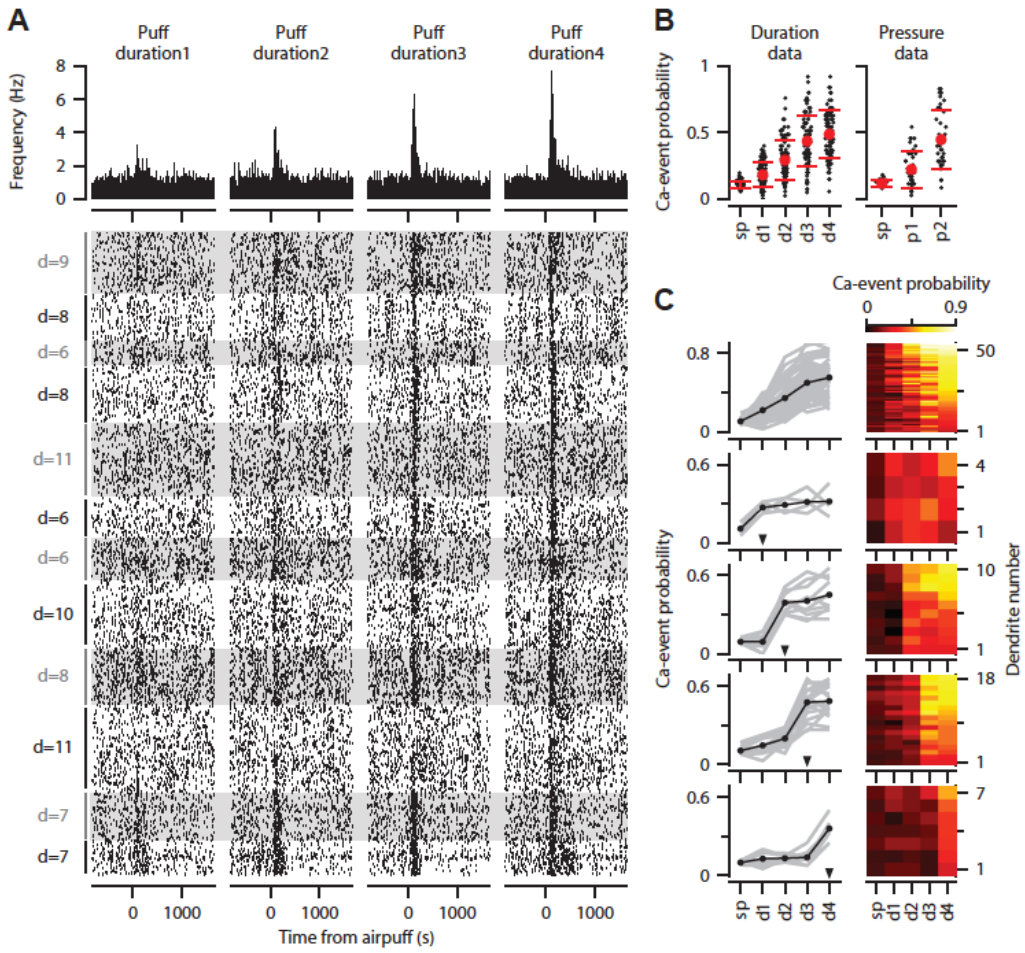

Figure 5-3 Calcium-event probability encodes stimulus intensity

(A) Bottom: raster plots represent all trials of the duration dataset. Dots indicate calcium events. White and gray shades mark different experiments. Within each experiment, trials from all dendrites are shown consecutively. Number of dendrites imaged in each experiment is shown on the left. **Top:** PSTHs, corresponding to the raster plots, indicate calcium event frequency at each time point. **(B)** Calcium-event probability for the spontaneous (sp) and airpuff-evoked conditions (d1-d4, p1-p2) is shown for all dendrites (black). Red: mean±s.e.m. Left: duration data. Right: pressure data. **(C)** Top to bottom: 5 dendrite categories based on how calcium-event probability varies with airpuff duration. For each category, the calcium-event probability of individual dendrites (left: gray lines; right: rows of heatmaps) and their average (left, black lines) is shown. Triangles (left): stimulus-strength threshold for evoking calcium events. Color intensities (right): calcium-event probability. d1-d4: different airpuff durations. p1-p2: different airpuff pressures.

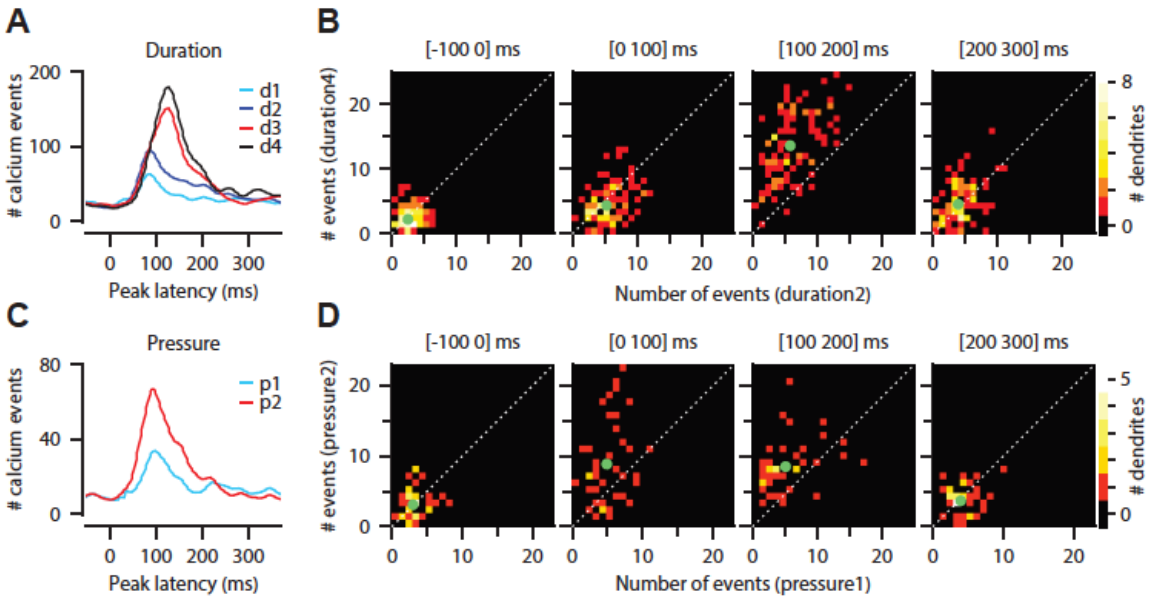

Figure 5-4 Calcium-event latency is modulated by stimulus intensity

(A) Peak-latency distributions of calcium events for duration data. **(B)** Each panel corresponds to a particular latency interval and compares, for each dendrite (dots), the number of events evoked by two different durations of airpuff (y-axis: longer duration; x-axis: shorter duration; green dot: mean; dashed: unity line). **(C,D)** Same as (A,B), but for pressure data.

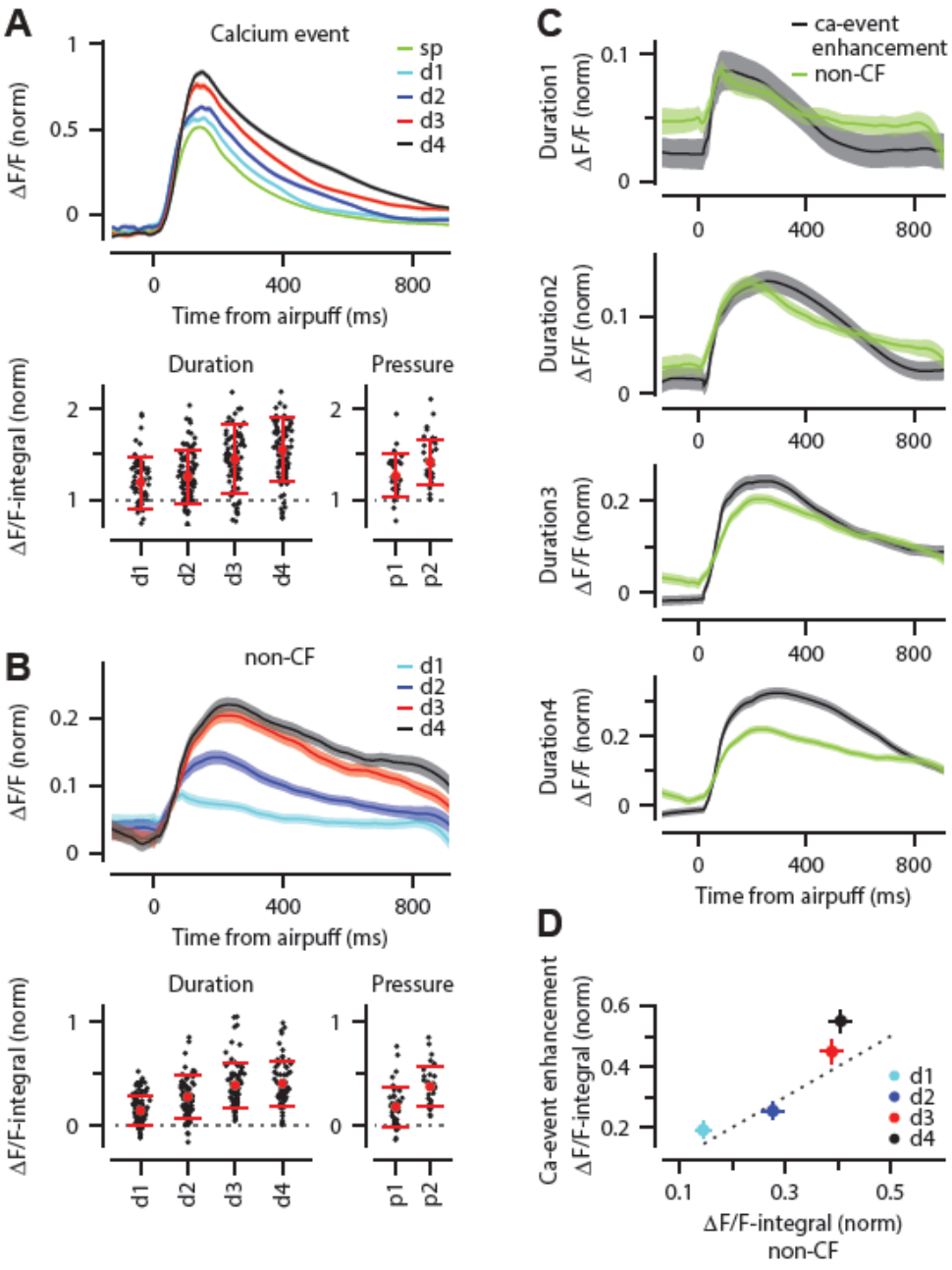
A
Calcium event
sp
d1
d2
d3
d4
ΔF/F (norm)
Time from airpuff (ms)
Duration
Pressure
ΔF/F-integral (norm)
B
non-CF
C
ca-event enhancement
non-CF
Duration1
Duration2
Duration3
Duration4
D
Ca-event enhancement ΔF/F-integral (norm)
ΔF/F-integral (norm) non-CF

Figure 5-5 Stimulus intensity is represented in the size of calcium events and size of non-CF signals

(A) Top: mean ΔF/F trace of calcium events across all dendrites for the spontaneous ('sp', green) and airpuff-evoked conditions (d1-d4: different airpuff durations; shades: s.e.m.). **Bottom:** mean size of calcium events ("ΔF/F-integral") is shown for each dendrite (black dots) for different durations (left, d1-d4) and pressures (right, p1-p2) of the airpuff. ΔF/F-integral values are normalized to the mean size of spontaneous events (dashed line). Red: mean±s.e.m. **(B)** Same as (A), but showing the non-CF signal. **(C)** Each panel corresponds to an airpuff duration, and compares ΔF/F traces of calcium-event enhancement (i.e. evoked minus spontaneous event; black) and non-CF signal (green) in response to a particular airpuff duration (solid lines: mean across dendrites; shades: s.e.m.). **(D)** Mean size of calcium-event enhancement is shown vs. mean size of non-CF signal for different airpuff durations (d1-d4; circles: average across dendrites; bars: s.e.m.; dashed: unity line; ΔF/F-integral values are normalized to the mean size of spontaneous events.)

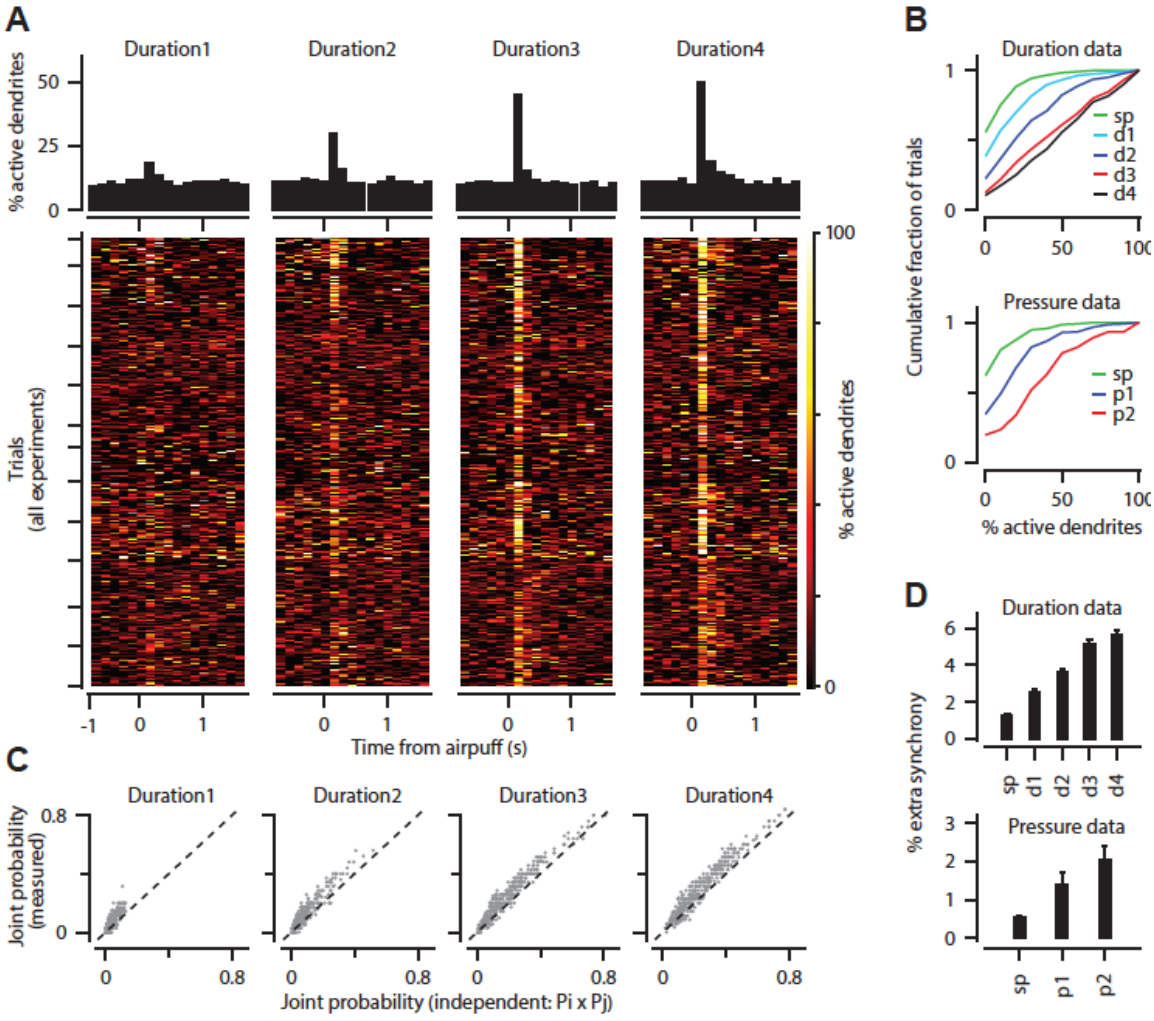

Figure 5-6 Population coding of stimulus intensity

(A) Bottom: % coactive dendrites at different time points for all trials of the duration data. Color intensities indicate % coactivation. **Top:** PSTHs correspond to heatmaps at the bottom and show the average coactivation across all trials at each time point surrounding the stimulus. **(B)** Cumulative distribution of % coactive dendrites across all trials for the spontaneous (sp) and airpuff-evoked conditions (top: duration data; bottom: pressure data). **(C)** Measured and independent joint probabilities is shown for each dendrite pair (gray; dashed: unity line) for different airpuff durations. **(D)** % extra synchrony (measured minus independent joint probability) averaged across all dendrite pairs (error bars: s.e.m; sp: spontaneous; d1-d4: different airpuff durations. p1-p2: different airpuff pressures.)

CHAPTER 6:

Conclusions and Future Directions

The studies presented in this dissertation have examined how climbing fibers encode the intensity of sensory stimuli that induce cerebellar learning ("teaching" stimuli). My behavioral data demonstrated that the amount of adaptation in a cerebellar-learning task is proportionate to the strength of the teaching stimulus. My two-photon imaging experiments explored the neural representation of the strength of the teaching stimulus in a non-learning paradigm in awake mice. In this final chapter, I will review my primary findings and describe some additional experiments that we have embarked on to further investigate cerebellar adaptation to the strength of the teaching stimuli.

6.1 What did we learn from this dissertation?

Figure 6-1 demonstrates a modified circuitry for eyeblink conditioning which incorporates the findings presented in this dissertation. We suggest that information about the unconditioned stimulus (US) not only is relayed through the climbing fiber pathway (CF), but it also involves the parallel fiber (PF) pathway (ref. chapters 3-4). Our hypothesis is corroborated by previous evidence that has shown both CF and PF inputs occur in Purkinje cells (PC) in response to sensory stimulation (Eccles et al., 1972; Bosman et al., 2010). In particular, anatomical and physiological studies have demonstrated that tactile stimuli carried through the trigeminal nucleus, such as the periocular airpuff, not only are transferred to the olivary neurons, they are as well sent to

cerebellar granule cells (i.e. the source of PFs) (Watson and Switzer, 1978; Vos et al., 2000). Therefore, we think it is plausible that PFs, in addition to CFs, provide the neural representation of unconditioned stimuli during cerebellar-dependent conditioning. This hypothesis contrasts the common belief in the field of eyeblink conditioning which considers CFs as the sole neural substrate of unconditioned stimuli.

What are the functional consequences of parallel-fiber contribution to the representation of unconditioned stimuli? Our hypothesis is that the activation of PFs could modulate the amplitude of the concurrent US-evoked CF response in PCs. This modulation will provide individual PCs with a graded calcium signal, whose magnitude reflects the strength of the US in single trials. Such graded encoding of US strength at the level of individual PCs can potentially contribute to the population-based mechanisms, such as synchrony, that may principally underlie single-trial graded cerebellar learning. Cutting-edge genetic and optical techniques that allow single-neuron stimulation may unravel whether graded calcium signals in individual Purkinje cells could have any functional implications.

In this dissertation we also provided, for the first time, a trial-by-trial analysis of eyeblink conditioning. We showed that the magnitude of learning in this cerebellar paradigm depends on the strength of the unconditioned stimulus (teaching signal), and can be adapted trial-by-trial. Our single-perturbation experiments, in which the US strength was modified in single trials, suggest that each individual perturbation triggers a short-lived plasticity mechanism that lasts about 60 seconds. Such time course matches the temporal properties of endocannabinoid-mediated short-term plasticity, which has been observed in PC synapses with parallel fibers and inhibitory interneurons (Brown et

al., 2004; Safo et al., 2006; Carey et al., 2011; Fioravante et al., 2012; Hirano and Kawaguchi, 2014).

Interestingly, and especially relevant to our research, is the study that showed endocannabinoid-mediated plasticity depends on the magnitude of calcium signals in PC dendrites (Rancz and Hausser, 2006). Therefore, the graded calcium signals that we observed in PCs in response to different strength of the US, can potentially trigger graded amounts of plasticity on a short timescale. Additionally, the short-term plasticity induced by a single perturbation may mediate the long-term adaptation we observed following repeated presentations of the teaching unconditioned stimulus (ref. chapter 2). Indeed it has been shown that cannabinoid signaling mediates long-term plasticity mechanisms such as LTD of parallel fiber and Purkinje cell synapses (Safo and Regehr, 2005).

In brief, our findings suggest that different magnitudes of a teaching stimulus induce proportionate trial-by-trial learning, perhaps through the modulation of synchrony among climbing fibers (CF). Additionally, we propose that the modulation of the amplitude of CF-triggered calcium signals in Purkinje cell dendrites may provide an additional mechanism underlying the proportionate learning. This latter mechanism may provide single Purkinje cells with a graded amount of plasticity in single trials, which may subsequently contribute to graded trial-by-trial motor learning.

6.2 Single-trial adaptation in dynamic environments

I started **chapter 2** by presenting our novel method of eyeblink conditioning, which involves headfixed mice on a treadmill and leads to remarkable learning

standards. Next, I showed that the magnitude of conditioned responses (CR) is proportionate to the strength of the unconditioned stimulus (US, periocular airpuff), which provides the teaching signal in this cerebellar-driven task. I showed that single-session adaptations to scaled-up and scaled-down airpuff stimuli have different time courses. I described how mice adapt their eyelid movements even after a single “perturbation” (change) of the US intensity. Finally, I showed how this single-trial adaptation is modified by the passage of time.

Previous studies of motor adaptation in humans have shown that the statistical properties of the training environment play a key role in determining how movements will be adapted following perturbations. For instance, it has been suggested that the learning strategy adopted by humans in a reaching task is not always fixed and proportional to the size of the error; instead, it depends on the likelihood of perturbations in the environment (Thoroughman et al., 2007). Another study on reaching tasks in humans has demonstrated that uncertainty plays a key role in the degree to which movements are modified trial-by-trial (Wei and Kording, 2010). Human studies of non-cerebellar tasks have also demonstrated the influence of environmental variability on learning. Particularly, it has been shown that unexpected stimuli may not contribute to prediction updating and future decision-making in a changeable environment (Nassar et al., 2010).

My behavioral experiments in mice indicated that eyelid movements are modified, bidirectionally, after a single perturbation of the airpuff intensity. However, two features of my experiments need to be emphasized. 1) The initial training of mice was performed using airpuff stimuli of constant intensity. 2) Perturbation trials were interspersed among trials with constant airpuff intensity. To characterize if motor learning

in our cerebellar task might be influenced by the statistical properties of the environment, I would like to study single-trial adaptation of eyelid responses in a probabilistic, variable environment. In a recent set of experiments, I have started to address this question by training two groups of mice: one group receives constant airpuff stimuli throughout conditioning, and the other is trained with a range of randomly varied airpuff intensities. After mice fully acquire conditioned responses, I will introduce perturbation trials in order to compare single-trial adaptation between the constant and the variable group.

6.3 Imaging prediction error signals in eyeblink-conditioned mice

Chapters 4 and 5 of this dissertation included data from my two-photon microscopy experiments on awake, naïve mice. First, the neural representation of the airpuff stimulus was discussed (chapter 4). Next, the mechanisms of encoding the intensity of the airpuff were presented (chapter 5). More specifically, in **Chapter 4** I showed that in response to airpuff stimulation the amplitude of climbing-fiber-triggered calcium events is enhanced in Purkinje cell (PC) dendrites. I showed that this enhancement partly arises from the activation of a non-climbing-fiber source. Additionally, it differentiates sensory-driven from spontaneous calcium events. In **chapter 5** I discussed the representation of airpuff intensity in PC dendrites through several coding mechanisms, which involved graded modulation of probability, latency, amplitude, and synchrony of calcium events. Particular emphasis was laid upon the single-trial encoding of stimulus intensity, due to its relevance to my behavioral findings on single-trial adaptation to US intensity.

My imaging data were collected in a non-learning paradigm. Ensuing experiments include combining two-photon imaging and eyeblink conditioning. This will open avenues for further exploration of cerebellar motor learning. Below I describe a number of open questions that are pertinent to my behavioral experiments, and can provide insight about the underlying neural mechanisms.

- How would PC calcium responses be modified when a conditioned mouse receives blocks of trials at different US intensities? Is there a neural correlate for the graded CR magnitude that we observed in our behavioral data (Fig. 1.3)? Occasional no-puff trials interspersed within each block of US intensity can serve as probes to study cerebellar predictions of US intensity.

- How would PC calcium signals be adapted, trial-by-trial, during single-session gain-up and gain-down adaptations (Fig. 1.4)? This experiment could shed light upon the adaptive mechanisms that underlie gain-up and gain-down learning in eyeblink conditioning. For instance, if in contrast to our behavioral results, we observe comparable rates of PC calcium-response modulation for gain-up and gain-down conditions, it will corroborate the hypothesis we proposed in chapter 2; i.e. a non-cerebellar structure contributes to gain-up learning. This underlies the fast adaptive process following the gain-up condition, and leads to different temporal properties for gain-up and gain-down adaptations.

- How would a single perturbation of the US intensity modify PC calcium responses? In other words, do we see a PC neural correlate for the single-trial adaptation that we observed in our behavioral experiments (Fig. 1.5)? Can this explain our finding about

the largely non-associative nature of adaptation following a single strong-puff trial, in contrast to its associative nature following a no-puff trial?

- How would PC calcium responses vary with the passage of time after a single perturbation trial? In particular, can we find a neural correlate for the transient adaptation that we observed after a single change of US intensity (Fig. 1.6)? We can address this question by analyzing PC calcium responses to occasional probe (no-puff) trials that we introduce at various time points (e.g. 1-80sec) following a perturbation trial. This strategy could help us monitor time-dependent changes of single-trial cerebellar memory.

- Our behavioral data indicates that learned blinks start to decay within 10 seconds after a "normal" (no perturbation) trial (Fig. 1.6B). Can PC calcium signals explain this time-dependent modification of motor responses even in the absence of perturbations? PC calcium responses to probe trials that occur at various intervals following a normal trial could cast light on the underlying mechanisms.

By doing two-photon imaging and eyeblink conditioning we will be able to address the questions posed above at the following levels: 1) **Single-cell activity**: based on my imaging results, individual PCs have access, in single trials, to an analogue calcium signal whose amplitude correlates with the strength of the unconditioned stimulus. Such an analogue signal can hypothetically induce, in each PC and after each trial, a graded amount of plasticity that will be proportional to US magnitude. The experiments described above would allow us to test this hypothesis and examine the functional implication of the graded calcium signals that we found in PCs in response to airpuff stimuli. 2) **Population-level activity**. Two-photon imaging provides the advantage of

monitoring the activity of a population of PCs simultaneously. This is significant since synchronous climbing fiber responses have been suggested to play a major role in cerebellar-dependent learning (De Zeeuw et al., 1998).

We have taken an initial step towards investigating the aforementioned questions by imaging PC calcium signals in eyeblink-conditioned mice. The novel head-fixed method that we developed for doing eyeblink conditioning in mice (ref. chapter 2), not only proved to be remarkably efficient, it also enabled us to do two-photon microscopy while doing behavioral experiments (Fig. 6.2). Below, I discuss some of the findings from our ongoing work on simultaneous calcium imaging and eyeblink conditioning in mice (Giovannucci et al., 2011).

In order to examine the ensemble coding of US-related signals during eyeblink conditioning, we have imaged populations of climbing fiber responses in lobulus simplex while recording the eyelid movements in a conditioned mouse (Fig. 6.2 A,B). As a first step, we studied how CF responses are modulated by prediction error signals. Figure 6.2 compares the CF-evoked calcium signals in a conditioned mouse among the following three conditions: 1) US-alone trials; 2) paired trials without a conditioned response; 3) paired trials with a conditioned response. Mean eyelid closure for each of the conditions is also shown (Fig. 6.3 bottom, blue traces). PSTH plots of example dendrites (Fig. 6.3 top) and their averages (Fig. 6.3 bottom) demonstrate that airpuff-evoked CF responses are inhibited when conditioned responses occur. In other words, climbing fibers are activated by the periocular airpuff stimulus only when it is not predicted, such as in US-alone trials (Fig. 6.3 left) or those CS-US paired trials without a conditioned response (Fig. 6.3 middle). This finding supports the role of the cerebellum

as an error predictor and the idea that cerebello-olivary pathway is a feedback controller of Purkinje cell activity (Fig. 6.2C).

6.4 Concluding remarks

Errors in predicting outcomes act as teaching signals that will be used by the brain to update predictions on a trial-by-trial basis. The degree by which predictions will be updated is determined by the magnitude of prediction errors. Theoretical frameworks of cerebellar learning have suggested that climbing fibers (CF) convey prediction error signals to the cerebellar cortex. Therefore, in theory, CFs must be capable of encoding the magnitude of prediction errors in single trials. However, there is a critical lack of experimental evidence for this hypothesis.

The aim of this dissertation was to lay the groundwork for the study of error-magnitude encoding through the climbing fiber pathway. To achieve this purpose we modified the intensity of the unconditioned stimulus that represents the “actual outcome” in eyeblink conditioning. Our trial-by-trial analysis of adaptation in this cerebellar-conditioning task represents a departure from traditional methods of studying conditioning, which relied on averaging behavior across many trials. Our behavioral experiments in mice support the trail-by-trial adaptation of motor memories that has been observed in primate studies. Our two-photon imaging experiments propose mechanisms that can be potentially employed by climbing fibers to represent the magnitude of prediction errors in a learning paradigm. Finally, our finding about the contribution of a non-climbing fiber source to the neural representation of the

unconditioned stimulus suggests a reexamination of current theories of cerebellar learning.

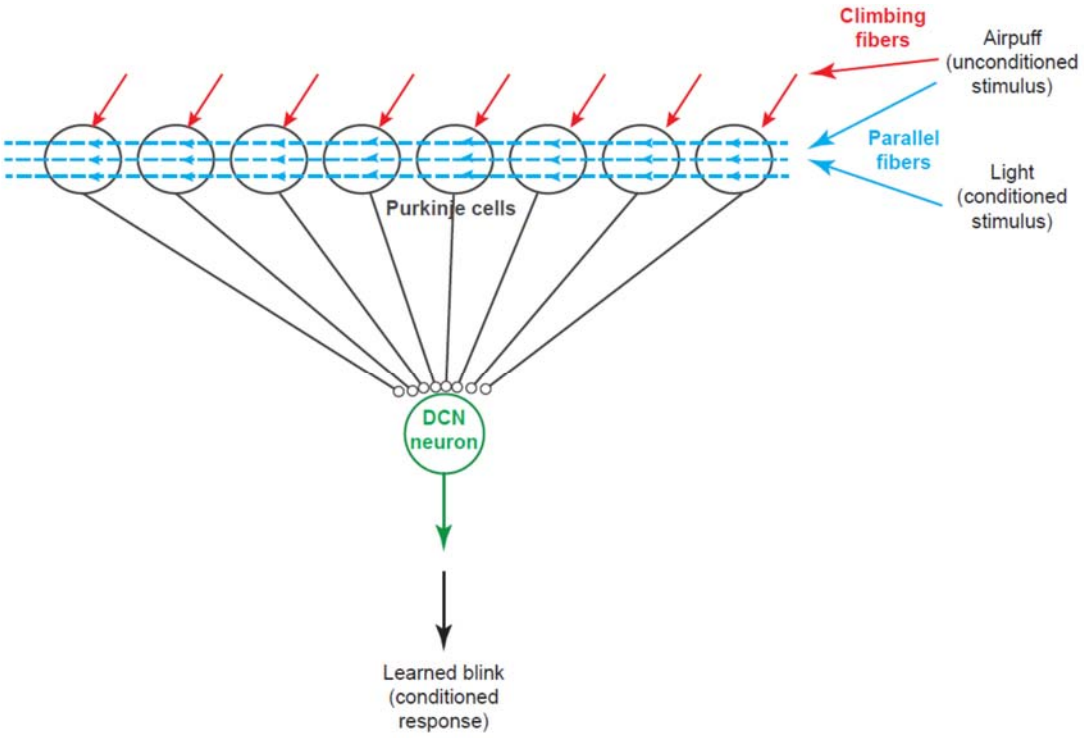

Figure 6-1 Modified cerebellar circuitry for eyeblink conditioning.

In our proposed circuitry, the unconditioned stimulus (US) is relayed to Purkinje cells not only through climbing fibers but also through parallel fibers (PF). [Refer to the text for an explanation of the potential functional role of PF contribution in relaying US-related information during eyeblink conditioning.]

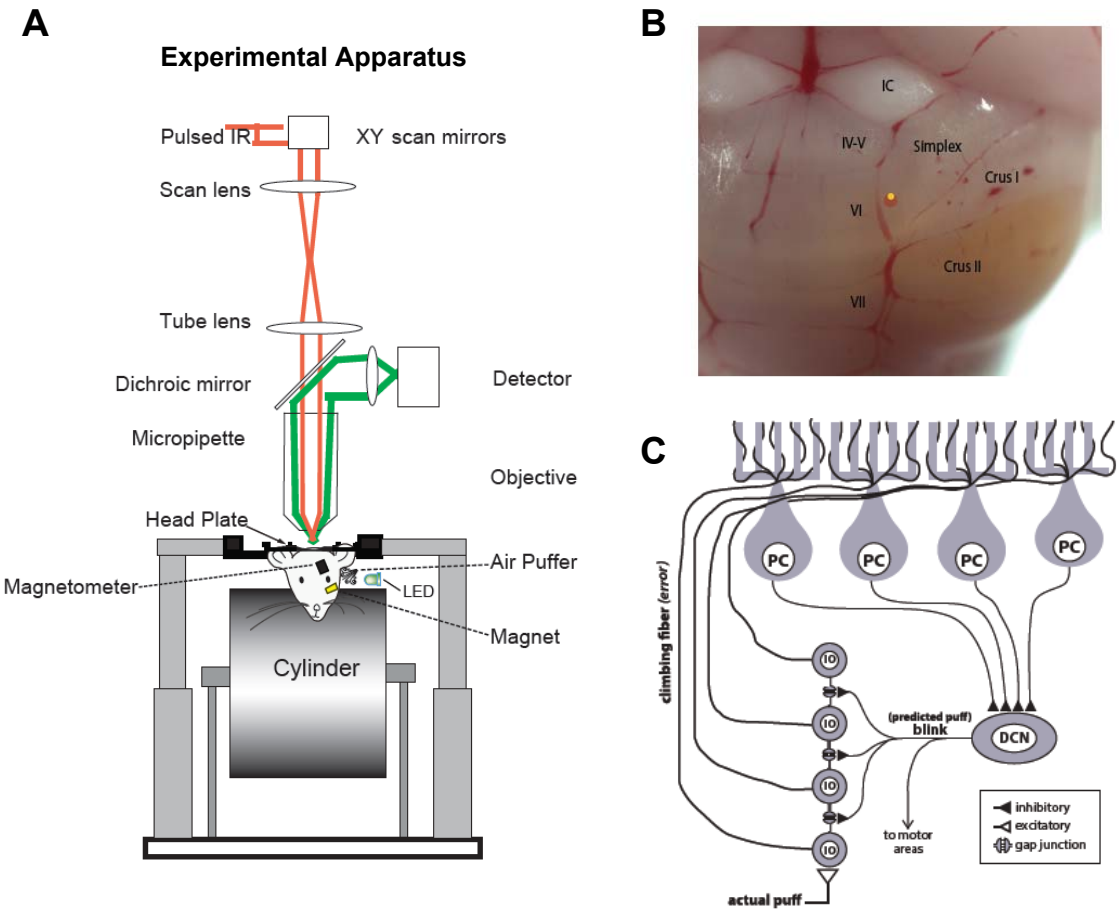

Figure 6-2 Simultaneous two-photon imaging and eyeblink conditioning in awake mice

(A) Mice are head-fixed on a cylindrical treadmill. Eyelid position is measured using a magnetometer. Conditional stimulus is a blue LED. Unconditional stimulus is an airpuff directed at the cornea. In mice reaching a performance of ~60% CRs, a craniotomy was made above the simplex lobule (**B**, yellow dot indicates the imaged area). Purkinje cells and other structures were labeled with Oregon Green BAPTA-1/AM. **(C)** Inferior olivary (IO) neurons are thought to be neural comparators that produce a prediction error signal by comparing their excitatory input (from external stimuli such the periocular airpuff), and inhibitory input (from deep cerebellar nuclei, DCN).

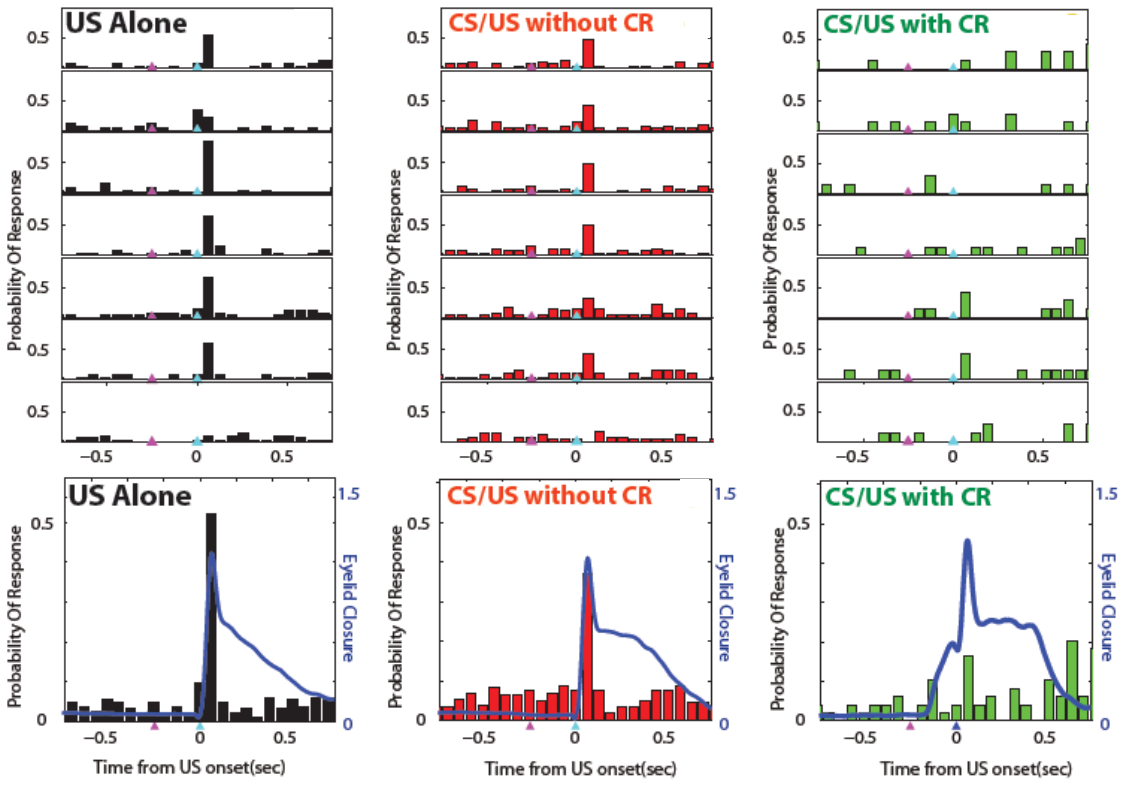

Figure 6-3 Climbing-fiber responses are inhibited when conditioned responses occur

Top: PSTH of 7 example dendrites that were simultaneously imaged is shown for three types of trials: US-alone (left), paired without CR (middle) and paired with CR (right). **Bottom:** mean PSTH across the dendrites. Eyelid traces are superimposed (blue).

BIBLIOGRAPHY

Albus JS (1971) A theory of cerebellar function. Math Biosci 10:25-61.

Andersson G, Armstrong DM (1987) Complex spikes in Purkinje cells in the lateral vermis (b zone) of the cat cerebellum during locomotion. J Physiol 385:107-134.

Andersson G, Hesslow G (1987a) Inferior olive excitability after high frequency climbing fibre activation in the cat. Exp Brain Res 67:523-532.

Andersson G, Hesslow G (1987b) Activity of Purkinje cells and interpositus neurones during and after periods of high frequency climbing fibre activation in the cat. Exp Brain Res 67:533-542.

Andersson G, Garwicz M, Hesslow G (1988) Evidence for a GABA-mediated cerebellar inhibition of the inferior olive in the cat. Exp Brain Res 72:450-456.

Apps R (1999) Movement-related gating of climbing fibre input to cerebellar cortical zones. Prog Neurobiol 57:537-562.

Apps R, Garwicz M (2005) Anatomical and physiological foundations of cerebellar information processing. Nat Rev Neurosci 6:297-311.

Apps R, Hawkes R (2009) Cerebellar cortical organization: a one-map hypothesis. Nat Rev Neurosci 10:670-681.

Armstrong D, Rawson J (1979) Activity patterns of cerebellar cortical neurones and climbing fibre afferents in the awake cat. J Physiol 289:425-448.

Armstrong DM (1974) Functional significance of connections of the inferior olive. Physiol Rev 54:358-417.

Batchelor AM, Garthwaite J (1997) Frequency detection and temporally dispersed synaptic signal association through a metabotropic glutamate receptor pathway. Nature 385:74-77.

Bazzigaluppi P, De Gruijl JR, van der Giessen RS, Khosrovani S, De Zeeuw CI, de Jeu MT (2012) Olivary subthreshold oscillations and burst activity revisited. Frontiers in neural circuits 6:91.

Bell CC, Kawasaki T (1972) Relations among climbing fiber responses of nearby Purkinje Cells. J Neurophysiol 35:155-169.

Bengtsson F, Ekerot CF, Jorntell H (2011) In vivo analysis of inhibitory synaptic inputs and rebounds in deep cerebellar nuclear neurons. PLoS One 6:e18822.

Bermudez MA, Schultz W (2010) Responses of amygdala neurons to positive reward-predicting stimuli depend on background reward (contingency) rather than stimulus-reward pairing (contiguity). J Neurophysiol 103:1158-1170.

Boele HJ, Koekkoek SK, De Zeeuw CI (2010) Cerebellar and extracerebellar involvement in mouse eyeblink conditioning: the ACDC model. Front Cell Neurosci 3:19.

Bosman LW, Takechi H, Hartmann J, Eilers J, Konnerth A (2008) Homosynaptic long-term synaptic potentiation of the "winner" climbing fiber synapse in developing Purkinje cells. J Neurosci 28:798-807.

Bosman LW, Koekkoek SK, Shapiro J, Rijken BF, Zandstra F, van der Ende B, Owens CB, Potters JW, de Gruijl JR, Ruigrok TJ, De Zeeuw CI (2010) Encoding of whisker input by cerebellar Purkinje cells. J Physiol 588:3757-3783.

Boyden ES, Raymond JL (2003) Active reversal of motor memories reveals rules governing memory encoding. Neuron 39:1031-1042.

Brenowitz SD, Regehr WG (2003) Calcium dependence of retrograde inhibition by endocannabinoids at synapses onto Purkinje cells. J Neurosci 23:6373-6384.

Brown IE, Bower JM (2001) Congruence of mossy fiber and climbing fiber tactile projections in the lateral hemispheres of the rat cerebellum. J Comp Neurol 429:59-70.

Brown SP, Safo PK, Regehr WG (2004) Endocannabinoids inhibit transmission at granule cell to Purkinje cell synapses by modulating three types of presynaptic calcium channels. J Neurosci 24:5623-5631.

Callaway JC, Lasser-Ross N, Ross WN (1995) IPSPs strongly inhibit climbing fiber-activated [Ca2+]i increases in the dendrites of cerebellar Purkinje neurons. J Neurosci 15:2777-2787.

Campbell NC, Ekerot CF, Hesslow G, Oscarsson O (1983) Dendritic plateau potentials evoked in Purkinje cells by parallel fibre volleys in the cat. J Physiol 340:209-223.

Carey MR, Regehr WG (2009) Noradrenergic control of associative synaptic plasticity by selective modulation of instructive signals. Neuron 62:112-122.

Carey MR, Myoga MH, McDaniels KR, Marsicano G, Lutz B, Mackie K, Regehr WG (2011) Presynaptic CB1 receptors regulate synaptic plasticity at cerebellar parallel fiber synapses. J Neurophysiol 105:958-963.

Chen TW, Wardill TJ, Sun Y, Pulver SR, Renninger SL, Baohan A, Schreiter ER, Kerr RA, Orger MB, Jayaraman V, Looger LL, Svoboda K, Kim DS (2013) Ultrasensitive fluorescent proteins for imaging neuronal activity. Nature 499:295-300.

Chettih SN, McDougle SD, Ruffolo LI, Medina JF (2011) Adaptive timing of motor output in the mouse: the role of movement oscillations in eyelid conditioning. Front Integr Neurosci 5:72.

Coddington LT, Rudolph S, Vande Lune P, Overstreet-Wadiche L, Wadiche JI (2013) Spillover-mediated feedforward inhibition functionally segregates interneuron activity. Neuron 78:1050-1062.

Coesmans M, Weber JT, De Zeeuw CI, Hansel C (2004) Bidirectional parallel fiber plasticity in the cerebellum under climbing fiber control. Neuron 44:691-700.

Cohen D, Yarom Y (1998) Patches of synchronized activity in the cerebellar cortex evoked by mossy-fiber stimulation: questioning the role of parallel fibers. Proc Natl Acad Sci U S A 95:15032-15036.

Crill WE (1970) Unitary multiple-spiked responses in cat inferior olive nucleus. J Neurophysiol 33:199-209.

Davie JT, Clark BA, Hausser M (2008) The origin of the complex spike in cerebellar Purkinje cells. J Neurosci 28:7599-7609.

De Gruijl JR, Bazzigaluppi P, de Jeu MT, De Zeeuw CI (2012) Climbing fiber burst size and olivary sub-threshold oscillations in a network setting. PLoS Comput Biol 8:e1002814.

De Schutter E, Maex R (1996) The cerebellum: cortical processing and theory. Curr Opin Neurobiol 6:759-764.

De Zeeuw CI, Koekkoek SK, Wylie DR, Simpson JI (1997) Association between dendritic lamellar bodies and complex spike synchrony in the olivocerebellar system. J Neurophysiol 77:1747-1758.
De Zeeuw CI, Simpson JI, Hoogenraad CC, Galjart N, Koekkoek SK, Ruigrok TJ (1998) Microcircuitry and function of the inferior olive. Trends Neurosci 21:391-400.
De Zeeuw CI, Lang EJ, Sugihara I, Ruigrok TJ, Eisenman LM, Mugnaini E, Llinas R (1996) Morphological correlates of bilateral synchrony in the rat cerebellar cortex. J Neurosci 16:3412-3426.
De Zeeuw CI, Elgersma Y, Hulscher HC, Dortland BR, Hensbroek RA, Ruigrok TJH, Koekkoek SKE (2004) Response to Comment on "Cerebellar LTD and Learning-Dependent Timing of Conditioned Eyelid Responses". Science 304:211.
Dean P, Porrill J, Ekerot CF, Jorntell H (2010) The cerebellar microcircuit as an adaptive filter: experimental and computational evidence. Nat Rev Neurosci 11:30-43.
Denk W, Sugimori M, Llinas R (1995) Two types of calcium response limited to single spines in cerebellar Purkinje cells. Proc Natl Acad Sci U S A 92:8279-8282.
Desclin JC (1974) Histological evidence supporting the inferior olive as the major source of cerebellar climbing fibers in the rat. Brain Res 77:365-384.
Devor A, Yarom Y (2002) Generation and propagation of subthreshold waves in a network of inferior olivary neurons. J Neurophysiol 87:3059-3069.
Dizon MJ, Khodakhah K (2011) The role of interneurons in shaping Purkinje cell responses in the cerebellar cortex. J Neurosci 31:10463-10473.
Dombeck DA, Khabbaz AN, Collman F, Adelman TL, Tank DW (2007) Imaging large-scale neural activity with cellular resolution in awake, mobile mice. Neuron 56:43-57.
Duguid IC, Smart TG (2004) Retrograde activation of presynaptic NMDA receptors enhances GABA release at cerebellar interneuron-Purkinje cell synapses. Nat Neurosci 7:525-533.
Eccles JC (1973) The cerebellum as a computer: patterns in space and time. J Physiol 229:1-32.
Eccles JC, et al. (1967) The cerebellum as a neuronal machine. Oxford, England: Springer-Verlag.
Eccles JC, Llinas R, Sasaki K (1966a) The excitatory synaptic action of climbing fibres on the purinje cells of the cerebellum. J Physiol 182:268-296.
Eccles JC, Llinas R, Sasaki K (1966b) The excitatory synaptic action of climbing fibres on the Purkinje cells of the cerebellum. J Physiol 182:268-296.
Eccles JC, Sabah NH, Schmidt RF, Taborikova H (1972) Integration by Purkyne cells of mossy and climbing fiber inputs from cutaneous mechanoreceptors. Exp Brain Res 15:498-520.
Eilers J, Augustine G, Konnerth A (1995) Subthreshold synaptic Ca2+ signalling in fine dendrites and spines of cerebellar Purkinje neurons. Nature 373:155-158.
Ekerot C, Jorntell H (2001) Parallel fibre receptive fields of Purkinje cells and interneurons are climbing fibre-specific. The European journal of neuroscience 13:1303-1310.
Ekerot CF, Jorntell H (2003) Parallel fiber receptive fields: a key to understanding cerebellar operation and learning. Cerebellum 2:101-109.
Ekerot CF, Gustavsson P, Oscarsson O, Schouenborg J (1987) Climbing fibres projecting to cat cerebellar anterior lobe activated by cutaneous A and C fibres. J Physiol 386:529-538.
Fioravante D, Myoga MH, Leitges M, Regehr WG (2012) Adaptive regulation maintains posttetanic potentiation at cerebellar granule cell synapses in the absence of calcium-dependent PKC. J Neurosci 32:13004-13009.

Franklin DW, Wolpert DM (2008) Specificity of reflex adaptation for task-relevant variability. J Neurosci 28:14165-14175.
Gao W, Chen G, Reinert KC, Ebner TJ (2006) Cerebellar cortical molecular layer inhibition is organized in parasagittal zones. J Neurosci 26:8377-8387.
Gao Z, van Beugen BJ, De Zeeuw CI (2012) Distributed synergistic plasticity and cerebellar learning. Nat Rev Neurosci 13:619-635.
Garwicz M, Jorntell H, Ekerot C-F (1998) Cutaneous receptive fields and topography of mossy fibres and climbing fibres projecting to cat cerebellar C3 zone. J Physiol 512.
Gellman R, Gibson A, Houk J (1985) Inferior olivary neurons in the awake cat: detection of contact and passive body displacement. J Neurophysiol 54:40-60.
Gibson AR, Horn KM, Pong M (2004) Activation of climbing fibers. Cerebellum 3:212-221.
Gilbert P (1975) How the cerebellum could memorise movements. Nature 254:688-689.
Gilbert PF (1993) Theories of motor learning by the cerebellum. Trends Neurosci 16:177-178.
Gilbert PF, Thach WT (1977) Purkinje cell activity during motor learning. Brain Res 128:309-328.
Giovannucci A, Najafi F, Kloth AD, Medina JF, Wang SS (2011) Calcium imaging from cerebellar neuronal populations after eyeblink conditioning in head-fixed mice. In: Program No. 83.19/QQ30. 2011 Neuroscience Meeting Planner.

Washington DC: Society for Neuroscience, 2011. Online.
Glitsch M, Parra P, Llano I (2000) The retrograde inhibition of IPSCs in rat cerebellar purkinje cells is highly sensitive to intracellular Ca2+. Eur J Neurosci 12:987-993.
Gormezano I, Schneiderman N, Deaux E, Fuentes I (1962) Nictitating membrane: classical conditioning and extinction in the albino rabbit. Science 138:33-34.
Green DM, Swets JA (1966) Signal Detection Theory and Psychophysics: John Wiley and Sons.
Hansel C, Linden DJ (2000) Long-term depression of the cerebellar climbing fiber--Purkinje neuron synapse. Neuron 26:473-482.
Hansel C, Linden DJ, D'Angelo E (2001) Beyond parallel fiber LTD: the diversity of synaptic and non-synaptic plasticity in the cerebellum. Nat Neurosci 4:467-475.
Heiney SA, Kim J, Augustine GJ, Medina JF (2014) Precise control of movement kinematics by optogenetic inhibition of Purkinje cell activity. J Neurosci 34:2321-2330.
Hesslow G (1994) Correspondence between climbing fibre input and motor output in eyeblink-related areas in cat cerebellar cortex. J Physiol 476:229-244.
Hesslow G, Ivarsson M (1996) Inhibition of the inferior olive during conditioned responses in the decerebrate ferret. Exp Brain Res 110:36-46.
Hirano T, Kawaguchi SY (2014) Regulation and functional roles of rebound potentiation at cerebellar stellate cell-Purkinje cell synapses. Front Cell Neurosci 8:42.
Hoehler F, Leonard D (1981) Motivational vs. associative role of the US in classical conditioning of the rabbit's nictitating membrane response. Anim Learn Behav 9:239-244.
Houk JC, Buckingham JT, Barto AG (1996) Models of the cerebellum and motor learning. Behav Brain Sci 19:368-383.
Huang VS, Shadmehr R (2007) Evolution of motor memory during the seconds after observation of motor error. J Neurophysiol 97:3976-3985.
Hyvarinen A (1999) Fast and robust fixed-point algorithms for independent component analysis. IEEE transactions on neural networks / a publication of the IEEE Neural Networks Council 10:626-634.

Ito M (1984) The cerebellum and neural control: New York, Raven Press.
Ito M (1989) Long-term depression. Annu Rev Neurosci 12:85-102.
Ito M (2006) Cerebellar circuitry as a neuronal machine. Prog Neurobiol 78:272-303.
Ito M (2013) Error detection and representation in the olivo-cerebellar system. Frontiers in neural circuits 7:1.
Ito M, Kano M (1982) Long-lasting depression of parallel fiber-Purkinje cell transmission induced by conjunctive stimulation of parallel fibers and climbing fibers in the cerebellar cortex. Neurosci Lett 33:253-258.
Kano M, Rexhausen U, Dreessen J, Konnerth A (1992) Synaptic excitation produces a long-lasting rebound potentiation of inhibitory synaptic signals in cerebellar Purkinje cells. Nature 356:601-604.
Kano M, Kano M, Fukunaga K, Konnerth A (1996) Ca(2+)-induced rebound potentiation of gamma-aminobutyric acid-mediated currents requires activation of Ca2+/calmodulin-dependent kinase II. Proc Natl Acad Sci U S A 93:13351-13356.
Kawato M, Gomi H (1992) A computational model of four regions of the cerebellum based on feedback-error learning. Biol Cybern 68:95-103.
Kehoe EJ, White NE (2002) Extinction revisited: similarities between extinction and reductions in US intensity in classical conditioning of the rabbit's nictitating membrane response. Anim Learn Behav 30:96-111.
Kenyon GT, Medina JF, Mauk MD (1998) A mathematical model of the cerebellar-olivary system II: motor adaptation through systematic disruption of climbing fiber equilibrium. J Comput Neurosci 5:71-90.
Kim JJ, Thompson RE (1997) Cerebellar circuits and synaptic mechanisms involved in classical eyeblink conditioning. Trends Neurosci 20:177-181.
Kim JJ, Krupa DJ, Thompson RF (1998) Inhibitory cerebello-olivary projections and blocking effect in classical conditioning. Science 279:570-573.
Kitamura K, Hausser M (2011) Dendritic calcium signaling triggered by spontaneous and sensory-evoked climbing fiber input to cerebellar Purkinje cells in vivo. J Neurosci 31:10847-10858.
Kitamura K, Kano M (2013) Dendritic calcium signaling in cerebellar Purkinje cell. Neural networks : the official journal of the International Neural Network Society 47:11-17.
Kitazawa S, Wolpert DM (2005) Rhythmicity, randomness and synchrony in climbing fiber signals. Trends Neurosci 28:611-619.
Kitazawa S, Kimura T, Yin PB (1998) Cerebellar complex spikes encode both destinations and errors in arm movements. Nature 392:494-497.
Kobayashi Y, Kawano K, Takemura A, Inoue Y, Kitama T, Gomi H, Kawato M (1998) Temporal firing patterns of Purkinje cells in the cerebellar ventral paraflocculus during ocular following responses in monkeys II. Complex spikes. J Neurophysiol 80:832-848.
Koekkoek SK, Den Ouden WL, Perry G, Highstein SM, De Zeeuw CI (2002) Monitoring kinetic and frequency-domain properties of eyelid responses in mice with magnetic distance measurement technique. J Neurophysiol 88:2124-2133.
Kojima Y, Iwamoto Y, Yoshida K (2004) Memory of learning facilitates saccadic adaptation in the monkey. J Neurosci 24:7531-7539.

Konnerth A, Dreessen J, Augustine GJ (1992) Brief dendritic calcium signals initiate long-lasting synaptic depression in cerebellar Purkinje cells. Proc Natl Acad Sci U S A 89:7051-7055.
Lampl I, Yarom Y (1993) Subthreshold oscillations of the membrane potential: a functional synchronizing and timing device. J Neurophysiol 70:2181-2186.
Lampl I, Yarom Y (1997) Subthreshold oscillations and resonant behavior: two manifestations of the same mechanism. Neuroscience 78:325-341.
Lang EJ (2002) GABAergic and glutamatergic modulation of spontaneous and motor-cortex-evoked complex spike activity. J Neurophysiol 87:1993-2008.
Lang EJ, Sugihara I, Welsh JP, Llinas R (1999) Patterns of spontaneous purkinje cell complex spike activity in the awake rat. J Neurosci 19:2728-2739.
Leznik E, Llinas R (2005) Role of gap junctions in synchronized neuronal oscillations in the inferior olive. J Neurophysiol 94:2447-2456.
Li J, Smith SS, McElligott JG (1995) Cerebellar nitric oxide is necessary for vestibulo-ocular reflex adaptation, a sensorimotor model of learning. J Neurophysiol 74:489-494.
Llinas R, Sugimori M (1980) Electrophysiological properties of in vitro Purkinje cell dendrites in mammalian cerebellar slices. J Physiol 305:197-213.
Llinas R, Yarom Y (1981) Electrophysiology of mammalian inferior olivary neurones in vitro. Different types of voltage-dependent ionic conductances. J Physiol 315:549-567.
Llinas R, Sasaki K (1989) The Functional Organization of the Olivo-Cerebellar System as Examined by Multiple Purkinje Cell Recordings. Eur J Neurosci 1:587-602.
Llinas R, Welsh JP (1993) On the cerebellum and motor learning. Curr Opin Neurobiol 3:958-965.
Llinas R, Baker R, Sotelo C (1974) Electrotonic coupling between neurons in cat inferior olive. J Neurophysiol 37:560-571.
Llinas R, Lang EJ, Welsh JP (1997) The cerebellum, LTD, and memory: alternative views. Learn Mem 3:445-455.
Llinas RR (2011) Cerebellar motor learning versus cerebellar motor timing: the climbing fibre story. J Physiol 589:3423-3432.
Lou JS, Bloedel JR (1992) Responses of sagittally aligned Purkinje cells during perturbed locomotion: synchronous activation of climbing fiber inputs. J Neurophysiol 68:570-580.
Maejima T, Oka S, Hashimotodani Y, Ohno-Shosaku T, Aiba A, Wu D, Waku K, Sugiura T, Kano M (2005) Synaptically driven endocannabinoid release requires Ca2+-assisted metabotropic glutamate receptor subtype 1 to phospholipase Cbeta4 signaling cascade in the cerebellum. J Neurosci 25:6826-6835.
Manni E, Petrosini L (2004) A century of cerebellar somatotopy: a debated representation. Nat Rev Neurosci 5:241-249.
Maren S (2001) Neurobiology of Pavlovian fear conditioning. Annu Rev Neurosci 24:897-931.
Marr D (1969) A theory of cerebellar cortex. J Physiol 202:437-470.
Marshall SP, van der Giessen RS, de Zeeuw CI, Lang EJ (2007) Altered olivocerebellar activity patterns in the connexin36 knockout mouse. Cerebellum 6:287-299.
Maruta J, Hensbroek RA, Simpson JI (2007) Intraburst and interburst signaling by climbing fibers. J Neurosci 27:11263-11270.
Mathews PJ, Lee KH, Peng Z, Houser CR, Otis TS (2012) Effects of climbing fiber driven inhibition on Purkinje neuron spiking. J Neurosci 32:17988-17997.

Mathy A, Ho SS, Davie JT, Duguid IC, Clark BA, Hausser M (2009) Encoding of oscillations by axonal bursts in inferior olive neurons. Neuron 62:388-399.
Mauk MD, Donegan NH (1997) A model of Pavlovian eyelid conditioning based on the synaptic organization of the cerebellum. Learn Mem 4:130-158.
Mauk MD, Steinmetz JE, Thompson RF (1986) Classical conditioning using stimulation of the inferior olive as the unconditioned stimulus. Proc Natl Acad Sci U S A 83:5349-5353.
Mauk MD, Steele PM, Medina JF (1997) Cerebellar involvement in motor learning. Neuroscientist 3:301-313.
McCormick DA, Thompson RF (1984) Cerebellum: essential involvement in the classically conditioned eyelid response. Science 223:296-299.
Medina JF, Lisberger SG (2008) Links from complex spikes to local plasticity and motor learning in the cerebellum of awake-behaving monkeys. Nat Neurosci 11:1185-1192.
Medina JF, Nores WL, Mauk MD (2002) Inhibition of climbing fibres is a signal for the extinction of conditioned eyelid responses. Nature 416:330-333.
Medina JF, Nores WL, Ohyama T, Mauk MD (2000) Mechanisms of cerebellar learning suggested by eyelid conditioning. Curr Opin Neurobiol 10:717-724.
Midtgaard J, Lasser-Ross N, Ross WN (1993) Spatial distribution of Ca2+ influx in turtle Purkinje cell dendrites in vitro: role of a transient outward current. J Neurophysiol 70:2455-2469.
Miles T, Wiesendanger M (1975a) Climbing fibre inputs to cerebellar Purkinje cells from trigeminal cutaneous afferents and the SI face area of the cerebral cortex in the cat. J Physiol 245:425-445.
Miles TS, Wiesendanger M (1975b) Organization of climbing fibre projections to the cerebellar cortex from trigeminal cutaneous afferents and from the SI face area of the cerebral cortex in the cat. J Physiol 245:409-424.
Mittmann W, Hausser M (2007) Linking synaptic plasticity and spike output at excitatory and inhibitory synapses onto cerebellar Purkinje cells. J Neurosci 27:5559-5570.
Miyakawa H, Lev-Ram V, Lasser-Ross N, Ross W (1992) Calcium transients evoked by climbing fiber and parallel fiber synaptic inputs in guinea pig cerebellar Purkinje neurons. J Neurophysiol 68:1178-1189.
Miyata M, Finch EA, Khiroug L, Hashimoto K, Hayasaka S, Oda SI, Inouye M, Takagishi Y, Augustine GJ, Kano M (2000) Local calcium release in dendritic spines required for long-term synaptic depression. Neuron 28:233-244.
Moises HC, Waterhouse BD, Woodward DJ (1981) Locus coeruleus stimulation potentiates Purkinje cell responses to afferent input: the climbing fiber system. Brain Res 222:43-64.
Mostofi A, Holtzman T, Grout AS, Yeo CH, Edgley SA (2010) Electrophysiological localization of eyeblink-related microzones in rabbit cerebellar cortex. J Neurosci 30:8920-8934.
Najafi F, Medina JF (2013) Beyond "all-or-nothing" climbing fibers: graded representation of teaching signals in Purkinje cells. Frontiers in neural circuits 7:115.
Najafi F, Giovannucci A, Wang SS, Medina JF (2014) Sensory-driven enhancement of calcium signals in individual purkinje cell dendrites of awake mice. Cell Rep 6:792-798.
Nassar MR, Wilson RC, Heasly B, Gold JI (2010) An approximately Bayesian delta-rule model explains the dynamics of belief updating in a changing environment. J Neurosci 30:12366-12378.

Nicholson DA, Freeman JH (2003) Developmental changes in evoked Purkinje cell complex spike responses. J Neurophysiol 90:2349-2357.
Niv Y, Schoenbaum G (2008) Dialogues on prediction errors. Trends in cognitive sciences 12:265-272.
Odeh F, Ackerley R, Bjaalie JG, Apps R (2005) Pontine maps linking somatosensory and cerebellar cortices are in register with climbing fiber somatotopy. J Neurosci 25:5680-5690.
Ohtsuki G, Hirano T (2008) Bidirectional plasticity at developing climbing fiber-Purkinje neuron synapses. Eur J Neurosci 28:2393-2400.
Ohtsuki G, Piochon C, Hansel C (2009) Climbing fiber signaling and cerebellar gain control. Front Cell Neurosci 3:4.
Oscarsson O (1979) Functional units of the cerebellum - sagittal zones and microzones. Trends Neurosci 2:143-145.
Otis TS, Mathews PJ, Lee KH, Maiz J (2012) How do climbing fibers teach? Frontiers in neural circuits 6:95.
Ozden I, Lee H, Sullivan M, Wang S (2008) Identification and clustering of event patterns from in vivo multiphoton optical recordings of neuronal ensembles. J Neurophysiol 100:495-503.
Ozden I, Sullivan M, Lee H, Wang S (2009) Reliable coding emerges from coactivation of climbing fibers in microbands of cerebellar Purkinje neurons. J Neurosci 29:10463-10473.
Ozden I, Dombeck DA, Hoogland TM, Tank DW, Wang SS (2012) Widespread state-dependent shifts in cerebellar activity in locomoting mice. PLoS One 7:e42650.
Palay SL, Chan-Palay V (1974) Cerebellar cortex: cytology and organization: Springer.
Palkovits M, Mezey E, Hamori J, Szentagothai J (1977) Quantitative histological analysis of the cerebellar nuclei in the cat. I. Numerical data on cells and on synapses. Exp Brain Res 28:189-209.
Passey GE (1948) The influence of intensity of unconditioned stimulus upon acquisition of a conditioned response. J Exp Psychol 38:420-428.
Pavlov IP, Anrep GV (1927) Conditioned Reflexes: An Investigation of the Physiological Activity of the Cerebral Cortex: Oxford University Press.
Person AL, Raman IM (2012) Purkinje neuron synchrony elicits time-locked spiking in the cerebellar nuclei. Nature 481:502-505.
Pijpers A, Apps R, Pardoe J, Voogd J, Ruigrok TJ (2006) Precise spatial relationships between mossy fibers and climbing fibers in rat cerebellar cortical zones. J Neurosci 26:12067-12080.
Pologruto TA, Sabatini BL, Svoboda K (2003) ScanImage: flexible software for operating laser scanning microscopes. Biomedical engineering online 2:13.
Raman IM, Bean BP (1997) Resurgent sodium current and action potential formation in dissociated cerebellar Purkinje neurons. J Neurosci 17:4517-4526.
Raman IM, Bean BP (1999a) Ionic currents underlying spontaneous action potentials in isolated cerebellar Purkinje neurons. J Neurosci 19:1663-1674.
Raman IM, Bean BP (1999b) Properties of sodium currents and action potential firing in isolated cerebellar Purkinje neurons. Ann N Y Acad Sci 868:93-96.

Rancz E, Hausser M (2006) Dendritic calcium spikes are tunable triggers of cannabinoid release and short-term synaptic plasticity in cerebellar Purkinje neurons. J Neurosci 26:5428-5437.
Rasmussen A, Jirenhed DA, Hesslow G (2008) Simple and complex spike firing patterns in Purkinje cells during classical conditioning. Cerebellum 7:563-566.
Raymond JL, Lisberger SG (1998) Neural learning rules for the vestibulo-ocular reflex. J Neurosci 18:9112-9129.
Raymond JL, Lisberger SG, Mauk MD (1996) The cerebellum: a neuronal learning machine? Science 272:1126-1131.
Rescorla RA, Wagner AW (1972) A theory of Pavlovian conditioning: Variations in the effectiveness of reinforcement and nonreinforcement. Classical Conditioning II: Current Research and Theory 64-99.
Ross WN, Werman R (1987) Mapping calcium transients in the dendrites of Purkinje cells from the guinea-pig cerebellum in vitro. J Physiol 389:319-336.
Ruigrok TJ, Voogd J (1995) Cerebellar influence on olivary excitability in the cat. Eur J Neurosci 7:679-693.
Rushmer DS, Roberts WJ, Augter GK (1976) Climbing fiber responses of cerebellar Purkinje cells to passive movement of the cat forepaw. Brain Res 106:1-20.
Safo PK, Regehr WG (2005) Endocannabinoids control the induction of cerebellar LTD. Neuron 48:647-659.
Safo PK, Cravatt BF, Regehr WG (2006) Retrograde endocannabinoid signaling in the cerebellar cortex. Cerebellum 5:134-145.
Sakurai M (1990) Calcium is an intracellular mediator of the climbing fiber in induction of cerebellar long-term depression. Proc Natl Acad Sci U S A 87:3383-3385.
Sasaki K, Bower JM, Llinas R (1989) Multiple Purkinje Cell Recording in Rodent Cerebellar Cortex. Eur J Neurosci 1:572-586.
Scheidt RA, Dingwell JB, Mussa-Ivaldi FA (2001) Learning to move amid uncertainty. J Neurophysiol 86:971-985.
Schmolesky MT, Weber JT, De Zeeuw CI, Hansel C (2002) The making of a complex spike: ionic composition and plasticity. Ann N Y Acad Sci 978:359-390.
Schultz SR, Kitamura K, Post-Uiterweer A, Krupic J, Hausser M (2009) Spatial pattern coding of sensory information by climbing fiber-evoked calcium signals in networks of neighboring cerebellar Purkinje cells. J Neurosci 29:8005-8015.
Schultz W (1986) Responses of midbrain dopamine neurons to behavioral trigger stimuli in the monkey. J Neurophysiol 56:1439-1461.
Schultz W, Dickinson A (2000) Neuronal coding of prediction errors. Annu Rev Neurosci 23:473-500.
Schultz W, Dayan P, Montague PR (1997) A neural substrate of prediction and reward. Science 275:1593-1599.
Sears LL, Steinmetz JE (1991) Dorsal accessory inferior olive activity diminishes during acquisition of the rabbit classically conditioned eyelid response. Brain Res 545:114-122.
Sejnowski TJ (1977) Storing covariance with nonlinearly interacting neurons. J Math Biol 4:303-321.

Shadmehr R, Mussa-Ivaldi FA (1994) Adaptive representation of dynamics during learning of a motor task. J Neurosci 14:3208-3224.
Simpson JI, Wylie DR, De Zeeuw CI (1996) On climbing fiber signals and their consequence(s). Behav Brain Sci 19:384-398.
Sjostrom PJ, Nelson SB (2002) Spike timing, calcium signals and synaptic plasticity. Curr Opin Neurobiol 12:305-314.
Smith MA, Ghazizadeh A, Shadmehr R (2006) Interacting adaptive processes with different timescales underlie short-term motor learning. PLoS Biol 4:e179.
Smith MC (1968) CS-US interval and US intensity in classical conditioning of the rabbit's nictitating membrane response. J Comp Physiol Psychol 66:679-687.
Soetedjo R, Kojima Y, Fuchs AF (2008a) Complex spike activity in the oculomotor vermis of the cerebellum: a vectorial error signal for saccade motor learning? J Neurophysiol 100:1949-1966.
Soetedjo R, Kojima Y, Fuchs A (2008b) Complex spike activity signals the direction and size of dysmetric saccade errors. Prog Brain Res 171:153-159.
Sotelo C, Llinas R, Baker R (1974) Structural study of inferior olivary nucleus of the cat: morphological correlates of electrotonic coupling. J Neurophysiol 37:541-559.
Spence KW (1953) Learning and performance in eyelid conditioning as a function of intensity of the UCS. J Exp Psychol 45:57-63.
Spence KW, Taylor J (1951) Anxiety and strength of the UCS as determiners of the amount of eyelid conditioning. J Exp Psychol 42:183-188.
Spence KW, Haggard DF, Ross LE (1958) UCS intensity and the associative (habit) strength of the eyelid CR. J Exp Psychol 55:404-411.
Spoelstra J, Schweighofer N, Arbib MA (2000) Cerebellar learning of accurate predictive control for fast-reaching movements. Biol Cybern 82:321-333.
Steinberg EE, Keiflin R, Boivin JR, Witten IB, Deisseroth K, Janak PH (2013) A causal link between prediction errors, dopamine neurons and learning. Nat Neurosci 16:966-973.
Strata P, Rossi F (1998) Plasticity of the olivocerebellar pathway. Trends Neurosci 21:407-413.
Strughold H (1930) THE MECHANICAL THRESHOLD OF THE CORNEA-REFLEX OF THE USUAL LABORATORY ANIMALS. American Journal of Physiology -- Legacy Content 94:235-240.
Sturrock RR (1989) Changes in neuron number in the cerebellar cortex of the ageing mouse. J Hirnforsch 30:499-503.
Sugihara I, Lang EJ, Llinas R (1993) Uniform olivocerebellar conduction time underlies Purkinje cell complex spike synchronicity in the rat cerebellum. J Physiol 470:243-271.
Sullivan M, Nimmerjahn A, Sarkisov D, Helmchen F, Wang S (2005) In vivo calcium imaging of circuit activity in cerebellar cortex. J Neurophysiol 94:1636-1644.
Sutton RS, Barto AG (1998) Introduction to Reinforcement Learning: MIT Press.
Szapiro G, Barbour B (2007) Multiple climbing fibers signal to molecular layer interneurons exclusively via glutamate spillover. Nat Neurosci 10:735-742.
Takatsuki K, Kawahara S, Takehara K, Kishimoto Y, Kirino Y (2001) Effects of the noncompetitive NMDA receptor antagonist MK-801 on classical eyeblink conditioning in mice. Neuropharmacology 41:618-628.
Takechi H, Eilers J, Konnerth A (1998) A new class of synaptic response involving calcium release in dendritic spines. Nature 396:757-760.

Tanaka K, Khiroug L, Santamaria F, Doi T, Ogasawara H, Ellis-Davies GC, Kawato M, Augustine GJ (2007) Ca2+ requirements for cerebellar long-term synaptic depression: role for a postsynaptic leaky integrator. Neuron 54:787-800.

Tank DW, Sugimori M, Connor JA, Llinas RR (1988) Spatially resolved calcium dynamics of mammalian Purkinje cells in cerebellar slice. Science 242:773-777.

Thach W (1968) Discharge of Purkinje and cerebellar nuclear neurons during rapidly alternating arm movements in the monkey. J Neurophysiol 31:785-797.

Thach WT, Goodkin HP, Keating JG (1992) The cerebellum and the adaptive coordination of movement. Annu Rev Neurosci 15:403-442.

Thach WT, Jr. (1967) Somatosensory receptive fields of single units in cat cerebellar cortex. J Neurophysiol 30:675-696.

Thompson R, Steinmetz J (2009) The role of the cerebellum in classical conditioning of discrete behavioral responses. Neuroscience 162:732-755.

Thoroughman KA, Fine MS, Taylor JA (2007) Trial-by-trial motor adaptation: a window into elemental neural computation. Prog Brain Res 165:373-382.

Voogd J, Pardoe J, Ruigrok TJ, Apps R (2003) The distribution of climbing and mossy fiber collateral branches from the copula pyramidis and the paramedian lobule: congruence of climbing fiber cortical zones and the pattern of zebrin banding within the rat cerebellum. J Neurosci 23:4645-4656.

Vos BP, Volny-Luraghi A, Maex R, De Schutter E (2000) Precise spike timing of tactile-evoked cerebellar Golgi cell responses: a reflection of combined mossy fiber and parallel fiber activation? Prog Brain Res 124:95-106.

Wang S, Denk W, Hausser M (2000) Coincidence detection in single dendritic spines mediated by calcium release. Nat Neurosci 3:1266-1273.

Watson CR, Switzer RC, 3rd (1978) Trigeminal projections to cerebellar tactile areas in the rat-origin mainly from n. interpolaris and n. principalis. Neurosci Lett 10:77-82.

Wei K, Kording K (2010) Uncertainty of feedback and state estimation determines the speed of motor adaptation. Front Comput Neurosci 4:11.

Welsh JP, Lang EJ, Suglhara I, Llinas R (1995) Dynamic organization of motor control within the olivocerebellar system. Nature 374:453-457.

Wise AK, Cerminara NL, Marple-Horvat DE, Apps R (2010) Mechanisms of synchronous activity in cerebellar Purkinje cells. J Physiol 588:2373-2390.

Woodruff-Pak DS (2006) Stereological estimation of Purkinje neuron number in C57BL/6 mice and its relation to associative learning. Neuroscience 141:233-243.

Wylie DR, De Zeeuw CI, Simpson JI (1995) Temporal relations of the complex spike activity of Purkinje cell pairs in the vestibulocerebellum of rabbits. J Neurosci 15:2875-2887.

Yang Y, Lisberger SG (2010) Learning on multiple timescales in smooth pursuit eye movements. J Neurophysiol 104:2850-2862.

Zucker RS (1999) Calcium- and activity-dependent synaptic plasticity. Curr Opin Neurobiol 9:305-313.